Peninsula Technikon

Faculty of Engineering

Center for Research in Applied Technology

Approximate Analytical Solutions for Vibration Control of Smart Composite Beams

Da Huang

B. Sc. Eng. (P. R. China)

Submitted towards the degree of
Master of Technology in Mechanical Engineering

Under Supervision of

Dr Bohua Sun

CAPE TOWN, 1999

Acknowledgments

There are a number of people who sincere deserve my thanks for their effort in the support of my master's thesis. Special thanks goes to my supervisor Dr. Bohua Sun who gave the perfect balance of technical direction and freedom in the pursuit of my research interests. I would like to thank Dr. Nawaz Mahomed (Head of Research at Faculty of Engineering) and Mr. Keith Jacobs (HoD of Mechanical Engineering) for their financial assistance. I also wish to thank Dr. Wei Cheng (Visiting Post-Doctoral Researcher) for being especially helpful with my study. Thanks also go to Mr. Brian Hendricks and Mr. Xun Li for many important discussions and supports. I would also like to thank all the members of Center for Research in Applied Technology (CRATech) and staff members at Department of Mechanical Engineering for the fantastic environment for learning, friendly atmosphere, and technical support.

Specially, I would like to thank my father, Professor Yih Huang, for his encouragement, guidance, and many important suggestions. I would also like to give a special thanks to all my family (my mother, my sister and brother-in-law and their daughter), for their endearing encouragement, patience, and love. I would like to thank all my friends and classmates for their years of support and motivation to partake in social activities: Mark Ludick, Oscar Philander, Abed Mennad, Mornay Riddles, Philemon Simelane. I would also like to thank Ms. Bernedette Gonzalves (Secretary of CRATech) for checking spelling of thesis and Mrs. Elvina Moosa (Secretary of Dept. Mechanical Engineering) for her help and use of equipment.

Finally, I would like to thank the National Research Foundation (NRF) of South Africa for supporting this work under the project: Smart Composite Structures (GUN2038139). The Peninsula Technikon scholarship is also gratefully acknowledged.

Abstract

Title of Thesis:	Approximate Analytical Solutions for Vibration Control of Smart Composite Beams
Degree candidate:	Da Huang
Degree and Year:	Master of Technology, 1999
Thesis directed by:	Dr. Bo-hua Sun Department of Mechanical Engineering and Center for Research in Applied Technology

Smart structures technology featuring a network of sensors and actuators, real-time control capabilities, computational capabilities and host material will have tremendous impact upon the design, development and manufacture of the next generation of products in diverse industries. The idea of applying smart materials to mechanical and structural systems has been studied by researchers in various disciplines. Among the promising materials with adaptable properties such as piezoelectric polymers and ceramics, shape memory alloys, electrorheological fluids and optical fibers, piezoelectric materials can be used both as sensors and actuators because of their high direct and converse piezoelectric effects. The advantage of incorporating these special types of material into the structure is that the sensing and actuating mechanism becomes part of the structure by sensing and actuating strains directly. This advantage is especially apparent for structures that are deployed in aerospace and civil engineering.

Active control systems that rely on piezoelectric materials are effective in controlling the vibrations of structural elements such as beams, plates and shells. The beam as a fundamental structural element is widely used in all construction. The purpose of the present project is to derive a set of approximate governing equations of smart composite beams. The approximate analytical solution for laminated beams with piezoelectric laminae and its control effect will be also presented. According to the review of the related literature, active vibration control analysis of smart beams subjected to an impulsive loading and a periodic excitation are simulated numerically and tested experimentally. The research currently in progress is highly industry related and will have definite benefits for designers as well as engineers in the future.

The present beam model is to demonstrate the vibration control effects of smart composite beam structures with piezoelectric sensor and actuator layers. The equations of motion are developed using Hamilton's principle (energy principle). These equations are based on Mindlin laminated theory, and include the coupling between mechanical deformation and the charge equations of electrostatics. The approximate analytical solutions by using software package MATLAB and MATHEMATICA is to study the effectiveness of piezoelectric sensors and actuators in actively controlling the transverse response of smart laminated beams. The behaviour of the output voltage from the sensor layer and the input voltage acting on the actuator layer is also studied. In this thesis, the following three important issues have been presented. Firstly, the governing equations of smart laminated beams, which include the charge equation, are derived and

evaluated. The formulations of the output voltage from sensor and input voltage acting on actuator have been clearly expressed. Secondly, the significant idea of this thesis is to, creatively introduce a mathematical tool - complex numbers, to simplify the governing equations. This is the first presentation of this form. Finally, the approximate analytical solutions of smart laminated composite beams have been derived by using software package MATLAB. The graphical outputs are generated using the software package MATHEMATICA. From these graphical results, the experiential formulation of the amplitude of beam vibration and negative velocity feedback control gain has also been evaluated.

This thesis includes five chapters. Chapter 1 is the background of smart structures. The constitutive equation of smart laminated beams is introduced in chapter 2. In chapter 3, we will discuss the governing equations of smart composite beams. Approximate analytical solutions of smart composite beams are derived in chapter 4 and the results and discussions are included in chapter 5.

Table of Contents

Chapter 1

Introduction

1.1 Background of Smart Composite Materials and Structures

Composite materials consist of two or more different materials that form regions large enough to be regarded as continua and which are usually firmly bonded together at the interface. Many natural and artificial materials are of this nature, such as: reinforced rubber, filled polymers, mortar and concrete, alloys, porous and cracked media, aligned and chopped fiber composites, polycrystalline aggregates (metals), etc.

Analytical determination of the properties of composite materials originates with some of the most illustrious names in science. J. C. Maxwell in 1873 and Lord Rayleigh in 1892 computed the effective conductivity of composites consisting of a matrix and certain distributions of spherical particles. Analysis of mechanical properties apparently originated with a famous paper by Albert Einstein in 1906 in which he computed the effective viscosity of fluid containing a small amount of rigid spherical particles. Until about 1960, work was primarily concerned with macroscopically isotropic composites, in particular, matrix/particle composites and also polycrystalline aggregates. During this period the primary motivation was scientific. While the composite materials investigated were of technological importance, a technology of composite materials did not as yet exist. Such a technology began to emerge about 1960 with the advent of modern fiber composites consisting of very stiff and strong aligned fibers (glass, boron, carbon, graphite) in a polymeric matrix and later also in a light weight metal matrix.

The engineering significance of reliable analysis of properties is quite different for particulate composites and for fiber composites. For the former, such capability is desirable, while for the latter it is crucial. The reason is that the range of realizable properties and the ability to control the internal geometry are quite different in two cases. For example: the effective Young's modulus of an isotropic composite consisting of matrix and very much stiffer and stronger spherical type particles will depend primarily on volume fractions and can be increased in practice only up to about four-five times the matrix modulus. The strength of such a composite is only of the order of the matrix strength and may even be lower. The effect of stiffening and strengthening increases if particles have elongated shapes but at the price of lowering the maximum attainable particle volume fraction.

A unidirectional fiber composite is highly anisotropic and therefore has many more stiffness and strength parameters than a particulate composite. Stiffness and strength in the fiber direction are of fiber value order, and thus very high. Stiffnesses and strengths transverse to fiber direction are of matrix order, similar to that of a particulate composite, and thus much lower. Carbon and graphite are themselves significantly anisotropic, their elastic properties being defined by five numbers instead of the usual two for an isotropic material. Furthermore, matrix properties may be strongly influenced

by environmental changes such as heating, cooling, and moisture absorption. All of this creates an enormous variety of properties, of a much wider range than for a particulate composite.

The generally low values of stiffness and strength transversely to the fibers provide the motivation for *laminate* construction consisting of thin unidirectional layers with different reinforcement directions. The laminates are formed into laminated structures. The layer thickness, fiber directions, choice of fibers, and matrix are at the designers disposal and should, ideally, be chosen from the point of view of optimization of such structures is an integrated process leading from constituents to structure in the sequence: FIBERS AND MATRIX → UNIDIRECTIONAL COMPOSITE → LAMINATE → LAMINATED STRUCTURE.

Traditionally, material properties have been obtained by experiment and material improvement has been achieved empirically and qualitatively. The structural designer had at his disposal a limited number of material options provided by the materials developer. This situation is entirely different for fiber composite structures. The only constituents that are materials in the traditional sense are fibers and matrix. Everything following in the sequence, including the unidirectional material, is of such immense variety that analysis, rather than experimentation, is the practical procedure to obtain properties. Thus, the relevant methods are those of applied mechanics rather than those of materials science.

Normally, the analysis of composite materials include the following properties of various kinds of composite materials: elasticity, thermal expansion, moisture swelling, viscoelasticity, conductivity (which includes, by mathematical analogy, dielectrics, magnetics, and diffusion), static strength, and fatigue. The other two important subjects are plasticity of composite materials, and dynamic behaviour and wave propagation in composites. In the above statement, the subjects of strength and failure of composite materials are of special nature. Engineering design requirements have motivated an immense literature much of which is confined to unpublished reports. At the same time the problem are of such difficulty that an analytical definition and/or solution has not been achieved in many cases and therefore much of the available work is of semiempirical nature. The many important problems that require analytical solution continue to be a primary challenge in composite materials research.

- **Smart Materials and Structures**

The history of science of materials from its conception in paleolithic times through the Stone Age, the Bronze Age and Iron Age to the current Synthetic Materials Age and beyond to the Smart Materials Age is pictorially chronicled in Figure 1.1. A review of the historical evolution of this science is presented in Figure 1.2 which highlights the distinct transition from structural materials to functional materials; and now smart materials; as humankind's scientific and technological prowess has matured.

Structural materials are those materials that are principally characterized by their mechanical strength and are generally employed in load-bearing situations. Consequently some one million years ago *Homo Habilis* selected flint as the most appropriate material for tools and weapons because it was structurally superior to other natural materials available such as bone and wood. Similarly aeronautical engineers in

the 1990s will design the load-bearing members of advanced fighter aircraft in polymeric fiberous composite materials, because they possess structural properties which are substantially superior to those of the monolithic structural materials.

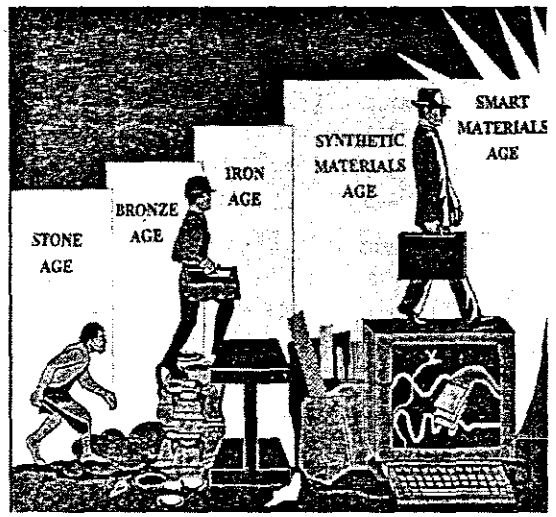

Figure 1.1 The eras of materials science [19]

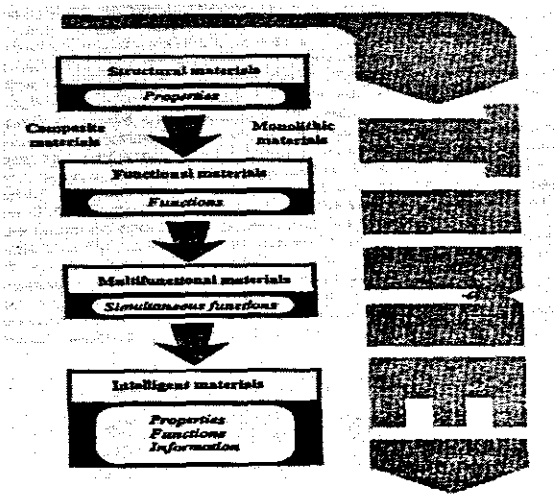

Figure 1.2 Evolution of materials science [19]

The most sophisticated class of smart materials and structures are currently based upon notions of biomimetics, and feature appropriately configured actuators, sensors, signal-processing capabilities and control algorithms which enable the materials to respond actonomously to external stimuli. Smart materials will have the capability to select and execute specific functions intelligently in response to changes in environmental stimuli. This ability may be complemented by several other capabilities that are characteristic of intelligent system, such as self-diagnosis, self-repair, self-multiplication, self-degradation, and self-learning. Furthermore, these features may be augmented by capabilities for anticipating future challenges and missions and the ability to recognize and discriminate. It is clearly evident, therefore, that all aspects of our lives will be significantly touched as the development of smart materials impacts industries as diverse as automotive, aerospace, defense, biomedical devices, advanced manufacturing, robotics, industrial machinery, sporting goods, high-precision instruments, highways, buildings and bridges.

These material functions of structure, actuator and sensor are currently incorporated into a smart structure in a discrete global sense. Thus, for example, a generation smart structure might feature a load-bearing graphite-epoxy, fiberous polymeric structural materials, in which piezoelectric discs are embedded for sensing and actuation purposes. Research is currently being pursued on embedding these material functions of sensor, actuator, and structure at a much more local level. These generation of smart materials and structures incorporate one or more of the following features:

1. *Sensors* which are either embedded within a structural material or else bonded to the surface of that material. Alternatively the sensing function can be performed by a functional material which, for example, measures the intensity of the stimulus associated with a stress, strain, electrical, thermal, radiative, or chemical phenomenon. This functional material may, in some circumstances, also serve as a structural material.

2. *Actuators* which are embedded within a structural material or else bonded on the surface of the material. These actuators are typically excited by an external stimulus, such as electricity in order to either change their geometrical configuration or else change their stiffness and energy-dissipation properties in a controlled manner. Alternatively, the actuator function can be performed directly by a hybrid material which serves as both a structural material and also as a functional material.

3. *Control capabilities* which permit the behaviour of the material to an external stimulus according to a prescribed functional relationship or control algorithm. These capabilities typically involve one or more microprocessors and data transmission links which are based upon the utilization of an automatic control theory.

Materials with the above features are indeed worthy of being described by the adjective "smart", as defined by *Webster's Third International Dictionary of the English Language*, which states that the meaning of 'smart' is: *having or showing mental alertness and quickness of perception, shrewd informed calculation, or contrived resourcefulness, marked by or suggesting brisk vigor, speedy effective activity, or spirited-liveliness*. Clearly, materials featuring control capabilities possess 'mental alertness', and some will certainly be 'informed' and 'resourceful' within specified limitations. Materials featuring sensing characteristics have the opportunity to demonstrate an 'informed' response along with 'quickness of perception'. Finally, materials featuring actuator functions possess 'spirited-liveliness' characteristics. Thus 'smart' materials clearly exist today in the arsenal of weapons for deployment by the materials scientist. We also can call the 'smart materials and structures' as 'intelligent materials and structures'. But actually, the 'intelligent' materials are an order of magnitude more sophisticated than smart materials because 'intelligence' is associated with learning, abstract thought, and the ability to think and reason. These capabilities have not been demonstrated at this time and they shall be the focus of much research and development during the coming decades.

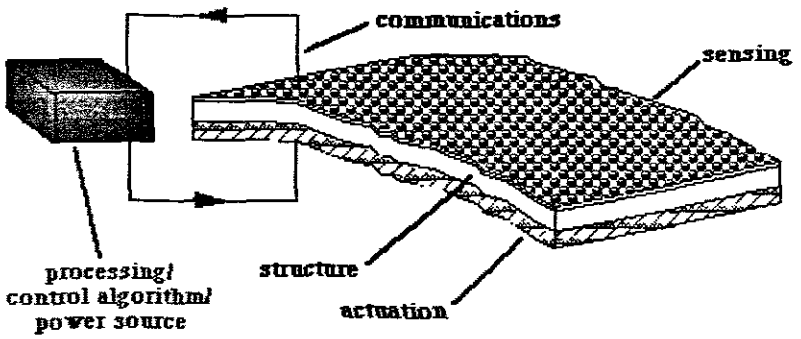

Figure 1.3 The loop control system of smart structure

- **Smart Control System**

The previous sections have been devoted to the discussion of the definition of smart materials and structures and its features. The next section, which will be discussed here, is a control system featuring computational capabilities, in order to orchestrate the

behaviour of the actuators in smart structure in response to the excitation data furnished by the sensors embedded in the smart structure. The smart structure loop control system is shown in Figure 1.3. The field of automatic control is a mature discipline, consequently, comprehensive literature on linear, nonlinear, adaptative, and optimal control system is relevant to the synthesis of viable smart structures featuring intelligent control system. To the knowledge-domain of automatic control, the designer of smart materials must consider adjoining theory and knowledge from the embryonic fields of artificial intelligence and neural networks. These fields embody notions of biomimetics, as with many other sub-fields of the smart materials discipline. Neural networks mimic the structure and capabilities of the human brain where approximately 12×10^9 nerve cells, or neurons, each have between 6000 and 60 000 dendritic connections with a signal carrying capacity. Furthermore, each processing element of neural network is relatively simple, and because of the parallel structure of the network, the computational time for complex problem is very fast. This is especially true where approximate solutions are acceptable wherein rules of fuzzy logic can be exploited.

Networks feature unstructured decision making logic while being devoid of the precise rule-based computer program characteristics of expert systems. Furthermore, every decision is the result of complex interactions between the interconnected network of processors, and the neural network features self-learning characteristics because it incorporates previous experiences into the interconnection patterns of neurons.

In this project, the active vibration control is the main objective of this research. The following description is the simple introduction of vibration control of smart structures by using neural networks. Many advanced systems are often required to be stiffer, lighter, and have sufficient damping for high precision pointing accuracy. These performance requirements have motivated a new approach in structural control: smart structures with build-in sensors and actuators that can actively and adaptively change their physical geometry and properties. Recent research has focused on the applications of piezoelectric sensor and actuator in smart structures. Crawley and de Luis (1987) were among the first to embed piezoelectric materials in composite laminated beams. Yang and Chiu (1993) also developed the manufacturing technique for composite structures with embedded piezoelectric sensors and actuators. Effective applications in vibration control, however, require that the system dynamics can be adequately and/or accurately determined and that controller design can be easily implemented. Vibration control of smart structures using neural networks has thus been receiving attention for their advantages in self-learning, fault tolerance, and parallel processing. Snyder and Tanaka (1993) developed a nonlinear feedforward controller for smart structures, and they showed that the neural network is essentially a transversal filter with a nonlinear hidden layer between the input and output. Bryant et al. (1993) presented a neural network model for the vibration isolation of a three-leg table by magnetostrictive terfenol actuators. Chen et al (1994) numerically investigated the vibration control of a cantilevered beam by using modified independent modal space control with a neural network state estimator. Damle et al (1994) also implemented a neural network for the identification of a clamp-free beam; model reference adaptive control with a shape memory alloy actuator was then applied in the later work (Rao et al., 1994). Clark (1994) analyzed the relationship between velocity feedback and the monosynaptic pathway of the central nervous system by using a simply supported beam with a pair of piezoelectric sensor and actuator. Zeinoun and Khorrami (1994) also proposed a fuzzy-

logic algorithm for vibration suppression of a clamp-free beam with piezoelectric sensor/actuator.

Although there has been much work on the active control of structural systems, the implementation of neural networks for vibration suppression of composite smart structures is still very limited. Mathematical and numerical analysis of this concept is presented in this research work. The experimental research and validation of this analysis will be included towards a PhD study.

This section presents an overview and assessment of technology leading to the development of smart structures. Smart structures are those which incorporate actuators and sensors that are highly integrated into the structure and have structural functionality, as well as highly integrated control logic, signal conditioning, and power amplification electronics. Such actuating, sensing, and signal processing elements are incorporated into a structure for the purpose of influencing its states or characteristics, be they mechanical, thermal, optical, chemical, electrical, or magnetic. For example, a mechanically intelligent structure is capable of altering both its mechanical states (its position or velocity) or its mechanical characteristics (its stiffness or damping). An optically intelligent structure could, for example, change color to match its background.

Smart structures are a subset of a much larger field of research, as shown in Figure 1.4. Those structures which have actuators distributed throughout are defined as adaptive or, alternatively, actuated. Classical examples of such mechanically adaptive structures are conventional aircraft wings with articulated leading- and trailing-edge control surfaces and robotic systems with articulated manipulators and end effectors. More advanced examples currently in research include highly articulated adaptive space cranes.

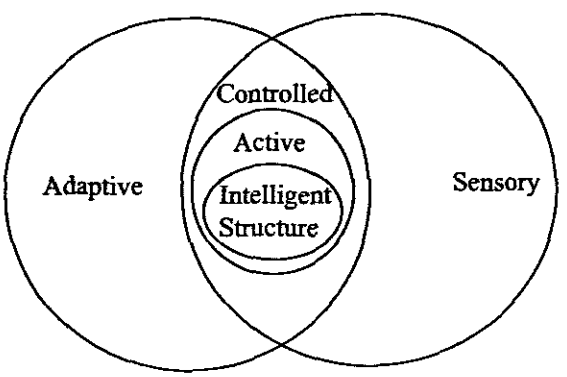

Figure 1.4 Intelligent structures as a subset of active and controlled structures

Structures which have sensors distributed throughout are a subset referred to as sensory. These structures have sensors which might detect displacements, strains or other mechanical states or properties, electromagnetic states or properties, temperature or heat flow, or the presence or accumulation of damage. Applications of this technology might include damage detection in long life structures, or embedded or conformal RF antennas within a structure. The smart structures which contain both actuators and sensors (implicitly linked by closed-loop control) are referred to as controlled structures. Any

structure whose properties or states can be influenced in this category. A subset of controlled structures is active structures, distinguished from controlled structures by highly distributed actuators which have structural functionality and are part of the load bearing system. Also, smart structures are a subset of active structures that have highly distributed actuator and sensor systems with structural functionality and, in addition, distributed control functions and computing architecture. To date, such intelligent structures have not been built. The ultimate realization of intelligent structures is a goal which has motivated this technology assessment.

For the development background of smart structure, there are three historical trends which have combined to establish the potential feasibility of smart structures. The first is a transition to laminated materials. In the past, structures were manufactured from large pieces of monolithic material which were machined, forged, or formed to a final structural shape, make it difficult to imagine the incorporation of active elements. However, in the past 30 years a transition to laminated material technology has occurred. Laminated materials, which are built up from smaller constitutive elements, allow for the easy incorporation of active elements within the structural form. One can now envision the incorporation of an intelligent ply carrying actuators, sensors, processors, and interconnections within the laminated materials.

Exploitation of the off-diagonal terms in the material constitutive relations is a second trend which enables intelligent structures at this time. The full constitutive relations of a material include characterizations of its mechanical, optical, electromagnetic, chemical, physical, and thermal properties. For the most part, researchers have focused only on block diagonal terms. Those interested in exploiting a material for its structural benefits have focused only on the mechanical characterization, and those interested in exploiting its electrical properties have focused on the electrical characterization. However, much can be gained by exploiting the off-diagonal terms in the constitutive relations which, for example, couple the mechanical and electrical properties. The characterization and exploitation of these off-diagonal material constitutive relations has led to much of the progress in the creation of intelligent structures.

The third and perhaps most obvious comes in the electrical engineering and computer science disciplines. These include the development of microelectronics, bus architectures, switching circuitry, and fiber optic technology. Also central to the emergence of intelligent structures is the development of information processing, artificial intelligence, and control disciplines.

The sum of these three evolving technologies (the transition to laminated materials, the exploitation of the off-diagonal terms in material constitutive relations, and the advances in microelectronics) has created the enabling infrastructure in which intelligent structures can develop.

There are four component technologies critical to the evolution and application of intelligent structures: actuators for intelligent structures, sensory elements, control methodologies and algorithms, and controller architecture and implementation hardware. Advances in these component technologies must be matched by a cost effective manufacturing technology which allows for the incorporation of the active elements and interconnections onto or into the structure in a structurally robust manner

and in such a way that the inherent properties of the host structure are not degraded. The requirements, capabilities, and manufacturability of four component technologies for mechanically intelligent structures are discussed in this section.

- **Actuator for Intelligent Structures**

Actuator for intelligent structures must be capable of being highly distributed and influencing the mechanical states of the structure. The ideal mechanical actuator would directly convert electrical inputs into strain or displacement in the host structures. Its primary performance parameters include its maximum achievable stroke or strain, stiffness, and bandwidth. Secondary performance parameters include linearity, temperature sensitivity, strength, density, and efficiency. These properties will be assessed and compared for several types of strain actuators.

The principal actuating mechanism of strain actuators is referred to as actuation strain, which is the controllable strain not due to stress. Actuation strains are produced by a variety of phenomena, with the most common but least controllable being temperature and moisture absorption. Other examples, less common but more useful for active control, include piezoelectricity, electrostriction, magnetostriction, and the shape memory effect.

- **Sensory Elements**

Sensory elements of intelligent structures must be sensitive to the mechanical states of the structure and capable of being highly distributed. The ideal sensor for intelligent structure converts strain or displacement (or their temporal derivatives) directly into electrical outputs. The primary functional requirements for such sensors are their sensitivity to the strain or displacement (or their time derivatives), spatial resolution, and bandwidth. Secondary requirements include the transverse and temperature sensitivity, linearity and hysteresis, electromagnetic compatibility, and size of sensor packaging. Although actuators are so large they must be explicitly accommodated in the built-up laminates, it is desirable to make sensors small enough to be placed in interlaminar or otherwise unobtrusive positions.

- **Control Methodologies and Algorithms**

The real intelligent structures stem from their highly distributed control functionality. There are three levels of control methodology and algorithm design which must be considered for smart structures: local control, global algorithms control, and higher cognitive functions. The objectives of local control are to add damping and/or absorb energy and minimize residual displacements. The objectives of global algorithmic control are to stabilize the structure, control shapes, and reject disturbances. These two levels are achievable within the current technology. In the future, controller with higher cognitive functions will have objectives such as system identification, identification and diagnosis of component failures, the ability to reconfigure and adapt after failures, and eventually to learn.

- **Controller Architecture and Implementation Hardware**

The presence of actuators, sensors, and highly distributed control functionality throughout the structure implies that there must be a distributed computing architecture.

The functional requirements for such a computing architecture include a bus architecture, an interconnection scheme, and distributed processing. The bus architecture should be chosen to yield a high transmission rate of data in convenient (probably digital) form throughout the structure. The interconnections must be suitable for connecting a (potentially) large number of devices, actuators, sensors, and processor with the least degradation of structural integrity. If the actuators and sensors are embedded within the structure, the interconnections should also be embedded within the structure to avoid the necessity of running the electrical connections through otherwise structurally important plies. The processing requirements are that the full functionality (signal conditioning, amplification, digital/analog (D/A) and analog/digital (A/D) conversion, and digital computation) be distributed throughout the structure. Secondary requirements for the computing architecture include minimizing electromagnetic interference, maintaining the mechanical strength and longevity of the structure and of the electronics components, and thermal chemical compatibility of electronic components within the host structure.

- **Application for Smart Structures**

A wide variety of application exist for smart structures technologies. Despite the fact that truly intelligent structures (i.e., those with embedded controllers as well as actuators and sensors) have not yet been built, a number of experimental implementations of active structures (i.e., those with distributed actuators and sensors) have been successfully demonstrated. Notable experimental implementations include aeroelastic control and maneuver enhancement, reduction of vibration and structure borne noise and acoustic transmission, jitter reduction in precision pointing system, shape control of plates and mirrors, trusses and lifting surfaces, isolation of offending machinery and sensitive instruments, and robotic control. To understand the potential and limitations of current technology, four examples found in the recent literature are discussed subsequently: the aeroservoelastic control of a lifting surface, precision control of truss, seismic control of building, and the control of radiated sound.

In the first example, a typical high performance aircraft-like wing was built of a graphite epoxy laminate with piezoelectric actuators distributed over 71% of its surfaces. The actuators were arranged into three banks which consisted of the vertical strips shown in Figure 1.5. The actuators were wired so as to induce bending in the laminate. Three tip displacement measurements were used for feedback. The controller implemented was a reduced order, 14-state, LOG controller. The control objective was gust disturbance rejection and flutter suppression. Shown in Figure 1.6 are the analytically predicted and experimentally measured open- and closed-loop transfer functions from disturbance to tip displacement. As can be seen, the static response of the structure was reduced by almost 10 dB, which corresponds to approximately a threefold stiffening in the structure due to the application of the closed-loop control. The first mode was virtually eliminated from dynamic consideration, being reduced 30 dB from an initial 1% damping. The second mode, which was torsional, was less strongly influenced, with a 10 dB reduction. This was due to the fact that this mode was less controllable than the first or third mode. The third mode achieved a 20 dB reduction. Overall the rms response in bandwidth up to 100 Hz was reduced by 15.4 dB. This is an example of the relatively high gain control which can be introduced into a structure, and is probably the largest control authority which has yet been reported on a structural test article in experimental implementation.

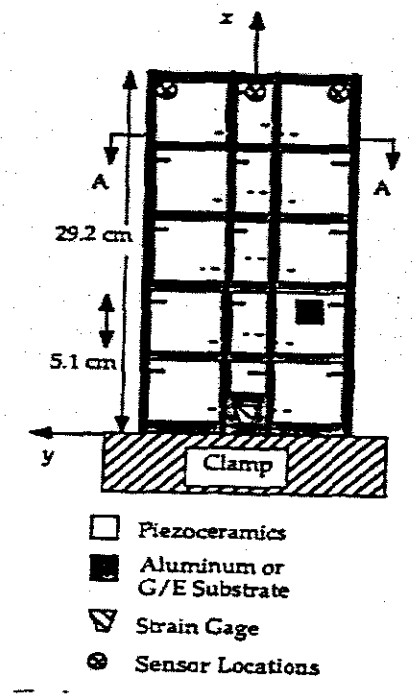

Figure 1.5 Active aeroservoelastic wing [14]

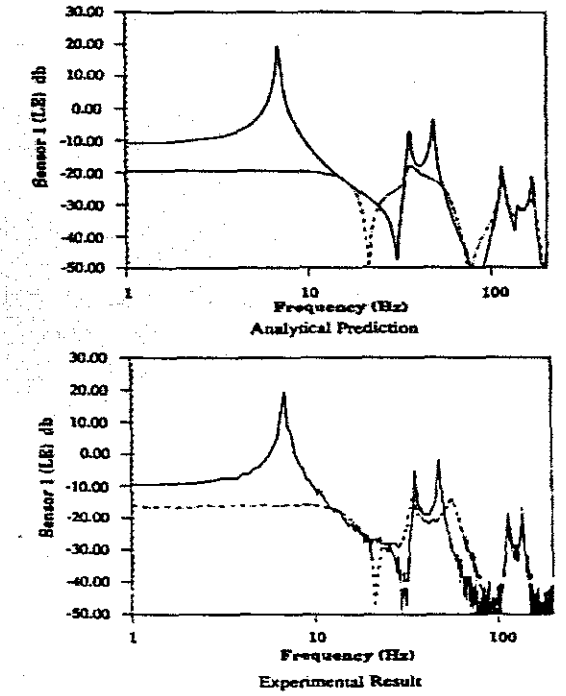

Figure 1.6 Comparison of analytical prediction and experimental results of the open (solid) and closed loop (dashed) for bench top testing of the active wing [14]

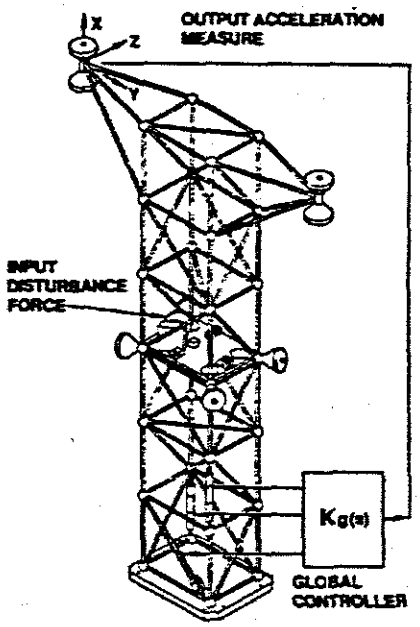

Figure 1.7 Precision truss with dial-a-strut [14]

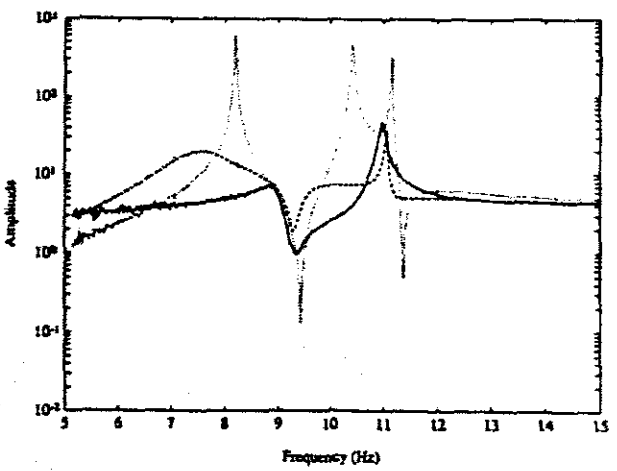

Figure 1.8 Open loop (dotted) vs closed loop for one (dashed) and two (solid) dial-a-struts [14]

The second example of a prototypical intelligent structure is the 'dial-a-strut' or locally controlled strut, which is part of a precision control truss experiment (Figure 1.7). In this case, the structure contains two active piezoelectric struts. Each strut has a collocated displacement and force feedback. By making measurements of the collocated

displacement and force, the previously described localized optimal impedance matching can be implemented. The control objective of this experiment was rejection of disturbances due to onboard machinery, typical of a jitter reduction task in precision interferemetric spacecraft. Figure 1.8 shows typical transfer functions (open loop and closed loop) for one and two of the dial-a-struts. By comparing the open-loop and two strut closed-loop responses, it can be seen that the first and second structural modes were significantly modified. Both the first and second mode response was reduced by 40 dB from an initial structural damping of a few tenths of a present. Thus, the local collocated approximation to the optimal noncausal controller is seen to achieve good performance in a realistic structural configuration.

The seismic control of buildings is a considerably larger scale application of smart structure. Experiments were performed on a model building with a simulated large earthquake disturbance (Figure 1.9). Control was effected by an active shear brace incorporated into the structure. Five transverse accelerometers were used to monitor the control response of the structure, and two were used for feedback control. The control objective was to minimize building acceleration in response to the disturbance. Figure 1.10 shows the building excitation with the control system. As a result of the closed-loop control, the damping factor was increased from nearly zero to 20% in the first three modes, with significant reduction in the low frequency response.

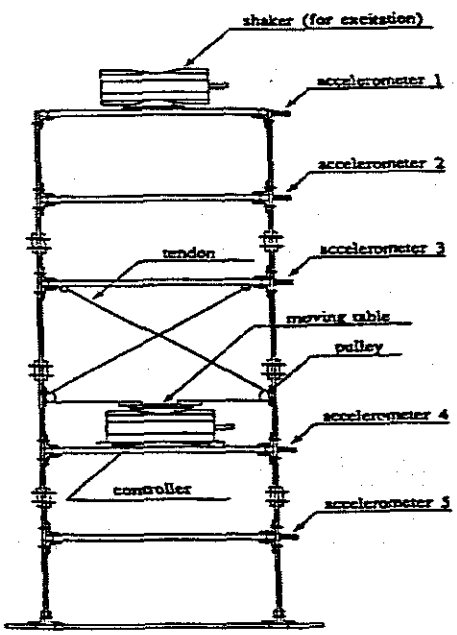

Figure 1.9 Building model for controlled seismic response [14]

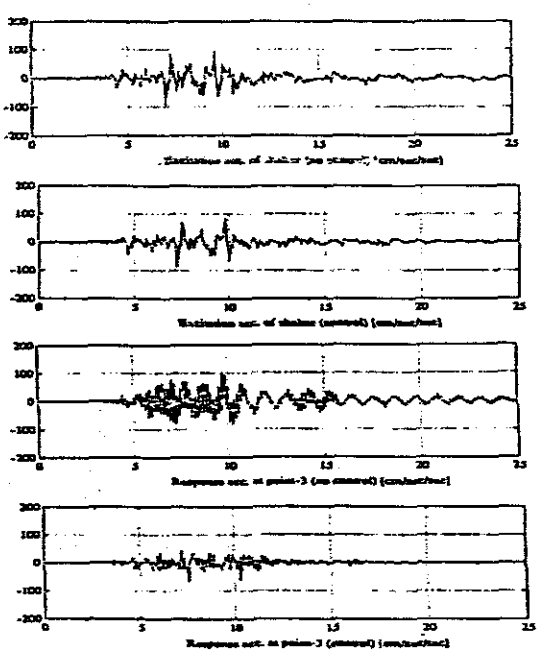

Figure 1.10 Comparison of open-loop response of midbuilding accelerometer under simulated seismic excitation [14]

The final example considers the reduction of sound radiated into a room or aircraft cabin by active control of shell-like members which form the walls. To simulate this situation, a rectangular plate was placed inside a test chamber. The plate was controlled by three piezoceramic actuators placed as shown in Figure 1.11. Two PVDF piezoelectric film sensors were used to measure the vibration of the plate. The excitation

source was an electromagnetic shaker which drove the plate at known frequency corresponding to, for example, the excitation of aircraft cabin wall from the rotation of an external propeller at a known rpm. In these cases, adaptive least-mean-square algorithms are likely candidates for control scheme. These schemes make use of knowledge of frequency at which the primary excitation is occurring. The control objective in this example was narrow-band reduction of the radiated far-field noise.

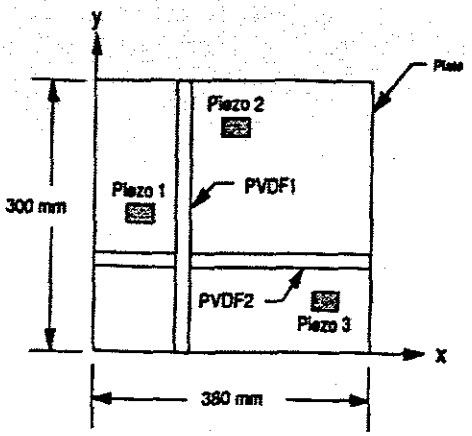

Figure 1.11 Actively controlled panel for control of sound radiation [14]

These four examples are but a few of the cases in which investigators throughout the world are now applying distributed actuation and sensing to a wide variety of control problems. It is encouraging that these early experiments show not only the feasibility of intelligent structures applications show not only the feasibility of smart structures application but also remarkably good agreement between theory and experimental result as well. Of course, further experimentation is necessary to establish the technological limitations as well as feasibility of distributing the processing and control architectures.

- **Anticipated Research and Development**

In the next decades, it is expected that there will be widespread application of the technology under development, in its current and evolutionary forms. The breadth of application of this technology is expected to not only span the aerospace industry but become widespread in the construction, automotive, and machine tool industries as well.

In the more distant future, the evolution of new physical-bio-logical technology is anticipated. This technology will have two trends which are complementary. The first is the natural evolution of the technology discussed earlier: the introduction of intelligence into the physical world, by the application of machine electronic intelligence to otherwise unintelligent devices. The second is more revolutionary: the introduction of life into engineering application, i.e., the application of biological processes to the solution of engineering problems. Much as the steam engine drove the technology of the 19^{th} century and electronics drove the technology of the 20^{th} century, one can envision that the application of biological concepts to engineering will drive the technology of the 21^{st} century. Engineering will cease to be the application of only the physical sciences for the betterment of mankind and become the application of all sciences, including both physical and life sciences, for the betterment of humanity.

1.2 Theoretical Background of Composite laminates

A composite laminae is a building block for laminates. Lamina are bonded together to form a laminate with the desired thickness and stiffness. In most applications, the thickness of a laminae is small compared to the planar dimensions (*i.e.*, the side-to-thickness ratio of a laminate is greater than 20). Therefore, laminate theories based on equivalent two-dimensional descriptions are used to analyze laminated composite structures. The two-dimensional theories, termed *equivalent-single layer theories*, are obtained from the three-dimensional elasticity theory by making assumptions concerning the variation of displacements and/or stresses through the thickness of the laminae.

In the *classical laminated plate theory* (CLPT), which is an extension of the classical plate theory to laminated plates, the inplane displacements are assumed to vary linearly through the thickness and the transverse displacement is assumed to be constant through the thickness. The classical laminate theory is found to be adequate for most applications where the thickness of laminate is small, by two orders of magnitude compared to the inplane dimensions. When the classical laminate theory is not applicable, a refine theory that accounts for the transverse shear strains is used. The *first-order shear deformation theory* (FSDT) accounts for constant state of transverse shear strains through the thickness. There are higher-order, equivalent-single-layer shear deformation theories as well as layerwise theories, which are not covered in this project.

- **The Classical Laminated Plate Theory (Kirchhoff Plate Theory)**

The classical laminated plate theory is an extension of the classical plate theory of plates to laminated composite plates. In the classical plate theory one assumes that straight lines perpendicular to midplane before deformation remain (1) straight, (2) inextensible, and (3) normal to the midplane after deformation. These three assumptions, collectively known as the *Kirchhoff-Love Hypothesis*, lead to zero transverse shear strains (ε_{xz}, ε_{yz}) and transverse normal strain (ε_{zz}). Since the (virtual) work done by the actual internal forces of the plate in moving through the virtual displacements is the product of forces associated with the stress field and the (virtual) displacements, which result in (virtual) strains, the (virtual) work done by the transverse stresses is zero because of the zero transverse (virtual) strains. Consequently, transverse stresses σ_{xz}, σ_{yz} and σ_{zz} do not contribute to the equations of motion. This amounts of omitting the transverse stresses in the classical laminated theory. This is equivalent to, from a physical point of view, assuming that the plate is 'infinitely' rigid in the transverse direction. When plates are very thin, this assumption is not so bad as it may appear on the surface.

Consider a laminate of total thickness h composed of N orthotropic layers. A typical lamina, say the kth layer ($k = 1,2, \ldots L$), has a uniform thickness h_k, material properties E_1^k, E_2^k, etc., and its principal material coordinates oriented at an angle $\theta = k$ to the laminate (global) coordinate, x. For the classical laminated plate theory, as mentioned before, the following assumptions have been made:

(a) The layers are perfectly bonded together,
(b) The material of each layer is linearly elastic and has three planes of material symmertry (*i.e.*, orthotropic),
(c) Each layer is uniform thickness,

(d) The strains are small, and
(e) The Kirchhoff-Love hypothesis holds.

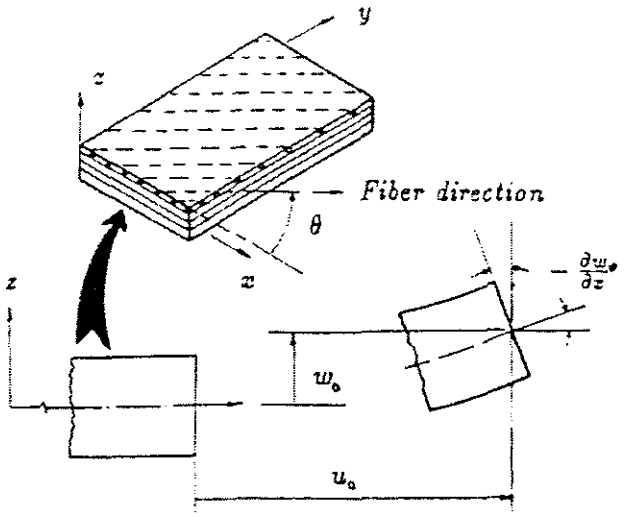

Figure 1.12 Bending of laminated plates under the Love-Kirchhoff hypothesis

The laminate coordinate system is chosen such that the xy-plane coincides with the midplane of the laminate. Although this is not necessary, it makes the derivations simple and consistent with the approach taken in a vast majority of the literature. The assumptions of the Kirchhoff hypothesis require that the displacements (u, v, w) be such that (see Figure 1.12)

$$\begin{aligned} u(x,y,z,t) &= u_0(x,y,t) - z\frac{\partial w_0}{\partial x}(x,y,t) \\ v(x,y,z,t) &= v_0(x,y,t) - z\frac{\partial w_0}{\partial x}(x,y,t) \\ w(x,y,z,t) &= w_0(x,y,t) \end{aligned} \tag{1.1}$$

where (u_0, v_0, w_0) is the displacement of a point on the xy-plane (or midplane), and t denotes time.

It is important to note that, in modelling a laminated plate composed of multiple layers of possibly dissimilar-material layers, we tacitly assume that the strains are continuous through the thickness, including the interfaces of dissimilar-material layers. This assumption plays a significant role in the developing laminate theories; it allows us to replace a laminate with an equivalent single layer with material coefficients which are averaged over the laminate thickness.

- **The First-Order Shear Deformation Theory (Mindlin Plate Theory)**

The classical plate theory is adequate for the analysis of thin laminates, especially when the transverse deformation is negligible. However, laminates made of advanced fiber-reinforced composite materials, whose elastic to linear modulus ratio (E_1/G_{13} and E_1/G_{23}) are very large, are susceptible to thickness failures because their effective transverse shear moduli (G_{13} and G_{23}) are significantly smaller than the effective moduli

(E_1) along the fiber direction. Although the transverse shear and normal stresses (σ_{xz}, σ_{yz}, σ_z) are an order of magnitude smaller than the inplane stresses (σ_x, σ_y, σ_{xy}), the material strength allowables for the transverse stresses are also an order of magnitude smaller than the allowables for the inplane stresses. Thus, the classical laminate theory mentioned here is not to be used for composites that are likely to fail in transverse shear or delamination.

The most widely used displacement based on shear deformation theory is the first-order shear deformation theory, which is also called Mindlin plate theory. In this theory the normality condition of the Kirchhoff-Love hypothesis is removed, allowing for independent rotation of transverse normals. Thus, the straight line normal to the midplane of laminate remains straight and inextensible after deformation, but it does not necessarily remain perpendicular to the midsurface. Thus, the displacement field of the first-order deformation theory is assumed to be of the form

$$\begin{aligned} u(x,y,z,t) &= u_0(x,y,t) - z\psi_x(x,y,t) \\ v(x,y,z,t) &= v_0(x,y,t) - z\psi_y(x,y,t) \\ w(x,y,z,t) &= w_0(x,y,t) \end{aligned} \tag{1.2}$$

where ψ_x and ψ_y are rotations of the transverse normal about the y-axis and x-axis, respectively.

In this project, the first-order shear deformation theory (Mindlin plate theory) will be used to develop a set of the governing equations of smart composite laminate beams (see Chapter 2). The laminate constitutive equations of smart composite structures will be introduced in Chapter 2.

As we know, the stiffness of laminated structure can be affected by the laminated stacking sequence. This is significant to design analysts. Here, it is useful to discuss the terminology and notation used in connection with lamination schemes or stacking sequences. The lamination scheme of a laminate can be denoted by [α/β/90/-α/0/...], where α is the orientation of the first ply, β is the orientation of the second ply, and so on. The plies are counted in the positive z direction (see Figure 1.12). Unless stated otherwise, this project also implies that all layers are of the same thickness and mode of the same material. A general laminate has layers of different orientations θ where -90°≤ $\theta \leq 90°$. *Angle-ply* laminates have ply orientations of θ or -θ where $0° \leq \theta \leq 90°$, with at least one layer having an orientation other than 0° 90°. *Cross-ply* laminates are those which have ply orientations of 0° or ± 90°. The effect of some special cases of lamination scheme of laminates with four and eight layers will be discussed in Chapter 5, such as *Symmetric laminates with isotropic layers*, *Symmetric laminates with specially orthotropic layers*, *Symmetric laminates with generally orthotropic layers*, *Antisymmetric cross-ply laminates*, *Antisymmetric cross-ply laminates* and *nonsymmetric laminates*, and so on.

1.3 Review

Advanced structures with integrated self-monitoring and control capabilities are increasingly becoming important due to the rapid development of 'intelligent' space

structures and mechanical systems. Since these structures are, in general, distributed and flexible in nature, distributed dynamic measurement and active vibration suppression are essential to their performance. Vibration suppression and control of distributed parameter system (e.g., beams, plates and shells) always represents a challenge, both in theory and practice. Theoretical development has been constantly advanced in the past 20 years. However, due to the limitation of materials and actuator design, practical application of theory to general distributed parameter systems will need to be further explored.

Due to the increasing demands of high structural performance requirement and the coupled mechanical and electrical properties, the modelling and control of light weight composite structures with embedded or surface-mounted piezoelectric materials in structures have attracted a considerable amount of research in recent years. One reason for this is that it may be possible to create certain types of structures and systems capable of adapting to or correcting for changing operating conditions. The rapid developments in space exploration have reached a level which calls for a departure from the conventional control approaches in order to satisfy the stringent system performance requirements, such as pointing and displacement requirements, set forth for space structures. The advantage of incorporating these special types of material into the structure is that the sensing and actuating mechanism becomes part of the structure by sensing and actuating strains directly. Active control counters undesirable forces by auxiliary mechanisms such as sensors, actuators and feedback controllers. Piezoelectric materials, which exhibit mechanical deformation when an electric field is applied and conversely, generate a change in response to mechanical deformation, can be used as actuators and sensors, respectively. By employing piezoelectric materials, it is feasible to achieve accurate response monitoring and effective control of flexible structures. This advantage is especially apparent for structures that are deployed in aerospace and civil engineering. In view of these advantages and characters, researching mechanical characters of smart structures vibration and its control methodology is becoming very important.

Polyvinylidene fluoride (PVDF) was initially discovered by Kawai in 1969. Raw polymetric PVDF (α-phase) is an electrical insulator and it does not have any intrinsic piezoelectric properties. If the raw material is polarized during the manufacturing process, PVDF transforms to β-phase – a tough and flexible semi-crystalline material and it can be made to strain either in one or two directions in the film plane. Since β-phase PVDF possesses a strong direct piezoelectric effect, it has been in many transducer applications: e.g., sonar, medical ultrasonic equipment, robot tactile sensors, acoustic pick-ups, forces and strains gages, etc. Due to its distinct characteristics, such as flexibility, durability, manufacturability, etc., PVDF is an ideal material for the distributed sensing and vibration suppression/control of distributed parameter systems (e.g., beams, plates, shells, etc.).

In order to utilize the strain-sensing and actuating properties of piezoelectric materials, the interaction between the structure and SSA (strain sensing and actuating) material must be well understood. There have been many theories and models proposed for analysis of laminated composite beams and plates containing active and passive piezoelectric layers. Bailey and Hubbard (1985) designed a distributed-parameter actuator and control theory. They used the angular velocity at the tip of cantilever

isotropic beam with constant-gain and constant-amplitude negative velocity algorithms and experimentally achieved vibration control. Hangud et al. (1985) presented a procedure, combining theory and experiments, to quantify the effects of an active feedback system on the damping matrix of an isotropic beam. Mechanical model for studying the interaction of piezoelectric patches surface-mounted to beams have been developed by Crawley and de Luis (1987), Im and Atluri (1989), and Chandra and Chopra (1993). The study presented here is different from these in that we study laminated beams containing piezoelectric laminae. The strain sensing and actuating (SSA) lamina can offer both discrete effects similar to patches as well as distributed effect. Gerhold and Rocha (1989) used piezoelectric sensor/driver pairs that are collocated equidistant from the neutral axis for the active vibration control of free-free isotropic beams using constant-gain feedback control. They neglected the effect of piezoelectric elements on the mass and stiffness properties of the beam element. The modeling aspects of laminated plates incorporating the piezoelectric property of materials have been reported in Lee (1990) and Crawley and Lazarus (1991). Wang and Rogers (1991) used the assumptions of classical lamination theory combined with inclusion of the effects of spatially distributed, small-size induced strain actuators embedded at any location of the laminate. And Lee (1990) derived a theory for laminated piezoelectric plates, where the linear piezoelectric constitutive equations were the only source of coupling between the electric field and the mechanical displacement field. Lee and co-workers (1991) used the assumptions of Kirchhoff plate theory to derive a simple theory for piezoelectric plates, used primarily for the design of piezoelectric laminates for bending and torsional control. Pai et al. (1993) has presented a geometrically non-linear plate theory for the analysis of composite plates with distributed piezoelectric laminae. However, their model does not include the charge equations of electrostatics. And these models are based on classical laminated plate theory, which neglects the transverse shear effects. But the effects of transverse shear stresses are important in composite fiber-reinforced materials because the interlaminar shear module are usually much smaller than the in-plane Young's module. In contrast, Tzou and Gadre (1989) derived equations of motion for laminated shells with piezoelectric layers based upon Love's first-approximation shell theory and Hamilton's principle. At that time, they did not include the charge equations in the model. Later, Tzou and Zhong (1993) derived governing equations for piezoelectric shells using first-order shear deformation theory and include the change equations of electrostatics. And a finite element model for the active vibration control of laminated plate based on first-order shear deformation theory has been presented in Chandrashekhara and Agarwal (1993). An overview of recent developments in the area of sensing and control of structures by piezoelectric materials has been reported in Rao and Sunar (1994). Recently G. Mei and Y. Shen (1997) used optical fiber sensors to measure transient impact induced strain. The issue of the feedback control gain of smart composite structures has also been discussed in B. Sun and D. Huang (1999).

1.4 Research Motivation

Comparing with the analysis of laminated plates without piezoelectric layers, the work reported in the area of fiber-reinforced composite beams with piezoelectric layers is still quite limited, especially for active vibration control of composite beams with piezoelectric laminae. Also, according to the above description, there are quite extensive works done by using the finite element method. The kinds of different finite element model of smart laminated composite beams have been well established. However, for

the analytical solution or exact solution, there are very few studies concentrated on this research area. As we know, the analytical or exact solution is more accurate than the numerical solution. The present study will focus on this approach and try to bring more attraction to this field. The work, which will be done here, can be compared by other researchers in the future.

The major goal of this work is to develop a set of governing equations for laminated composite beams with piezoelectric laminae using Hamilton's principle by introducing the electric potential function. The approximate analytical solutions of smart laminated beams with piezoelectric laminae based on a first-order shear deformation theory (MINDLIN plate theory) is to be derived by using the special method. The present beam model accounts for lateral strains, which are often neglected in conventional beam models (Vinson and Sierakowsky, 1986). The behaviour of output voltage from sensor and input voltage acting on actuator will be discussed and the relation between amplitude of vibration and feedback control will be also investigated.

1.5 The Scope of Thesis

The scope of this thesis contains five chapters. Chapter 1 is the introduction, which covers the background of smart composite materials and structures. The theoretical background of composite laminates, the motivation and objective of this research are included in this chapter. The mathematical model of smart laminated composite beams will be established in chapter 2. In this chapter, we will discuss the constitutive relationship of the smart composite beam structure. We can notice that the constitutive equation of the present beam model derived from the plate theory and can be treated as a special plate structure. The governing equation of the present smart beam model, which includes the charge equation, will be derived in chapter 3. In order to derive the governing equation, some assumptions have been made for the electric field in this chapter. The approximate analytical solution is presented in chapter 4. The software package MATLAB that is used and its brief introduction will be contained here. Finally, chapter 5 will present the numerical results to study the effectiveness of piezoelectric sensors and actuators in sensory and actively controlling the transverse response of smart laminated beams. The graphical outputs presented are generated using the MATHEMATICA software package. Some conclusions have been obtained in this chapter as well.

Chapter 2

Constitutive Equations of Smart Laminated Beams

In this chapter, we will discuss the constitutive relations of smart composite laminate beams. The theory of piezoelectricity, which relates to the present smart composite structural model will also be presented in this chapter.

2.1 Theory of Piezoelectricity

In this section, the theory of piezoelectricity will be presented. The piezoelectric phenomenon is a very important feature and is the main idea of smart composite structures.

2.1.1 Introduction

Electricity provides the engineer confronted with the task of synthesizing a smart materials system with an attractive thread of commonality during the evaluation of candidate sensors, actuators, data transmission links, and microprocessors. The two groups are mature fields of scientific endeavour but in the context of materials exhibiting electro-mechanical phenomena for sensing and actuation functions, the field is somewhat embryonic in nature. This section opens with a brief review of basic electro-mechanical properties of some classes of materials prior to discussing piezoelectric materials and applications utilizing these materials.

Piezoelectricity is an electro-deformation phenomenon derived from the Greek word '*piezein*' for '*press*' from which is derived the term 'pressure electricity', the first appeared in the scientific literature in 1880 when Pierre and Paul-Jacques Curie published a paper, describing how various crystals developed an electrical charge on their surface when they were mechanically deformed in certain directions. This piezoelectric phenomenon is similar to electrostriction, which is a property of all dielectrics. The electrostriction phenomenon is evidenced in practice as a small change of geometry of a body when it is subjected to an electrical field. The direction of this small change in geometry does not change if the direction of electrical field is reversed. In sharp contrast to this situation, piezoelectric materials, which are a unique class of non-conducting materials, exhibit a reversal in the direction of geometrical change when the direction of the electrical field is reversed. The unique characteristics of piezoelectric materials permit them to be employed as actuators or sensors which can be exploited in the synthesis of smart materials utilizing electric energy for sensing, communication and actuation functions. Indeed, the deployment of piezoelectric materials in the synthesis of smart materials involves the exploitation of a biomimetics philosophy because the anatomy of *Homo sapiens* features piezoelectric materials. For example, both skin and bone have piezoelectric properties. Thus, our sensing system at the fingertips involves the generation of an electrical potential at the surface of skin which is then transmitted to the brain by the nervous system prior to evaluation, interpretation and subsequent action.

Currently, piezoelectric materials are employed in a variety of conventional commercial applications such as phonographic pickup cartridges, where the vibrational motion of the phonograph stylus is converted into a time-varying electrical signal; microphones, where sound pressure waves are converted signals and where the shape of the crystal is carefully shaped in order to ensure that only signals of a specific frequency pass through them.

In the next decades, it is expected that there will be widespread application of the technology under development, in its current and evolutionary forms. The breath of application of this technology is expected to not only span the aerospace industry but become widespread in the construction, automotive and machine tool industries as well. Some topics which are likely to attach research studies in the distributed sensing and control of flexible structures via piezoelectricity are listed below:

1. development of piezoelectric sensors/actuators which are robust with respect to thermal changes, thermo-piezoelectric sensors/actuators, may be important for advanced intelligent space structures as well as robotic manipulators operating in environments where thermal effects are important,

2. more research in exploring the unique features and versatility of placement of piezoelectric materials as actuators and sensors is needed and more control theory needs to be introduced and applied to this area of research,

3. although some papers have been reported in the past dealing with the finite element analysis of piezoelectric medium, further research in this area will be useful especially in developing thin-layer finite elements, for distributed control purposes, and

4. the distributed sensor/actuator output may be partially or completely cancelled in symmetrical models of structural vibrations. Possible solutions should be investigated to avoid these cancellation effects.

2.1.2 Piezoelectricity

Due to the increasing demands of high structural performance requirements, the modelling and control of flexible structures has attracted considerable amount of research in recent years. Control studies of flexible structures have coursed into new channels to design controlled structures with high performance characteristics. These control studies have resulted in emergence of various new research areas particularly over the last decade. The distributed modelling, sensing and control of flexible structures usually involve, without loss of generality, beam, plate and shell-like problems depending upon the structural configuration. In the present beam model, the top piezoelectric layer (piezoelectric sensor) senses the displacement of the beam by generating voltage in response to the beam displacement. This voltage is multiplied by some gain according to the control law implemented and is fed back to the bottom piezoelectric layer (piezoelectric actuator). The bottom layer reacts to the feedback voltage and generates mechanical motion. The structures with distributed sensors and controllers are often called intelligent structures due to their self-monitoring and self-adaptive capabilities, which have been stated in chapter 1. These structures contain highly integrated or hierarchic control architecture. The intelligent structures have

several distinct advantages over conventional actively controlled structures. Since the sensing of intelligent structures is distributed instead of being discrete in nature, a much more accurate structural response measurement is possible, and hence in return, the controller design is improved. Furthermore, the sensor/actuator selection problem characteristics of conventional actively controlled structures are alleviated.

In practice, piezoelectricity is the phenomenon used most in the distributed sensing and actuation of relation between applied electric field and strain, or applied strain and electric field in certain piezoelectric ceramics, films and crystals. Piezoelectric materials can be bonded to the surfaces of beams, plates, shells, etc, or they can be embedded in these structural elements. Surface mounted components are easy to access and maintain, but they may be easily damaged during service and have some adverse effects on the structural surface. Surface mounted piezoelectric devices were used by many researchers in strain prediction and control of structures. The advantage of embedding is the better mechanical and electrical link between the piezoelectric material and main structure and the absence of bondage materials from the surface of main structure.

As stated earlier, there are two basic phenomena, characteristic of piezoelectric materials which permit them to be used as sensors and actuators in a control system. The first phenomenon is called the direct piezoelectric effect which implies that when some mechanical force or pressure (strain) is applied on a piezoelectric component, some electrical charge or voltage is induced in the piezoelectric material. Conversely, if some charge or voltage is imposed on a piezoelectric material, the material reacts by generating some mechanical force and strain. This phenomenon is called the converse piezoelectric effect. These direct and converse piezoelectric effects form a basis in the use of a piezoelectric material as sensor and actuator, respectively. The direct and converse piezoelectric phenomena, involving an interaction between the mechanical and electrical behaviour of material, can be usefully modelled by linear constitutive equations involving two mechanical variables and two electrical variables. Thus in matrix form the equations governing the direct piezoelectric effect and converse piezoelectric effect are written respectively,

$$\{D\} = [e]\{\varepsilon\} + [g]\{E\} \tag{2.1}$$

$$\{\sigma\} = [C]\{\varepsilon\} + [e]^T \{E\} \tag{2.2}$$

where {D} is the electric displacement vector; $[e]^T$ the transpose of [e], the dielectric permittivity matrix; {ε} is the strain vector; [g] is the dielectric matrix at constant mechanical strain; {E} is the electric field vector; {σ}is the stress vector and [C] is the matrix of elastic coefficients at constant electric field strength.

Two basic equations readily distill from these linear constitutive expressions. The first is the electrical expression governing an unstressed material subjected to an electrical field. Since the strain vector contains zeros, equation (2.1) reduces to a relationship relating the field strength to the electric displacement. The second basic equation is the mechanical expression governing the material at zero field strength. Thus since the electrical field vector is only populated by zero elements, equation (2.2) reduces to a relationship relating the stress and strain components of deformation.

Piezoelectric materials possess anisotropic properties. Consequently, from a mathematical perspective, their mechanical and electrical behaviour is dependent upon the direction of the external electric field relative to a set of axes fixed in the material. Alternatively, the electrical response of the material is dependent upon the direction of external mechanical loads, and hence stresses and strains, relative to a set of axes fixed in the material. Thus, design methodologies involving piezoelectric materials must carefully accommodate these anisotropic features. Consequently, with reference to equations (2.1) and (2.2), if {D} comprises three elements, and {σ} and {ε} comprise six elements, then the designer must potentially have access to a comprehensive material data base of these electro-mechanical properties because [e] has 18 elements, [g] has nine elements, and [C] has 36 elements.

In order to define these electro-mechanical properties relative to prescribed body-fixed axis frames; conventions have been developed for piezoelectric plate-like gerometries. Consider a beam of length *l*, width *b* and thickness *h*, the standard convention dictates that subscript 1 corresponds to length direction, subscript 2 corresponds to the width direction, and subscript 3 corresponds to the thickness direction as shown in Figure 2.1. The coefficients in the matrices featured in equations (2.1) and (2.2) are defined using two subscripts: the first number identifies the axis of the applied electric field, while the second number identifies the axis of induced mechanical deformation. The axis of polarization is typically in the 03 or thickness direction.

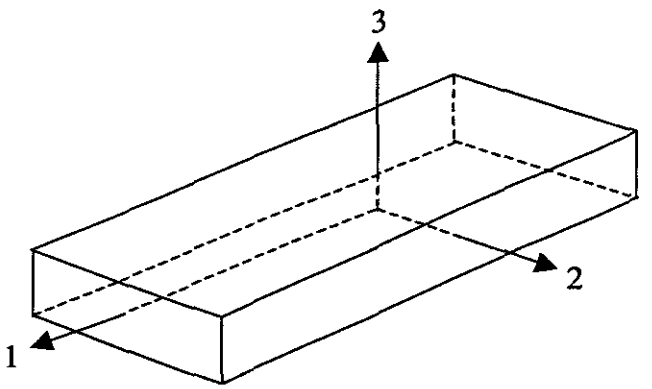

Figure 2.1 Body axes for defining piezoelectric constants

Several books in the phenomenon and theory of piezoelectricity have been written over the course of many years. Among the books are the references by Cady and Tiersten. The former treats the physical properties of piezoelectric crystal as well as their practical applications and the latter deals with the linear equations of vibrations in piezoelectric materials. A recent book written by Gandhi and Thompson is devoted entirely to the field of smart material systems and structures. In chapter 5 of this book, the physical description and use of piezoelectric materials are provided. The three piezoelectric materials of importance are lithium niobate ($LiNbO_3$), lead zirconate titanate (PZT) and polyvinylidene fluoride (PVDF or PVF_2). $LiNbO_3$ is a crystal with a high electro-mechanical coupling and a very low acoustical attenuation and is largely applied in surface wave devices. Recently, $LiNbO_3$ and PZT were used as piezoelectric tactile sensor materials in robotics by Shahinpoor.

In this project, Hamilton's principle is applied to derive a set of approximate governing equations for laminated plate with piezoelectric laminae base on the linear theory of piezoelectricity, which in turn is based on a sequence of two approximations. First, the non-linear theory of electro-elasticity is derived from the well-known conservation laws for a mechanical continuum and the conservation laws derived from Maxwells' equations [see Penfield and Haus (1967)]. In this step, a quasistatic electric field approximation is made, which allows for the electric field to be derivable from a scalar potential function. It is also assumed that the magnetic field and magnetization have negligible influence and that the electric field, polarization, and charge density are of primary concern when describing the motion and deformation of the material.

The second approximation, from whence the linear theory of piezoelectricity is derived, is that deformations are infinitesimal and that electric fields are small. In the theory, the charge equations of electrostatics are coupled to the mechanical deformations by using a modified Lagrangian function given by

$$L = \frac{1}{2}\rho \dot{u}_i \dot{u}_i - H(\varepsilon_{ij}, E_i) \tag{2.3}$$

where $H(\varepsilon_{ij}, E_i)$ is called the electric enthalpy density function, ε_{ij} are the components of the strain tensor, and E_i are the components of the electric field vector. In the present study $H(\varepsilon_{ij}, E_i)$ is taken as

$$H(\varepsilon_{ij}, E_i) = \frac{1}{2}C_{ijkl}\varepsilon_{ij}\varepsilon_{kl} - e_{ijk}E_i\varepsilon_{jk} - \frac{1}{2}g_{ij}E_iE_j \tag{2.4}$$

[see Tiersten (1969) and Reddy (1994)], where C_{ijkl} , e_{ijk} , and g_{ij} are the elastic, piezoelectric, and dielectric permittivity tensors, respectively. As described above, the electric field E_i is derived from a scalar potential function ϕ as follows:

$$E_i = -\frac{\partial \phi}{\partial x_i} \tag{2.5}$$

Equations (2.3), (2.4) and (2.5) describe the linear theory of piezoelectricity, which when combined with Hamilton's principle, can be used to derive a set of approximate governing equations for composite laminated beams.

σ_{ij} and D_i are the components of the stress tensor and the electric displacement vector, respectively. They can be derived from $H(\varepsilon_{ij}, E_i)$ as

$$D_i = -\frac{\partial H}{\partial E_i} \tag{2.6}$$

and

$$\sigma_{ij} = \frac{\partial H}{\partial \varepsilon_{ij}} \tag{2.7}$$

Piezoelectricity and its applications to various fields with an emphasis in the distributed sensing and control of flexible structures are discussed. Since its discovery by the Curie

brothers, piezoelectricity has always fascinated researchers in diverse fields and various piezoelectric materials have been used in many transducer designs, sonar applications, medical ultrasonic equipment, robot tactile sensors, acoustic pick-ups, force and strain gages, etc. In recent years, piezoelectric materials have attracted many research activities in the distributed sensing and control of structural system. The development of distributed piezoelectric sensor and actuators is expected to be essential for design of future light-weight and high-performance structures with intelligent adaptive capabilities. Hence, it appears that piezoelectricity will be an active research topic in the area of distributed sensing and control of structures and in other areas as well for many years to come.

2.2 Constitutive Equations of Smart Laminated Structures

A piezoelectric laminate theory that uses the piezoelectric phenomenon to effect distributed control and sensing of bending, shearing, torsion, shrinking, and stretching of a flexible plate has been developed. This newly developed theory is capable of modelling the electromechanical (actuating) and mechanoelectrical (sensing) behaviour. Because of their coupled mechanical and electrical properties, piezoelectric ceramics have recently attracted significant attention for their potential application as sensors for monitoring and as actuators for controlling the response of structures. The concept of using a network of actuators and sensors to form a self-controlling and self-monitoring 'smart' system in advanced structural design has drawn considerable interest among the research community. This new technology could possibly be applied to design of large-scale space structures, aircraft structures, satellites, and so forth. In this chapter, we will discuss the constitutive relationship on composite plate bonded with piezoelectric sensor and actuator layers. From the constitutive equation of the intelligent composite plate, we will derive the constitutive relationship of the smart composite beam.

The mathematical model proposed in this thesis is useful for laminates with laminae having arbitrary orientations through the thickness. However, in most cases, the principal material co-ordinate system does not coincide with the plate co-ordinate directions. Then, the transforming constitutive relations from the principal material directions to the plate (laminate) co-ordinate directions are becoming necessary. Also, in this project, the two types of constitutive relationships of the smart structures will be considered.

2.2.1 Constitutive Equations for Non-piezoelectric Laminae

For a plate of constant thickness h and composed of thin layers of orthotropic material, the constitutive equations for the k^{th} non-piezoelectric layer can be written as:

$$\begin{Bmatrix} \sigma_1 \\ \sigma_2 \\ \sigma_3 \\ \tau_{23} \\ \tau_{13} \\ \tau_{12} \end{Bmatrix}_k = \begin{bmatrix} Q_{11} & Q_{12} & Q_{13} & 0 & 0 & 0 \\ Q_{12} & Q_{22} & Q_{23} & 0 & 0 & 0 \\ Q_{13} & Q_{23} & Q_{33} & 0 & 0 & 0 \\ 0 & 0 & 0 & Q_{44} & 0 & 0 \\ 0 & 0 & 0 & 0 & Q_{55} & 0 \\ 0 & 0 & 0 & 0 & 0 & Q_{66} \end{bmatrix}_k \begin{Bmatrix} \varepsilon_1 \\ \varepsilon_2 \\ \varepsilon_3 \\ \gamma_{23} \\ \gamma_{13} \\ \gamma_{12} \end{Bmatrix}_k \tag{2.8}$$

where Q_{ij} are the plane-stress-reduced elastic constants in the material axes of the layer, and the bar over the quantities implies that the quantities are referred to principal material directions of the layer. In this analysis, the plane stress approximation is made, thus requiring modifications to the above constitutive relationship. By setting $\sigma_3 = 0$, the strain ε_3 is eliminated from the constitutive relationship. Then, the constitutive equation for non-piezoelectric laminae can be written as:

$$\begin{Bmatrix} \sigma_1 \\ \sigma_2 \\ \tau_{23} \\ \tau_{13} \\ \tau_{12} \end{Bmatrix}_k = \begin{bmatrix} \hat{Q}_{11} & \hat{Q}_{12} & 0 & 0 & 0 \\ \hat{Q}_{12} & \hat{Q}_{22} & 0 & 0 & 0 \\ 0 & 0 & \hat{Q}_{44} & 0 & 0 \\ 0 & 0 & 0 & \hat{Q}_{55} & 0 \\ 0 & 0 & 0 & 0 & \hat{Q}_{66} \end{bmatrix}_k \begin{Bmatrix} \varepsilon_1 \\ \varepsilon_2 \\ \gamma_{23} \\ \gamma_{13} \\ \gamma_{12} \end{Bmatrix}_k \tag{2.9}$$

where

$$\hat{Q}_{11} = Q_{11} - \frac{Q_{13}^{\,2}}{Q_{33}}, \quad \hat{Q}_{12} = Q_{12} - \frac{Q_{13}Q_{23}}{Q_{33}}, \quad \hat{Q}_{22} = Q_{22} - \frac{Q_{23}^{\,2}}{Q_{33}}$$

$$\hat{Q}_{44} = Q_{44}, \quad \hat{Q}_{55} = Q_{55}, \quad \hat{Q}_{66} = Q_{66}$$

Upon transformation by using transformation matrix [*T*] (see Appendix A), the lamina constitutive equations for non-piezoelectric layer can be expressed in term of stresses and strains in the plate (laminate) co-ordinates (x, y, z) as:

$$\begin{Bmatrix} \sigma_x \\ \sigma_y \\ \tau_{yz} \\ \tau_{xz} \\ \tau_{xy} \end{Bmatrix}_k = \begin{bmatrix} \overline{Q}_{11} & \overline{Q}_{12} & 0 & 0 & \overline{Q}_{16} \\ \overline{Q}_{12} & \overline{Q}_{22} & 0 & 0 & \overline{Q}_{26} \\ 0 & 0 & \overline{Q}_{44} & \overline{Q}_{45} & 0 \\ 0 & 0 & \overline{Q}_{45} & \overline{Q}_{55} & 0 \\ \overline{Q}_{16} & \overline{Q}_{26} & 0 & 0 & \overline{Q}_{66} \end{bmatrix}_k \begin{Bmatrix} \varepsilon_x \\ \varepsilon_y \\ \gamma_{yz} \\ \gamma_{xz} \\ \gamma_{xy} \end{Bmatrix}_k \tag{2.10}$$

where $\overline{Q}_{ij}$ are the transformed material constants (for more details, see Appendix A).

2.2.2 Constitutive Equations for Piezoelectric Laminae

The lamina constitutive equations accounting for piezoelectric effect for the k^{th} layer in the material axes can be written (here setting $\sigma_3 = 0$, the strain ε_3 is eliminated from the constitutive relationships) as:

$$\begin{Bmatrix} \sigma_1 \\ \sigma_2 \\ \tau_{23} \\ \tau_{13} \\ \tau_{12} \end{Bmatrix}_k = \begin{bmatrix} \hat{Q}_{11} & \hat{Q}_{12} & 0 & 0 & 0 \\ \hat{Q}_{12} & \hat{Q}_{22} & 0 & 0 & 0 \\ 0 & 0 & \hat{Q}_{44} & 0 & 0 \\ 0 & 0 & 0 & \hat{Q}_{55} & 0 \\ 0 & 0 & 0 & 0 & \hat{Q}_{66} \end{bmatrix}_k \begin{Bmatrix} \varepsilon_1 \\ \varepsilon_2 \\ \gamma_{23} \\ \gamma_{13} \\ \gamma_{12} \end{Bmatrix}_k - \begin{bmatrix} 0 & 0 & e_{31} \\ 0 & 0 & e_{32} \\ 0 & e_{24} & 0 \\ e_{15} & 0 & 0 \\ 0 & 0 & 0 \end{bmatrix}_k \begin{Bmatrix} E_1 \\ E_2 \\ E_3 \end{Bmatrix}_k \tag{2.11a}$$

$$\begin{Bmatrix} D_1 \\ D_2 \\ D_3 \end{Bmatrix}_k = \begin{bmatrix} 0 & 0 & 0 & e_{15} & 0 \\ 0 & 0 & e_{24} & 0 & 0 \\ e_{31} & e_{32} & 0 & 0 & 0 \end{bmatrix}_k \begin{Bmatrix} \varepsilon_1 \\ \varepsilon_2 \\ \gamma_{23} \\ \gamma_{13} \\ \gamma_{12} \end{Bmatrix}_k + \begin{bmatrix} g_{11} & 0 & 0 \\ 0 & g_{22} & 0 \\ 0 & 0 & g_{33} \end{bmatrix}_k \begin{Bmatrix} E_1 \\ E_2 \\ E_3 \end{Bmatrix}_k \tag{2.11b}$$

where D_i is the electric displacement, E_i is the electric field intensity, Q_{ij} is the elastic stiffness constants, e_{ij} is the piezoelectric stress coefficient and g_{ij} is the dielectric permittivity constants. Here, the labels for the elastic, piezoelectric stress and dielectric permittvity constants are not changed while the strain ε_3 is eliminated from the constitutive relationships, it is assumed that they have been adjusted to accommodate the plane stress approximation.

Upon transformation by using the transformation matrixes $[T]$ and $[T_0]$, the constitutive equations including piezoelectric effects with respect to the plane (laminate) co-ordinates (x, y, z), is given as:

$$\begin{Bmatrix} \sigma_x \\ \sigma_y \\ \tau_{yz} \\ \tau_{xz} \\ \tau_{xy} \end{Bmatrix}_k = \begin{bmatrix} \overline{Q}_{11} & \overline{Q}_{12} & 0 & 0 & \overline{Q}_{16} \\ \overline{Q}_{12} & \overline{Q}_{22} & 0 & 0 & \overline{Q}_{26} \\ 0 & 0 & \overline{Q}_{44} & \overline{Q}_{45} & 0 \\ 0 & 0 & \overline{Q}_{45} & \overline{Q}_{55} & 0 \\ \overline{Q}_{16} & \overline{Q}_{26} & 0 & 0 & \overline{Q}_{66} \end{bmatrix}_k \begin{Bmatrix} \varepsilon_x \\ \varepsilon_y \\ \gamma_{yz} \\ \gamma_{xz} \\ \gamma_{xy} \end{Bmatrix}_k - \begin{bmatrix} 0 & 0 & \overline{e}_{31} \\ 0 & 0 & \overline{e}_{32} \\ \overline{e}_{14} & \overline{e}_{24} & 0 \\ \overline{e}_{15} & \overline{e}_{25} & 0 \\ 0 & 0 & \overline{e}_{36} \end{bmatrix}_k \begin{Bmatrix} E_x \\ E_y \\ E_z \end{Bmatrix}_k \tag{2.12a}$$

$$\begin{Bmatrix} D_x \\ D_y \\ D_z \end{Bmatrix}_k = \begin{bmatrix} 0 & 0 & \overline{e}_{14} & \overline{e}_{15} & 0 \\ 0 & 0 & \overline{e}_{24} & \overline{e}_{25} & 0 \\ \overline{e}_{31} & \overline{e}_{32} & 0 & 0 & \overline{e}_{36} \end{bmatrix}_k \begin{Bmatrix} \varepsilon_x \\ \varepsilon_y \\ \gamma_{yz} \\ \gamma_{xz} \\ \gamma_{xy} \end{Bmatrix}_k + \begin{bmatrix} \overline{g}_{11} & \overline{g}_{12} & 0 \\ \overline{g}_{12} & \overline{g}_{22} & 0 \\ 0 & 0 & \overline{g}_{33} \end{bmatrix}_k \begin{Bmatrix} E_x \\ E_y \\ E_z \end{Bmatrix}_k \tag{2.12b}$$

where $\overline{Q}_{ij}$, $\overline{e}_{ij}$, $\overline{g}_{ij}$ are the coefficient after transformation (for more details, see Appendix A).

Using the matrix expression, these constitutive equations for the plate shape sensor and actuator are written as follows:

$$\{\sigma\}_k = [\overline{Q}]_k \{\varepsilon\}_k - [\overline{e}]_k^T \{E\}_k \tag{2.13a}$$

$$\{D\}_k = [\overline{e}]_k \{\varepsilon\}_k + [\overline{g}]_k \{E\}_k \tag{2.13b}$$

where $\{D\}$, $\{E\}$, $\{\varepsilon\}$ and $\{\sigma\}$ are the electric displacement, electric field, strain and stress vectors, and $[\overline{Q}], [\overline{e}], [\overline{g}]$ are the elasticity, piezoelectric and permittivity constant matrices, respectively. $[\overline{e}]^T$ is defined as the transpose of $[\overline{e}]$. Equation (2.13a)

describes the inverse piezoelectric effect and equation (2.13b) describes the direct piezoelectric effect.

The constitutive equation in the elastic field by using matrix expression is as follows:

$$[\sigma]_k = [\overline{Q}]_k \{\varepsilon\}_k \tag{2.14}$$

where $[\overline{Q}]$ is the elasticity constant matrix of the main structural laminae in the smart structure. Also, the equation (2.14) can be modelled by simply setting the piezoelectric constants to zero from equation (2.13a).

2.3 Constitutive Equations of Smart Laminated Beam Model

All structures, no matter what their dimensions are, should be treated as three-dimensional structures. It is well-known that the solution of the three-dimensional elasticity equations is too involved and in some cases is even unattainable. To overcome this difficulty it is usual engineering practice, depending on the dimensions of the structure, to make some assumptions and reduce the structure to a two-dimensional problem or even a one-dimensional problem. For example, in the case of plates, thickness is far less than length or width, and hence one can neglect the influence of strains and stresses in the thickness direction and model it as a two-dimensional problem using Kirchhoff's hypothesis. Similarly, beams are modelled as one-dimensional structures using the Euler-Bernoulli hypothesis because their width and depth are far less than their length.

Because of the type of assumption made, the solution of reduced problems, in the present beam problem, differs from the solution obtained from the three-dimensional elasticity theory or that obtained from the two-dimensional plate theory. It is to be noted here that the beam approximations that give us at least the comparable result with the two-dimensional plate theory result are best approximations to be considered. In the present case of the beam, one should consider such approximations that allow analysis of the structure as a one-dimensional problem, yet giving results that are as close as possible to those obtained from considering the same structure as two-dimensional plate problem. This means, the present model of beam comes from plate. It is a specific plate. The assumption to the point where existing theories can be utilised. At this point in development of composite technology, simplifications of plate theory appear to offer the most feasible approaches from which to begin.

In the present case, the beam is a smart composite beam model including the piezoelectric materials, which possess anisotropic properties. PVDF (polyvinylidene fluoride) and PZT (piezoceramics, such as lead zirconate Titanates) are excellent candidates for the role of sensors and actuators. In this project, the PVDF is chosen as sensors and actuators' materials. Piezoelectric material layers are polarised in the thickness direction and exhibit transversely isotropic properties in the xy-plane. Considering piezoelectric materials while retaining the anisotropic behaviour of the master structure, Eq. (2.12a) can be written as:

$$\begin{Bmatrix}\sigma_x\\ \sigma_y\\ \tau_{yz}\\ \tau_{xz}\\ \tau_{xy}\end{Bmatrix}_k = \begin{bmatrix}\overline{Q}_{11} & \overline{Q}_{12} & 0 & 0 & \overline{Q}_{16}\\ \overline{Q}_{12} & \overline{Q}_{22} & 0 & 0 & \overline{Q}_{26}\\ 0 & 0 & \overline{Q}_{44} & \overline{Q}_{45} & 0\\ 0 & 0 & \overline{Q}_{45} & \overline{Q}_{55} & 0\\ \overline{Q}_{16} & \overline{Q}_{26} & 0 & 0 & \overline{Q}_{66}\end{bmatrix}_k \begin{Bmatrix}\varepsilon_x\\ \varepsilon_y\\ \gamma_{yz}\\ \gamma_{xz}\\ \gamma_{xy}\end{Bmatrix}_k - \begin{bmatrix}0 & 0 & \bar{e}_{31}\\ 0 & 0 & \bar{e}_{31}\\ \bar{e}_{25} & \bar{e}_{15} & 0\\ \bar{e}_{15} & \bar{e}_{25} & 0\\ 0 & 0 & 0\end{bmatrix}_k \begin{Bmatrix}0\\ 0\\ E_z\end{Bmatrix}_k \tag{2.15}$$

where $\bar{e}_{31} = e_{31}$, $\bar{e}_{15} = e_{15}(\cos^2\theta - \sin^2\theta)$ and $\bar{e}_{25} = -2e_{15}\sin\theta\cos\theta$.

Thus, because of the above statement, for a beam problem, one can use $\sigma_y = \tau_{yz} = \tau_{xy} = 0$ while assuming the $\varepsilon_y \neq \gamma_{yz} \neq \gamma_{xy} \neq 0$, to obtain the following reduced constitutive equations of smart composite beams from Eq. (2.15):

$$\begin{Bmatrix}\sigma_x\\ \tau_{xz}\end{Bmatrix}_k = \begin{bmatrix}\tilde{Q}_{11} & 0\\ 0 & \tilde{Q}_{55}\end{bmatrix}_k \begin{Bmatrix}\varepsilon_x\\ \gamma_{xz}\end{Bmatrix}_k - \begin{Bmatrix}\tilde{e}_{31}\\ 0\end{Bmatrix}_k E_z^k \tag{2.16}$$

where

$$\begin{cases}\tilde{Q}_{11} = \overline{Q}_{11} + \dfrac{\overline{Q}_{16}\overline{Q}_{26} - \overline{Q}_{12}\overline{Q}_{66}}{\overline{Q}_{22}\overline{Q}_{66} - \overline{Q}_{26}^2}\overline{Q}_{12} + \dfrac{\overline{Q}_{12}\overline{Q}_{26} - \overline{Q}_{16}\overline{Q}_{22}}{\overline{Q}_{22}\overline{Q}_{66} - \overline{Q}_{26}^2}\overline{Q}_{16}\\ \tilde{Q}_{55} = \overline{Q}_{55} - \dfrac{\overline{Q}_{45}^2}{\overline{Q}_{44}}\\ \tilde{e}_{31} = (1 - \dfrac{\overline{Q}_{12}\overline{Q}_{66} - \overline{Q}_{16}\overline{Q}_{26}}{\overline{Q}_{22}\overline{Q}_{66} - \overline{Q}_{26}^2})\bar{e}_{31}\end{cases} \tag{2.17}$$

The relations for $\tilde{Q}_{ij}$ in terms of $\overline{Q}_{ij}$ and $\tilde{e}_{ij}$ in terms of $\bar{e}_{ij}$ are given in Appendix A.

Chapter 3

Vibration Analysis of Smart Composite Beams

3.1 Introduction

Composite materials have increasingly been accepted as suitable materials in the high-performance but weight-sensitive structures such as space vehicles and automobiles. This is due to the high strength-to-weight and high stiffness-to-weight ratios offered by composite materials. Laminated composite materials consist of two or more layers of different materials so as to achieve desired structural properties. Since the laminated composite is made of different material layers, the material property is discontinuous through its thickness. The material mis-match across the laminate interfaces, bending-stretching coupling, and geometric nonlinear effects make the analysis of composite structures very complicated.

In the analysis of laminated plates, the Kirchhoff plate theory, known as the classical plate theory is used. It is based on the assumptions, that: (i) straight lines normal to the mid-surface remain straight and normal after deformation, (ii) the displacement gradients are small, (iii) the length of a normal remains unchanged, and (iv) the transverse normal stress is small and it can be neglected. Thus the classical plate theory does not account for the transverse normal and shear deformations. Shear deformation theories are those in which the transverse shear stresses are accounted for. Such theories can be used to describe the kinematics of deformation of laminated plate accurately. The first-order shear deformation theory (FSDT), known as the Reissner-Mindlin plate theory, which is presented in this thesis, removes the normality assumption and includes transverse shear deformation.

3.2 Displacement Components and Stress Resultants

In chapter 2, we discussed that the present beam mathematical model came from the plate theory. This is a specific plate. For discussing the displacement components of the composite beam, we start from the Mindline plate theory (see chapter 1). In order to account for transverse shear deformation and rotary inertia effects in the plate, the displacement components of Reissner-Mindlin plate theory of the form for vibration problem are described as

$$\begin{cases} u_1(x, y, z, t) = u_0(x, y, t) + z\psi_x(x, y, t) \\ u_2(x, y, z, t) = v_0(x, y, t) + z\psi_y(x, y, t) \\ u_3(x, y, z, t) = w_0(x, y, t) \end{cases} \tag{3.1}$$

where u_0, v_0 and w_0 representing the mid-plane displacements in the x, y, z directions, and ψ_x, ψ_y represent the rotations of transverse normal to mid-plane about the y and x co-ordinates. For the composite beam problem, the displacement field can be written as

$$\begin{cases} u_1(x, y, z, t) = u_0(x, t) + z\psi_0(x, t) \\ u_2(x, y, z, t) = 0 \\ u_3(x, y, z, t) = w_0(x, t) \end{cases} \tag{3.2}$$

Here, we assume that the displacement for y-direction is neglected and u_0, v_0 and ψ_0 are only functions of x-axis and time (t) in the present model of beam.

Consider a beam length l, width b, and total thickness h, made up of a number of perfectly bonded layers including the piezoelectric layers as shown in Figure 3.1.

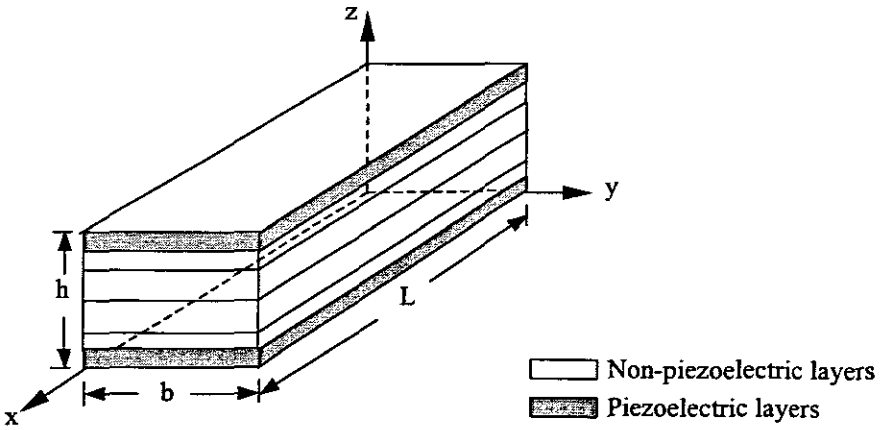

Figure 3.1 Laminated beam with integrated piezoelectric sensor and actuator

The strain displacement relations of a laminated beam based on a first order shear deformation theory associated with the displacement field are given by

$$\begin{cases} \varepsilon_x = \varepsilon_x^0 + z\kappa_x^1 \\ \gamma_{xz} = \gamma_{xz}^0 \end{cases} \tag{3.3}$$

where

$$\begin{cases} \varepsilon_x^0 = \dfrac{\partial u_0}{\partial x}, \quad \kappa_x^1 = \dfrac{\partial \psi_0}{\partial x} \\ \gamma_{xz}^0 = \psi_0 + \dfrac{\partial w_0}{\partial x} \end{cases} \tag{3.4}$$

In this project, we assume that the top and bottom layers are the actuator and sensor, respectively. Then, for non-piezoelectric laminae (main structure), the constitutive equation (2.16) for k^{th} layer can be written by setting the piezoelectric constants to zero as

$$\sigma_x = \tilde{Q}_{11}\varepsilon_x, \quad \tau_{xz} = \tilde{Q}_{55}\gamma_{xz} \tag{3.5a~b}$$

For piezoelectric laminae, the constitutive equation (2.16) for the top and bottom layers of the respecting actuator and sensor can be written as

$$\sigma_x = \tilde{Q}_{11}\varepsilon_x - \tilde{e}_{31}E_z^k, \quad \tau_{xz} = \tilde{Q}_{55}\gamma_{xz} \tag{3.6a~b}$$

The stress resultants of the first order shear deformation theory are defined as

$$N_x = \int_{-\frac{h}{2}}^{\frac{h}{2}} \sigma_x dz, \quad M_x = \int_{-\frac{h}{2}}^{\frac{h}{2}} \sigma_x z dz, \quad Q_{xz} = \int_{-\frac{h}{2}}^{\frac{h}{2}} \tau_{xz} dz \tag{3.7a~c}$$

Substituting Eqs. (3-5a~b) and (3-6a~b) in Eqs. (3-7a~c), we get

$$\begin{aligned} N_x &= \overbrace{\sum_{k=2}^{n-1} \int_{z_{k-1}}^{z_k} \tilde{Q}_{11}\varepsilon_x dz}^{non-piezoelectric\ layers} + \overbrace{\int_{z_{n-1}}^{z_n} \left(\tilde{Q}_{11}\varepsilon_x - \tilde{e}_{31}E_z^k\right)dz + \int_{z_0}^{z_1} \left(\tilde{Q}_{11}\varepsilon_x - \tilde{e}_{31}E_z^k\right)dz}^{piezoelectric\ layers} \\ &= \sum_{k=1}^{n} \int_{z_{k-1}}^{z_k} \tilde{Q}_{11}\varepsilon_x dz - \int_{z_{n-1}}^{z_n} \tilde{e}_{31}E_z^k dz - \int_{z_0}^{z_1} \tilde{e}_{31}E_z^k dz \end{aligned} \tag{3.8a}$$

$$\begin{aligned} M_x &= \overbrace{\sum_{k=2}^{n-1} \int_{z_{k-1}}^{z_k} \tilde{Q}_{11}\varepsilon_x z dz}^{non-piezoelectric\ layers} + \overbrace{\int_{z_{n-1}}^{z_n} \left(\tilde{Q}_{11}\varepsilon_x - \tilde{e}_{31}E_z^k\right)z dz + \int_{z_0}^{z_1} \left(\tilde{Q}_{11}\varepsilon_x - \tilde{e}_{31}E_z^k\right)z dz}^{piezoelectric\ layers} \\ &= \sum_{k=1}^{n} \int_{z_{k-1}}^{z_k} \tilde{Q}_{11}\varepsilon_x z dz - \int_{z_{n-1}}^{z_n} \tilde{e}_{31}E_z^k z dz - \int_{z_0}^{z_1} \tilde{e}_{31}E_z^k z dz \end{aligned} \tag{3.8b}$$

$$\begin{aligned} Q_{xz} &= \overbrace{\sum_{k=2}^{n-1} \int_{z_{k-1}}^{z_k} \tilde{Q}_{55}\gamma_{xz} dz}^{non-piezoelectric\ layers} + \overbrace{\int_{z_{n-1}}^{z_n} \tilde{Q}_{55}\gamma_{xz} dz + \int_{z_0}^{z_1} \tilde{Q}_{55}\gamma_{xz} dz}^{piezoelectric\ layers} \\ &= \sum_{k=1}^{n} \int_{z_{k-1}}^{z_k} \tilde{Q}_{55}\gamma_{xz} dz \end{aligned} \tag{3.8c}$$

where z_k and z_{k-1} are defined in Figure 3.2. Note that z_0=-h/2, z_n=h/2.

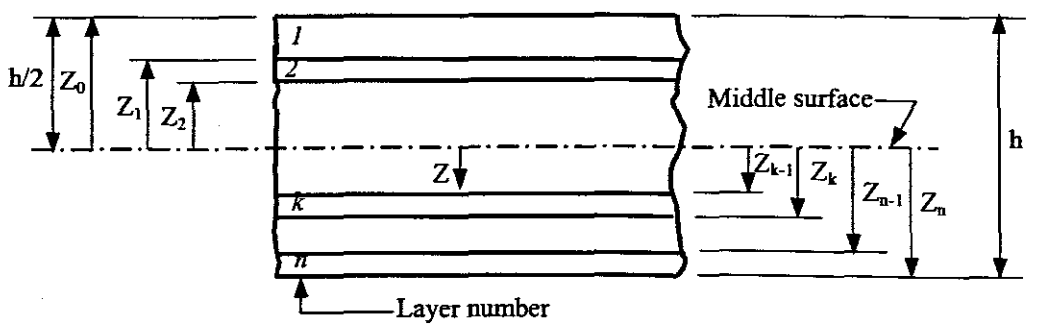

Figure 3.2 Geometry of an n-layered laminated beam

In the present beam model, we assume that the bottom and top layers are sensor and actuator layers, respectively. For sensor laminae, there is no external electric field is applied to this layer. Then, the electric field intensity for sensor is zero. Substituting Eq.

(3.3) in Eqs. (3.8a~c) and setting the sensor layer as $E_z^k = 0$, we can obtain the stress resultants as

$$\begin{Bmatrix} N_x \\ M_x \\ Q_{xz} \end{Bmatrix} = \begin{bmatrix} \overline{A}_{11} & \overline{B}_{11} & 0 \\ \overline{B}_{11} & \overline{D}_{11} & 0 \\ 0 & 0 & \overline{A}_{55} \end{bmatrix} \begin{Bmatrix} \varepsilon_x^0 \\ \kappa_x^1 \\ \gamma_{xz}^0 \end{Bmatrix} - \begin{Bmatrix} N_x^p \\ M_x^p \\ 0 \end{Bmatrix} \tag{3.9}$$

where

$$\left\{\overline{A}_{11} \quad \overline{B}_{11} \quad \overline{D}_{11}\right\} = \sum_{k=1}^{n} \int_{z_{k-1}}^{z_k} \widetilde{Q}_{11}(1, z, z^2)dz$$

$$\left\{\overline{A}_{55}\right\} = \sum_{k=1}^{n} \int_{z_{k-1}}^{z_k} \overline{Q}_{55}dz$$

$$\left\{N_x^p \quad M_x^p\right\} = \int_{z_{n-1}}^{z_n} \widetilde{e}_{31} E_z^k(1, z)dz$$

From Mitchell J.A. and Reddy J.N. in 1995 [36], the electric potential variable Φ can be expressed as

$$\Phi(x, y, z, t) = f(z)\phi_0(x, y, t) \tag{3.10}$$

For the beam problem, we do not consider the varying of y-axis because any physical variables are uniformed distributed through the Y-direction. The electric field of smart composite beams can be written as

$$\Phi(x, z, t) = f(z)\phi_0(x, t) \tag{3.11}$$

Because the thickness of the piezoelectric layers is very thin, we also assume that the voltage is uniformed distributed through the thickness (Z-direction) of the piezoelectric layers. That is $f(z) = 1$. Then the electric field intensity E_z^k can be expressed as

$$E_z^k = \frac{\phi_0(x, t)}{h_p} \tag{3.12}$$

where h_p is the thickness of the piezoelectric layers.

3.3 Governing Equations

In this section, we will use Hamilton's principle and the mechanoelectrical constitutive equation, as starting point to discuss the governing equation including the effect of piezoelectric layer and the closed circuit charge or current generated across the thickness direction of each individual lamina caused by the displacement of the laminates based on the first order shear deformation theory (Mindlin Theory). The charge or current can be easily measured through the surface of sensor laminae. The applied electric field through the actuator laminae can also be defined. The closed loop control system is shown in Figure 3.3.

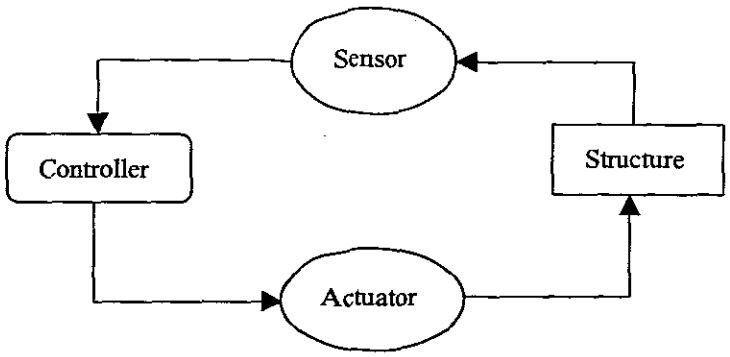

Figure 3.3 The active vibration control system for intelligent beam

The mathematical statement of Hamilton's principle can be expressed as

$$\int_{t_1}^{t_2} (\delta T - \delta U + \delta W) dt = 0 \tag{3.13}$$

where $U = U_M + U_E$, T is the kinetic energy, U_M is the strain energy, U_E is the electrical field potential energy of piezoelectric layers, and W is the work done by surface tractions and applied surface electrical charge density. In this project, the body forces are not considered. In Eq. (3.13), t_1 and t_2 are two arbitrary time variables and δ denotes the first variation. We begin with the first integral. Here, we assume that each layer of the present composite beam model has same the vibration speed. The kinetic energy can be expressed as

$$T = \sum_{k=1}^{n} \frac{1}{2} \int_{z_{k-1}}^{z_k} \int_{-\frac{b}{2}}^{\frac{b}{2}} \int_0^l \rho_k (\dot{u}_1 \dot{u}_1 + \dot{u}_3 \dot{u}_3) dx dy dz$$

where ρ_k is the kth layer mass intensity. Substituting Eq. (3.2) in the kinetic energy expression, we get

$$\begin{aligned} T &= \sum_{k=1}^{n} \frac{1}{2} \int_{z_{k-1}}^{z_k} \int_{-\frac{b}{2}}^{\frac{b}{2}} \int_0^l \rho_k \left[\left(\frac{\partial u_0}{\partial t} + z \frac{\partial \psi_0}{\partial t} \right)^2 + \left(\frac{\partial w_0}{\partial t} \right)^2 \right] dx dy dz \\ &= \frac{b}{2} \int_0^l \left[I_1 \left(\frac{\partial u_0}{\partial t} \right)^2 + I_1 \left(\frac{\partial w_0}{\partial t} \right)^2 + 2 I_2 \frac{\partial u_0}{\partial t} \frac{\partial \psi_0}{\partial t} + I_3 \left(\frac{\partial \psi_0}{\partial t} \right)^2 \right] dx \end{aligned} \tag{3.14}$$

The first variation of kinetic energy is given by

$$\delta T = \int_0^l \left[\left(I_1 \frac{\partial u_0}{\partial t} + I_2 \frac{\partial \psi_0}{\partial t} \right) \frac{\partial \delta u_0}{\partial t} + I_1 \frac{\partial w_0}{\partial t} \frac{\partial \delta w_0}{\partial t} + \left(I_2 \frac{\partial u_0}{\partial t} + I_3 \frac{\partial \psi_0}{\partial t} \right) \frac{\partial \delta \psi_0}{\partial t} \right] b dx \tag{3.15}$$

where

$$(I_1, I_2, I_3) = \sum_{k=1}^{n} \int_{z_{k-1}}^{z_k} \rho_k (1, z, z^2) dz$$

For the second integral of the Eq. (3.16), the strain energy of the smart composite beam can be expressed as

$$U_M = \frac{1}{2}\iiint(\sigma_x\varepsilon_x + \tau_{xz}\gamma_{xz})dxdydz$$

Substituting Eqs. (2.16) and (3.3) in the strain energy expression and in view of Eq. (3.9), we have

$$U_M = \frac{1}{2}\int_0^l (N_x\varepsilon_x^0 + M_x\kappa_x^1 + Q_{xz}\gamma_{xz}^0)bdx \tag{3.16}$$

Substitution of Eq. (3.4) into Eq. (3.16), then the second integral of Eq. (3.13) can be written as

$$\begin{aligned}\delta U_M &= \int_0^l (N_x\delta\varepsilon_x^0 + M_x\delta\kappa_x^1 + Q_{xz}\gamma_{xz}^0)bdx \\ &= \int_0^l \left[N_x\frac{\partial\delta u_0}{\partial x} + Q_{xz}\frac{\partial\delta w_0}{\partial x} + M_x\frac{\partial\delta\psi_0}{\partial x} + Q_{xz}\delta\psi_0\right]bdx\end{aligned} \tag{3.17}$$

Piezoelectric materials are polarized in the thickness direction and exhibit transversely isotropic properties in XY-plane. So for the equation (2.12b), only D_z is of interest to us. Considering piezoelectric materials while retaining the anisotropic behaviour of the master structure, the constitutive equation (2.12b) can be written as

$$D_z^k = \bar{e}_{31}\varepsilon_x + \bar{e}_{31}\varepsilon_y + \bar{g}_{33}E_z^k$$

For the present beam problem, we have $\varepsilon_y = \dfrac{\bar{Q}_{66}\bar{e}_{31}E_z^k - (\bar{Q}_{12}\bar{Q}_{66} - \bar{Q}_{16}\bar{Q}_{26})\varepsilon_x}{\bar{Q}_{22}\bar{Q}_{66} - \bar{Q}_{26}^2}$ (See Appendix A). Substitution of ε_y in above expression, we get

$$D_z^k = \tilde{e}_{31}\varepsilon_x + \tilde{g}_{33}E_z^k \tag{3.18}$$

where

$$\tilde{e}_{31} = (1 - \frac{\bar{Q}_{12}\bar{Q}_{66} - \bar{Q}_{16}\bar{Q}_{26}}{\bar{Q}_{22}\bar{Q}_{66} - \bar{Q}_{26}^2})\bar{e}_{31}\ ,\quad \tilde{g}_{33} = \frac{\bar{Q}_{66}\bar{e}_{31}^2}{\bar{Q}_{22}\bar{Q}_{66} - \bar{Q}_{26}^2} + \bar{g}_{33}$$

The electrical field potential energy of piezoelectric layers can be written as

$$\begin{aligned}U_E &= \frac{1}{2}\iiint_{\Omega_E} D_z^k E_z^k dxdydz = \frac{1}{2}\sum_{k=1}^{n}\int_{z_{k-1}}^{z_k}\int_{-\frac{b}{2}}^{\frac{b}{2}}\int_0^l D_z^k(\frac{\phi_0(x,t)}{h_p})dxdydz \\ &= \frac{b}{2}\int_0^l G_z^k\phi_0(x,t)dx\end{aligned}$$

where

$$G_z^k = \sum_{k=1}^{n} D_z^k\frac{1}{h_p}dz$$

and the first variation of the electrical field potential energy is

$$\delta U_E = \int_0^l G_z^k \delta\phi_0 b dx \tag{3.19}$$

The virtual work done by external surface force and the applied surface charge density is given by

$$W = \int_{S_M} p w_0 dA - \int_{S_E} q_0 \Phi(x,t) dA$$

where S_M and S_E are the surface area applied forces and the electrical charge, respectively. The variation of the virtual work can be expressed as

$$\delta W = \int_0^l p \delta w_0 b dx - \int_0^l q_0 \delta\phi_0 b dx \tag{3.20}$$

where p is the surface traction and q_0 is the surface charge density applied to the present intelligent composite beam model, respectively. Substituting the Eqs. (3.15), (3.17), (3.19) and (3.20) in the Hamilton's principle Eq. (3.13), we can obtain

$$\begin{aligned}\int_{t_1}^{t_2} \int_0^l \Bigg[& \left(I_1 \frac{\partial u_0}{\partial t} + I_2 \frac{\partial \psi_0}{\partial t} \right) \frac{\partial \delta u_0}{\partial t} + I_1 \frac{\partial w_0}{\partial t} \frac{\partial \delta w_0}{\partial t} + \left(I_2 \frac{\partial u_0}{\partial t} + I_3 \frac{\partial \psi_0}{\partial t} \right) \frac{\partial \delta \psi_0}{\partial t} - \\ & - N_x \frac{\partial \delta u_0}{\partial x} - Q_{xz} \frac{\partial \delta w_0}{\partial x} - M_x \frac{\partial \delta \psi_0}{\partial x} - Q_{xz} \delta \psi_0 - G_z^k \delta\phi_0 + p \delta w_0 - q_0 \delta\phi_0 \Bigg] b dx dt = 0\end{aligned} \tag{3.21}$$

Using the distributive (by parts) integral method on the above equation and collecting the coefficients of $(\delta u_0, \delta w_0, \delta \psi_0, \delta\phi_0)$ and setting them to zero, the governing equations for vibration of smart composite beams based on the Reissner-Mindlin plate theory can be expressed as

$$\delta u_0: \quad I_1 \ddot{u}_0 + I_2 \ddot{\psi}_0 - \frac{\partial N_x}{\partial x} = 0 \tag{3.22a}$$

$$\delta w_0: \quad I_1 \ddot{w}_0 - \frac{\partial Q_{xz}}{\partial x} = p \tag{3.22b}$$

$$\delta \psi_0: \quad I_2 \ddot{u}_0 + I_3 \ddot{\psi}_0 - \frac{\partial M_x}{\partial x} + Q_{xz} = 0 \tag{3.22c}$$

$$\delta\phi_0: \quad G_z^k + q_0 = 0 \tag{3.22d}$$

Equations (3.22) are subject to the following boundary conditions as

$$x = 0, \text{ and } x = l: \qquad N_x = \tilde{N}_x, \text{ or } u_0 = \tilde{u}_0$$

$$x=0, \text{ and } x=l: \qquad Q_{xz}=\tilde{Q}_{xz}, \text{ or } w_0=\tilde{w}_0$$

$$x=0, \text{ and } x=l: \qquad M_x=\tilde{M}_x, \text{ or } \psi_0=\tilde{\psi}_0$$

and "~" denotes the know value.

According to the Eq.(3.18), the coefficient G_z^k can be expanded as

$$G_z^k=\tilde{e}_{31}G_1^k\frac{\partial u_0}{\partial x}+\tilde{e}_{31}G_2^k\frac{\partial \psi_0}{\partial x}+\tilde{g}_{33}G_3^k\phi_0(x,t) \tag{3.23}$$

where

$$G_1^k=\sum_{k=1}^{n}\int_{z_{k-1}}^{z_k}(1/h_p)dz, \quad G_2^k=\sum_{k=1}^{n}\int_{z_{k-1}}^{z_k}(1/h_p)zdz, \quad G_3^k=\sum_{k=1}^{n}\int_{z_{k-1}}^{z_k}(1/h_p)^2dz$$

With the definitions for stress resultants, equation (3.9) can be re-written as

$$\begin{aligned}
N_x &= \bar{A}_{11}\frac{\partial u_0}{\partial x}+\bar{B}_{11}\frac{\partial \psi_0}{\partial x}-\tilde{e}_{31}G_1^k\phi_0(x,t)\\
M_x &= \bar{B}_{11}\frac{\partial u_0}{\partial x}+\bar{D}_{11}\frac{\partial \psi_0}{\partial x}-\tilde{e}_{31}G_2^k\phi_0(x,t)\\
Q_{xz} &= \bar{A}_{55}\left(\psi_0+\frac{\partial w_0}{\partial x}\right)
\end{aligned} \tag{3.24}$$

Substitution of Eq. (3.23) into Eq. (3.22d), we can obtain

$$\tilde{e}_{31}G_1^k\frac{\partial u_0}{\partial x}+\tilde{e}_{31}G_2^k\frac{\partial \psi_0}{\partial x}+\tilde{g}_{33}G_3^k\phi_0(x,t)=-q_0 \tag{3.25}$$

From the equation (3.25), the electrical field potential function can be expressed as

$$\phi_0(x,t)=-\frac{\tilde{e}_{31}G_1^k}{\tilde{g}_{33}G_3^k}\frac{\partial u_0}{\partial x}-\frac{\tilde{e}_{31}G_2^k}{\tilde{g}_{33}G_3^k}\frac{\partial \psi_0}{\partial x}+\phi_A(x,t) \tag{3.26}$$

where $\phi_A(x, t)$ is the input control electric potential voltage acting on the actuator layer.

Substituting Eqs. (3.24) and (3.26) in Eqs. (3.22a~c), we can get the governing equation in the following form:

$$\delta u_0: \quad I_1\frac{\partial^2 u_0}{\partial t^2}+I_2\frac{\partial^2 \psi_0}{\partial t^2}-\bar{A}_{11}\frac{\partial^2 u_0}{\partial x^2}-\bar{B}_{11}\frac{\partial^2 \psi_0}{\partial x^2}-\beta_1\frac{\partial^2 u_0}{\partial x^2}-\beta_2\frac{\partial^2 \psi_0}{\partial x^2}=\frac{\partial \phi_A}{\partial x} \tag{3.27a}$$

$$\delta w_0: \quad I_1\frac{\partial^2 w_0}{\partial t^2}-\bar{A}_{55}\frac{\partial \psi_0}{\partial x}-\bar{A}_{55}\frac{\partial^2 w_0}{\partial x^2}=p \tag{3.27b}$$

$$\delta \psi_0: \quad I_2\frac{\partial^2 u_0}{\partial t^2}+I_3\frac{\partial^2 \psi_0}{\partial t^2}-\bar{B}_{11}\frac{\partial^2 u_0}{\partial x^2}-\bar{D}_{11}\frac{\partial^2 \psi_0}{\partial x^2}-\beta_2\frac{\partial^2 u_0}{\partial x^2}-\beta_3\frac{\partial^2 \psi_0}{\partial x^2}=\frac{\partial \phi_A}{\partial x} \tag{3.27c}$$

where

$$\beta_1 = -\frac{\tilde{e}_{31}^2 G_1^{k^2}}{\tilde{g}_{33} G_3^k}, \quad \beta_2 = -\frac{\tilde{e}_{31}^2 G_1^k G_2^k}{\tilde{g}_{33} G_3^k}, \quad \beta_3 = -\frac{\tilde{e}_{31}^2 G_2^{k^2}}{\tilde{g}_{33} G_3^k}$$

If the sensing information is required, the electrical potential can be recovered by

$$\phi_0(x,t) = \alpha_1 \frac{\partial u_0}{\partial x} + \alpha_2 \frac{\partial \psi_0}{\partial x} + \phi_A(x,t) \tag{3.28}$$

where

$$\alpha_1 = -\frac{\tilde{e}_{31} G_1^k}{\tilde{g}_{33} G_3^k}, \quad \alpha_2 = -\frac{\tilde{e}_{31} G_2^k}{\tilde{g}_{33} G_3^k}$$

Note the $\phi_A(x,t)$ is usually zero in the piezoelectric sensor layer. Thus, the piezoelectric sensor electrical potential output is estimated by

$$\phi_S(x,t) = \alpha_{1S} \frac{\partial u_0}{\partial x} + \alpha_{2S} \frac{\partial \psi_0}{\partial x} \tag{3.29}$$

In the active vibration control application the electric force term can be regarded as the feedback control force. The piezoelectric actuator electrical potential input in terms of the output signal from the piezoelectric sensor layer can be written as

$$\phi_A(x,t) = -G_i \left(\alpha_{1A} \frac{\partial^2 u_0}{\partial x \partial t} + \alpha_{2A} \frac{\partial^2 \psi_0}{\partial x \partial t} \right) \tag{3.30}$$

where the negative velocity feedback control method is implemented and G_i is the feedback control gain. The symbol α_{jS} and α_{jA} (j=1,2) are the relative coefficients of sensor laminae and actuator laminae, respectively.

Substituting the equation (3.30) in equations (3.27a~c) and using the derivative operator forms, the governing equations can be written as simple form in term of the mechanical and piezoelectric resultants

$$\delta u_0: \quad L_{11} u_0 + L_{13} \psi_0 = 0 \tag{3.31a}$$

$$\delta w_0: \quad L_{22} w_0 + L_{23} \psi_0 = p \tag{3.31b}$$

$$\delta \psi_0: \quad L_{31} u_0 + L_{32} w_0 + L_{33} \psi_0 = 0 \tag{3.31c}$$

where L_{ij} are the derivative operators given by

$$L_{11} = -a \frac{\partial^2}{\partial x^2} + I_1 \frac{\partial^2}{\partial t^2} + G_i \alpha_1 \frac{\partial^3}{\partial x^2 \partial t}, \quad L_{12} = L_{21} = 0$$

$$L_{13} = -b\frac{\partial^2}{\partial x^2} + I_2\frac{\partial^2}{\partial t^2} + G_i\alpha_2\frac{\partial^3}{\partial x^2\partial t}$$

$$L_{22} = I_1\frac{\partial^2}{\partial t^2} - \bar{A}_{55}\frac{\partial^2}{\partial x^2}, \quad L_{23} = -\bar{A}_{55}\frac{\partial}{\partial x}$$

$$L_{31} = -b\frac{\partial^2}{\partial x^2} + I_2\frac{\partial^2}{\partial t^2} + G_i\alpha_1\frac{\partial^3}{\partial x^2\partial t}, \quad L_{32} = \bar{A}_{55}\frac{\partial}{\partial x}$$

$$L_{33} = -d\frac{\partial^2}{\partial x^2} + I_3\frac{\partial^2}{\partial t^2} + G_i\alpha_2\frac{\partial^3}{\partial x^2\partial t} + \bar{A}_{55}$$

and $\quad a = \bar{A}_{11} + \beta_1, \quad b = \bar{B}_{11} + \beta_2, \quad d = \bar{D}_{11} + \beta_3$

Chapter 4

Approximate Analytical Solutions of Smart Composite Beams

4.1 Introduction

In this chapter, the approximate analytical solutions of smart composite laminated beams will be presented. According to the governing equations, which is derived in chapter 3, we assume that the external exciting force has the characteristics of harmonic vibration. In this project, the significant idea is to use the mathematical tool of complex numbers to reduce the orders of the governing equations. *This method has never been applied before.* Also, from the relative references, the numerical results of smart composite beams have been presented by using the finite element method. The main objective of the present work is to find the approximate analytical solutions of smart laminate beams under the harmonic external exciting force. This is also the first analytical solution in the research field of smart composite beams. In this research work, we will find the displacements of the present mathematical beam model through solving the sixth-order differential equation of the displacement potential function $F(x, t)$ instead of finding the displacements of present beam model directly. The software package of MATLAB will be used in this procedure.

- **A Brief Introduction of MATLAB**

MATLAB is a high-performance language for technical computing. It integrates computation, visualization, and programming in an easy-to-use environment where problems and solutions are expressed in familiar mathematical notation. Typical uses include:

- Mathematics and computation
- Algorithm development
- Modelling, simulation, and prototyping
- Data analysis, exploration, and visualization
- Scientific and engineering graphics
- Application development, including Graphical User Interface building

MATLAB is an interactive system whose basic data element is an array that does not require dimensioning. This allows you to solve many technical computing problems, especially those with matrix and vector formulations, in a fraction of the time it would take to write a program in a scalar noninteractive language such as C or Fortran. The name MATLAB stands for matrix laboratory. It has evolved over a period of years with input from many users. In university environments, it is the standard instructional tool for introductory and advanced courses in mathematics, engineering, and science. In industry, MATLAB is the tool of choice for high-productivity research, development, and analysis.

MATLAB features a family of application-specific solutions called toolboxes. Very important to most users of this package, toolboxes allow you to learn and apply specialized technology. Toolboxes are comprehensive collections of MATLAB functions (M-files) that extend the MATLAB environment to solve particular classes of problems. Areas in which toolboxes are available include signal processing, control systems, neural networks, fuzzy logic, wavelets, simulation, and many others. The MATLAB system consists of five main parts:

The MATLAB language This is a high-level matrix/array language with control flow statements, functions, data structures, input/output, and object-oriented programming features. It allows both "programming in the small" to rapidly create quickly and dirty throwaway programs, and "programming in the large" to create complete large and complex application programs.

The MATLAB working environment This is the set of tools and facilities that you work with as the MATLAB user or programmer. It includes facilities for managing the variables in your workspace and importing and exporting data. It also includes tools for developing, managing, debugging, and profiling M-files, MATLAB's applications.

Handle Graphics This is the MATLAB graphics system. It includes high-level commands for two-dimensional and three-dimensional data visualization, image processing, animation, and presentation graphics. It also includes low-level commands that allow you to fully customize the appearance of graphics as well as to build complete Graphical User Interfaces on your MATLAB applications.

The MATLAB mathematical function library This is a vast collection of computational algorithms ranging from elementary functions like sum, sine, cosine, and complex arithmetic, to more sophisticated functions like matrix inverse, matrix eigenvalues, Bessel functions, and fast Fourier transforms.

The MATLAB Application Program Interface (API) This is a library that allows you to write C and Fortran programs that interact with MATLAB. It include facilities for calling routines from MATLAB (dynamic linking), calling MATLAB as a computational engine, and for reading and writing MAT-files.

In this project, the part of Mathematics and Computation in package MATLAB is used to solve the sixth-order differential equation.

4.2 Simplification of the Governing Equation

From the chapter 3, we can rewrite the governing equation (3.31) as

$$\delta u_0: \quad L_{11}u_0 + L_{12}w_0 + L_{13}\psi_0 = 0 \tag{4.1a}$$

$$\delta w_0: \quad L_{21}u_0 + L_{22}w_0 + L_{23}\psi_0 = p \tag{4.1b}$$

$$\delta \psi_0: \quad L_{31}u_0 + L_{32}w_0 + L_{33}\psi_0 = 0 \tag{4.1c}$$

where

$$L_{11} = -a\frac{\partial^2}{\partial x^2} + I_1\frac{\partial^2}{\partial t^2} + G_i\alpha_1\frac{\partial^3}{\partial x^2\partial t}, \quad L_{12} = L_{21} = 0$$

$$L_{13} = -b\frac{\partial^2}{\partial x^2} + I_2\frac{\partial^2}{\partial t^2} + G_i\alpha_2\frac{\partial^3}{\partial x^2\partial t}$$

$$L_{22} = I_1\frac{\partial^2}{\partial t^2} - \bar{A}_{55}\frac{\partial^2}{\partial x^2}, \quad L_{23} = -\bar{A}_{55}\frac{\partial}{\partial x}$$

$$L_{31} = -b\frac{\partial^2}{\partial x^2} + I_2\frac{\partial^2}{\partial t^2} + G_i\alpha_1\frac{\partial^3}{\partial x^2\partial t}, \quad L_{32} = \bar{A}_{55}\frac{\partial}{\partial x}$$

$$L_{33} = -d\frac{\partial^2}{\partial x^2} + I_3\frac{\partial^2}{\partial t^2} + G_i\alpha_2\frac{\partial^3}{\partial x^2\partial t} + \bar{A}_{55}$$

and

$$a = \bar{A}_{11} + \beta_1, \quad b = \bar{B}_{11} + \beta_2, \quad d = \bar{D}_{11} + \beta_3$$

The equations (4.1a) and (4.1c) can be rewritten as

$$\begin{aligned} L_{11}(u_0) + L_{12}(w_0) &= -L_{13}(\psi_0) \\ L_{31}(u_0) + L_{32}(w_0) &= -L_{33}(\psi_0) \end{aligned} \tag{4.2}$$

Using matrix form, the equation (4.2) can be expressed as

$$\begin{bmatrix} L_{11} & L_{12} \\ L_{31} & L_{32} \end{bmatrix} \begin{Bmatrix} u_0 \\ w_0 \end{Bmatrix} = \begin{Bmatrix} -L_{13}(\psi_0) \\ -L_{33}(\psi_0) \end{Bmatrix} \tag{4.3}$$

From Eq. (4.3), we can get

$$\begin{aligned} \Delta u_0 &= \left(-L_{13}L_{32} + L_{12}L_{33}\right)\psi_0 \\ \Delta w_0 &= \left(-L_{11}L_{33} + L_{13}L_{31}\right)\psi_0 \end{aligned} \tag{4.4}$$

where

$$\Delta = L_{11}L_{32} - L_{12}L_{31}$$

Introducing the displacement potential function $F(x, t)$ and taking into account $L_{12} = L_{21} = 0$, we can have

$$u_0 = L_1(F), \quad w_0 = L_2(F), \quad \psi_0 = L_3(F) \tag{4.5}$$

where

$$L_1 = -L_{13}L_{32}, \quad L_2 = -L_{11}L_{33} + L_{13}L_{31}, \quad L_3 = L_{11}L_{32}$$

Substituting Eq. (4.5) in Eq. (4.1b), we obtain the equation of the displacement potential function $F(x, t)$ as

$$L_{22}L_2(F) + L_{23}L_3(F) = p(x,t) \tag{4.6}$$

The derivative operators $L_1, L_2, L_3, L_{22}L_2$ and $L_{23}L_3$ are shown in Appendix B.

Substitution of the derivative operators $L_{22}L_2$ and $L_{23}L_3$ into equation (4.6), we can obtain

$$\begin{aligned} &a_1\frac{\partial^6 F}{\partial x^6}+a_2\frac{\partial^6 F}{\partial x^4 t^2}+a_3\frac{\partial^7 F}{\partial x^6 t}+a_4\frac{\partial^7 F}{\partial x^4 t^3}+a_5\frac{\partial^6 F}{\partial x^2 t^4}+a_6\frac{\partial^4 F}{\partial x^2 t^2}+ \\ &+a_7\frac{\partial^7 F}{\partial x^2 t^5}+a_8\frac{\partial^6 F}{\partial t^6}+a_9\frac{\partial^4 F}{\partial t^4}+a_{10}\frac{\partial^5 F}{\partial x^2 t^3}=p(x,t) \end{aligned} \tag{4.7}$$

where

$$\begin{aligned} &a_1=-\bar{A}_{55}b^2+\bar{A}_{55}ad, \quad a_2=-\bar{A}_{55}(I_3a+I_1d-2I_2b)+I_1(b^2-ad) \\ &a_3=-\bar{A}_{55}G_i(a\alpha_2+d\alpha_1-b\alpha_1-b\alpha_2) \\ &a_4=-\bar{A}_{55}G_i(I_2\alpha_1+I_2\alpha_2-I_1\alpha_2-I_3\alpha_1)+I_1G_i(a\alpha_2+d\alpha_1-b\alpha_1-b\alpha_2) \\ &a_5=-\bar{A}_{55}(I_2^{\,2}-I_1I_3)+I_1(I_3a+I_1d-2I_2b), \quad a_6=I_1a\bar{A}_{55} \\ &a_7=I_1G_i(I_2\alpha_1+I_2\alpha_2-I_1\alpha_2-I_3\alpha_1), \quad a_8=I_1(I_2^{\,2}-I_1I_3) \\ &a_9=-\bar{A}_{55}I_1^{\,2}, \quad a_{10}=-\bar{A}_{55}I_1G_i\alpha_1 \end{aligned}$$

Here, we assume that the external exciting force has the feature of harmonic vibration with the following form

$$p(x,t)=p_1(x)\sin(\omega t)+p_2(x)\cos(\omega t) \tag{4.8}$$

as well as the displacement potential function $F(x, t)$ is the form

$$F(x,t)=K_1(x)\sin(\omega t)+K_2(x)\cos(\omega t) \tag{4.9}$$

Substituting the Eqs. (4.8) and (4.9) in Eq. (4.7), we can obtain

$$\begin{aligned} &\Bigg[a_1\frac{d^6K_1(x)}{dx^6}-a_2\omega^2\frac{d^4K_1(x)}{dx^4}-a_3\omega\frac{d^6K_2(x)}{dx^6}+a_4\omega^3\frac{d^4K_2(x)}{dx^4}+ \\ &+a_5\omega^4\frac{d^2K_1(x)}{dx^2}-a_6\omega^2\frac{d^2K_1(x)}{dx^2}-a_7\omega^5\frac{d^2K_2(x)}{dx^2}-a_8\omega^6K_1(x)+ \\ &+a_9\omega^2K_1(x)+a_{10}\omega^3\frac{d^2K_2(x)}{dx^2}\Bigg]\sin(\omega t)+\Bigg[a_1\frac{d^6K_2(x)}{dx^6}-a_2\omega^2\frac{d^4K_2(x)}{dx^4}- \\ &-a_3\omega\frac{d^6K_1(x)}{dx^6}+a_4\omega^3\frac{d^4K_1(x)}{dx^4}+a_5\omega^4\frac{d^2K_2(x)}{dx^2}-a_6\omega^2\frac{d^2K_2(x)}{dx^2}- \\ &-a_7\omega^5\frac{d^2K_1(x)}{dx^2}-a_8\omega^6K_2(x)+a_9\omega^2K_2(x)+ \\ &a_{10}\omega^3\frac{d^2K_1(x)}{dx^2}\Bigg]\cos(\omega t)=p_1(x)\sin(\omega t)+p_2(x)\cos(\omega t) \end{aligned} \tag{4.10}$$

Separating the two variables of the field of space and time in equation (4.10), and canceling the terms $\sin(\omega t)$ and $\cos(\omega t)$, we can get the two coupled differentiation equations of functions $K_1(x)$ and $K_2(x)$ as

$$a_1\frac{d^6K_1(x)}{dx^6}-a_2\omega^2\frac{d^4K_1(x)}{dx^4}+(a_5\omega^4-a_6\omega^2)\frac{d^2K_1(x)}{dx^2}-(a_8\omega^6-a_9\omega^4)K_1(x)- \\ -\left[a_3\omega\frac{d^6K_2(x)}{dx^6}-a_4\omega^3\frac{d^4K_2(x)}{dx^4}+(a_7\omega^5-a_{10}\omega^3)\frac{d^2K_2(x)}{dx^2}\right]=p_1(x) \tag{4.11a}$$

$$a_1\frac{d^6K_2(x)}{dx^6}-a_2\omega^2\frac{d^4K_2(x)}{dx^4}+(a_5\omega^4-a_6\omega^2)\frac{d^2K_2(x)}{dx^2}-(a_8\omega^6-a_9\omega^4)K_2(x)- \\ -\left[a_3\omega\frac{d^6K_1(x)}{dx^6}-a_4\omega^3\frac{d^4K_1(x)}{dx^4}+(a_7\omega^5-a_{10}\omega^3)\frac{d^2K_1(x)}{dx^2}\right]=p_2(x) \tag{4.11b}$$

The equation (4.11) can be written as a simple form as following

$$b_6\frac{d^6K_1(x)}{dx^6}-b_4\frac{d^4K_1(x)}{dx^4}+b_2\frac{d^2K_1(x)}{dx^2}-b_1K_1(x)- \\ -\left[b_7\frac{d^6K_2(x)}{dx^6}-b_5\frac{d^4K_2(x)}{dx^4}+b_3\frac{d^2K_2(x)}{dx^2}\right]=p_1(x) \tag{4.12a}$$

$$b_6\frac{d^6K_2(x)}{dx^6}-b_4\frac{d^4K_2(x)}{dx^4}+b_2\frac{d^2K_2(x)}{dx^2}-b_1K_2(x)- \\ -\left[b_7\frac{d^6K_1(x)}{dx^6}-b_5\frac{d^4K_1(x)}{dx^4}+b_3\frac{d^2K_1(x)}{dx^2}\right]=p_2(x) \tag{4.12b}$$

where

$$b_1=(a_9-a_8\omega^2)\omega^4,\quad b_2=(a_6-a_5\omega^2)\omega^2$$
$$b_3=(a_{10}-a_7\omega^2)\omega^2,\quad b_4=a_2\omega^2,$$
$$b_5=a_4\omega^3,\quad b_6=a_1,\quad b_7=a_3\omega$$

The solution for the governing equations (4.1a~c) for the said smart laminate beam is derived in solving the two coupled differential equations (4.12a~b). It was found that the two coupled differential equations are twelfth-orders differential equation. Now, applying the mathematical tool, complex numbers, the twelfth-order differential equation is reduced to a sixth-order.

The product of Eq. (4.12b) and imaginary unit i, and consequently the sum of the above product and Eq. (4.12a), allowed us to present the reduced equation as

$$b_6\frac{d^6}{dx^6}[K_1(x)+iK_2(x)]-b_4\frac{d^4}{dx^4}[K_1(x)+iK_2(x)]-b_2\frac{d^2}{dx^2}[K_1(x)+iK_2(x)]+$$
$$+b_1[K_1(x)+iK_2(x)]-\left\{ib_7\frac{d^6}{dx^6}[K_2(x)-iK_1(x)]+ib_5\frac{d^4}{dx^4}[K_2(x)-iK_1(x)]+\right. \quad (4.13)$$
$$\left.+ib_3\frac{d^2}{dx^2}[K_2(x)-iK_1(x)]\right\}=p_1(x)+ip_2(x)$$

Where

$$K_2(x)-iK_1(x)=-i[K_1(x)-\frac{1}{i}K_2(x)]$$

and

$$\frac{1}{i}=\frac{i}{i^2}=-i$$

then we have

$$K_2(x)-iK_1(x)=i[K_1(x)+iK_2(x)]$$

Substitution of above expression into Eq. (4.13) and set $K(x)=K_1(x)+iK_2(x)$, we can get

$$b_6\frac{d^6K(x)}{dx^6}-b_4\frac{d^4K(x)}{dx^4}-b_2\frac{d^2K(x)}{dx^2}+b_1K(x)+$$
$$+ib_7\frac{d^6K(x)}{dx^6}-ib_5\frac{d^4K(x)}{dx^4}-ib_3\frac{d^2K(x)}{dx^2}=p_1(x)+ip_2(x) \quad (4.14)$$

The equation (4.14) can be also written as the simple form

$$A_6\frac{d^6K(x)}{dx^6}+A_4\frac{d^4K(x)}{dx^4}+A_2\frac{d^2K(x)}{dx^2}+A_0K(x)=\bar{p}(x) \quad (4.15)$$

where

$$A_6=b_6+ib_7,\quad A_4=-(b_4+ib_5),\quad A_2=-(b_2+ib_3)$$
$$A_0=b_1,\quad \bar{p}(x)=p_1(x)+ip_2(x)$$

4.3 Approximate Analytical Solutions

The solutions of equation (4.15) can be expressed as

$$K(x,t)=K_h(x,t)+K_p(x,t) \quad (4.16)$$

where $K_h(x,t)$ is the homogeneous solution and $K_p(x,t)$ is the particular solution, and they are satisfied the following equations, respectively,

$$A_6\frac{d^6K_h(x)}{dx^6}+A_4\frac{d^4K_h(x)}{dx^4}+A_2\frac{d^2K_h(x)}{dx^2}+A_0K_h(x)=0 \quad (4.17a)$$

$$A_6\frac{d^6K_p(x)}{dx^6}+A_4\frac{d^4K_p(x)}{dx^4}+A_2\frac{d^2K_p(x)}{dx^2}+A_0K_p(x)=\bar{p}(x) \qquad (4.17b)$$

Especially for uniform distributed load, $p_1(x)$ and $p_2(x)$ are constant, consequently $\bar{p}(x)$ is also constant. By using the option 'Dsolve' in Software Package MATLAB, the homogeneous solution of the present beam model (4.17a) can be written in the following form

$$K_h(x)=C_1e^{k_1x}+C_2e^{k_2x}+C_3e^{k_3x}+C_4e^{k_4x}+C_5e^{k_5x}+C_6e^{k_6x} \qquad (4.18)$$

where $C_1\sim C_6$ are six constants of integration produced in solving a sixth-order differential equation (4.17a) and the particular solution of equation (4.17b) can be easily evaluated as

$$K_p(x)=\frac{\bar{p}}{A_0} \qquad (4.19)$$

As we discussed before, the complete solution of Eq. (4.15) can be obtained as

$$\begin{aligned}K(x)&=K_h(x)+K_p(x)\\&=C_1e^{k_1x}+C_2e^{k_2x}+C_3e^{k_3x}+C_4e^{k_4x}+C_5e^{k_5x}+C_6e^{k_6x}+\frac{\bar{p}}{A_0}\end{aligned} \qquad (4.20)$$

where

$$k_1=-\frac{1}{\sqrt{6}A_6\xi}[A_6\xi(-2A_4\xi+\xi^2-12A_2A_6+4A_4^2)]^{\frac{1}{2}}$$

$$k_2=\frac{1}{\sqrt{6}A_6\xi}[A_6\xi(-2A_4\xi+\xi^2-12A_2A_6+4A_4^2)]^{\frac{1}{2}}$$

$$k_3=\frac{1}{\sqrt{3}A_6\xi}[-A_4A_6\xi^2-9A_2A_4A_6^2+27A_0A_6^3+2A_4^3A_6-3\sqrt{3}A_6^2\zeta+3A_2A_6^2\xi-$$

$$-A_4^2A_6\xi+i\sqrt{3}(9A_2A_4A_6^2-27A_0A_6^3-2A_4^3A_6+3\sqrt{3}A_6^2\zeta+3A_2A_6^2-A_4^2A_6\xi)]^{\frac{1}{2}}$$

$$k_4=-\frac{1}{\sqrt{3}A_6\xi}[-A_4A_6\xi^2-9A_2A_4A_6^2+27A_0A_6^3+2A_4^3A_6-3\sqrt{3}A_6^2\zeta+3A_2A_6^2\xi-$$

$$-A_4^2A_6\xi+i\sqrt{3}(9A_2A_4A_6^2-27A_0A_6^3-2A_4^3A_6+3\sqrt{3}A_6^2\zeta+3A_2A_6^2-A_4^2A_6\xi)]^{\frac{1}{2}}$$

$$k_5=\frac{1}{\sqrt{3}A_6\xi}[-A_4A_6\xi^2-9A_2A_4A_6^2+27A_0A_6^3+2A_4^3A_6-3\sqrt{3}A_6^2\zeta+3A_2A_6^2\xi-$$

$$-A_4^2A_6\xi-i\sqrt{3}(9A_2A_4A_6^2-27A_0A_6^3-2A_4^3A_6+3\sqrt{3}A_6^2\zeta+3A_2A_6^2-A_4^2A_6\xi)]^{\frac{1}{2}}$$

$$k_6=-\frac{1}{\sqrt{3}A_6\xi}[-A_4A_6\xi^2-9A_2A_4A_6^2+27A_0A_6^3+2A_4^3A_6-3\sqrt{3}A_6^2\zeta+3A_2A_6^2\xi-$$

$$-A_4^2A_6\xi-i\sqrt{3}(9A_2A_4A_6^2-27A_0A_6^3-2A_4^3A_6+3\sqrt{3}A_6^2\zeta+3A_2A_6^2-A_4^2A_6\xi)]^{\frac{1}{2}}$$

and

$$\zeta = (4A_2^3 A_6 - A_2^2 A_4^2 - 18A_0 A_2 A_4 A_6 + 27A_0^2 A_6^2 + 4A_0 A_4^3)^{\frac{1}{2}}$$

$$\xi = (36A_2 A_4 A_6 - 108A_0 A_6^2 - 8A_4^3 + 12\sqrt{3}A_6\zeta)^{\frac{1}{3}}$$

The original input and output files of Software Package MATLAB to solve the Eq.(4.17) is shown in Appendix C. In the solution (4.20), the six constants $C_1 \sim C_6$ can be determined by using the boundary conditions as shown in chapter 3.

The equation (4.17) is called the complex differentiation equation and the coefficients $A_2 \sim A_6$ are complex numbers. So the solution $K(x)$ is also the complex function. The two functions $K_1(x)$ and $K_2(x)$ can be derived by separating the real part and imaginary part of the complex function $K(x)$, respectively. After we obtain the functions $K_1(x)$ and $K_2(x)$, we can use the equations (4.9), (4.5) and (3.4), (3.9) to get the displacement and resultant force of smart composite laminate beams.

4.4 Special Condition of Governing Equation

In the previous section, we discussed the general analytical solution of smart composite laminate beams. The formulation and solution can apply to any type of beams, such as cantilever beam, simply supported beam, laminate beam symmetric-ply layers and unsymmetric-ply layers. But for the laminate beams with symmetric-ply layers, the governing equations (4.1a~c) have a special condition. In this section, we will mainly discuss this problem.

When the laminate beam has symmetric ply distribution, for the governing equation (4.1a~c), we have $\overline{B}_{11} = 0, \beta_2 = 0, b = 0$ and $I_2 = 0$. However when the external electrical field is applied to the actuator layer, that is the feedback control gain $G_i \neq 0$, the laminated beam still exhibits the electromechanical behaviour. The reason for this phenomenon is the external electrical field only applies to the actuator layer. But for the sensor layer, there is that not any external electrical force. For this condition, we can still use the solution that is shown in the previous section. But when the feedback control gain $G_i = 0$, that is, no external electrical field is applied to the beam structure. The derivative operators $L_{13} = L_{31} = 0$, then the governing equations (4.1a~c) can be simply rewritten as

$$L_{11}(u_0) = 0 \tag{4.21a}$$

$$L_{22}(w_0) + L_{23}(\psi_0) = p(x,t) \tag{4.21b}$$

$$L_{32}(w_0) + L_{33}(\psi_0) = 0 \tag{4.21c}$$

where the Eq. (4.21a) is not coupled with Eqs. (4.21b) and (4.21c). The equation (4.21a) is the axial vibration of beam and the equation (4.21b~c) are the transverse vibration of the beam accounting for the effect of transverse deformation.

Substitution of derivative operator L_{11} into Eq. (4.21a), we have

$$-a\frac{\partial^2 u_0}{\partial x^2}+I_1\frac{\partial^2 u_0}{\partial t^2}=0 \tag{4.22}$$

Applying the same procedure as in the section 4.3, from Eq. (4.21c), we have $L_{32}(w_0)=-L_{33}(\psi_0)$, introducing the displacement potential function $F(x, t)$, we can get the displacement w_0 and rotation ψ_0 as

$$w_0=-L_{33}(F),\quad \psi_0=L_{32}(F) \tag{4.23}$$

Substituting Eq. (4.23) in Eq. (4.21b), we can obtain the equation of the displacement potential function $F(x, t)$ as

$$-L_{22}L_{33}(F)+L_{23}L_{32}(F)=p(x,t) \tag{4.24}$$

From the above discussion, we can observe that if the beam has symmetric-ply distribution and the negative velocity feedback control gain is zero, the governing equation will change to two uncoupled equations (4.22) and (4.24).

Here, exactly same as in the previous section, we assume the forms of the external exciting force, the displacement potential function as Eqs. (4.8) and (4.9) and axial displacement as

$$u_0(x,t)=\bar{u}_0(x)[\sin(\omega t)+\cos(\omega t)] \tag{4.25}$$

Substituting Eq. (4.25) in Eq. (4.22) and setting $\frac{I_1}{a}=\frac{1}{k^2}$, we can get

$$\frac{d^2\bar{u}_0}{dx^2}+\frac{\omega^2}{k^2}\bar{u}_0=0 \tag{4.26}$$

and the solution of Eq. (4.26) can be easily obtained as

$$\bar{u}_0(x)=C_1e^{i\frac{\omega}{k}x}+C_2e^{-i\frac{\omega}{k}x} \tag{4.27}$$

Substitution of Eq. (4.27) into Eq. (4.25), we can get the complete solution of axial displacement as

$$u_0(x,t)=(C_1e^{i\frac{\omega}{k}x}+C_2e^{-i\frac{\omega}{k}x})[\sin(\omega t)+\cos(\omega t)] \tag{4.28}$$

Substituting Eqs. (4.8) and (4.9) in Eq. (4.24), expanding the derivative operators (for more detail, please see Appendix B) and simplifying the equations, we can obtain the two equations of functions $K_1(x)$ and $K_2(x)$ as

$$b_4 \frac{d^4 K_1(x)}{dx^4} + b_2 \frac{d^2 K_1(x)}{dx^2} + b_1 K_1(x) = p_1(x) \tag{4.29a}$$

$$b_4 \frac{d^4 K_2(x)}{dx^4} + b_2 \frac{d^2 K_2(x)}{dx^2} + b_1 K_2(x) = p_2(x) \tag{4.29b}$$

respectively, where

$$b_1 = (I_1 \bar{A}_{55} - I_1 I_3 \omega^2)\omega^2, \quad b_2 = -(I_3 \bar{A}_{55} - I_1 d)\omega^2, \quad b_4 = -\bar{A}_{55} d$$

The product of Eq. (4.12b) and imaginary unit i, and consequently the sum of the above product and Eq. (4.12a), allowed us to present the reduced equation as

$$\begin{aligned} &b_4 \frac{d^4}{dx^4}[K_1(x) + iK_2(x)] + b_2 \frac{d^2}{dx^2}[K_1(x) + iK_2(x)] + \\ &+ b_1[K_1(x) + iK_2(x)] = p_1(x) + ip_2(x) \end{aligned} \tag{4.30}$$

By setting $K(x) = K_1(x) + iK_2(x)$ and $\bar{p}(x) = p_1(x) + ip_2(x)$, the Eq. (4.30) can be written as

$$b_4 \frac{d^4 K(x)}{dx^4} + b_2 \frac{d^2 K(x)}{dx^2} + b_1 K(x) = \bar{p}(x) \tag{4.31}$$

Compare with equation (4.15), the equation (4.31) is only a fourth-order differentiation equation because of the symmetric-ply of laminated beam and negative velocity of feedback control gain $G_i = 0$. The solutions of Eq. (4.31) can also be written as

$$K(x,t) = K_h(x,t) + K_p(x,t) \tag{4.32}$$

where $K_h(x,t)$ is the homogeneous solution and $K_p(x,t)$ is the particular solution, and they satisfy the following equations,

$$b_4 \frac{d^4 K_h(x)}{dx^4} + b_2 \frac{d^2 K_h(x)}{dx^2} + b_1 K_h(x) = 0 \tag{4.33a}$$

$$b_4 \frac{d^4 K_p(x)}{dx^4} + b_2 \frac{d^2 K_p(x)}{dx^2} + b_1 K_p(x) = \bar{p}(x) \tag{4.33b}$$

respectively.

Similar to the previous section, for the uniform distributed load, $p_1(x)$ and $p_2(x)$ are constant and $\bar{p}(x)$ is also constant. Then the particular solution $K_p(x,t)$ can be easily found by observing the Eq. (4.33b) as

$$K_p(x) = \frac{\bar{p}}{b_1} \tag{4.34}$$

The homogeneous solution $K_h(x,t)$ can be obtained by using Software Package MATLAB as

$$K_h(x) = C_3 e^{k_1 x} + C_4 e^{k_2 x} + C_5 e^{k_3 x} + C_6 e^{k_4 x} \tag{4.35}$$

where

$$k_1 = -\sqrt{\frac{-b_2 - \sqrt{b_2^{\,2} - 4b_1 b_4}}{2b_4}}, \qquad k_2 = \sqrt{\frac{-b_2 - \sqrt{b_2^{\,2} - 4b_1 b_4}}{2b_4}}$$

$$k_3 = -\sqrt{\frac{-b_2 + \sqrt{b_2^{\,2} - 4b_1 b_4}}{2b_4}}, \qquad k_4 = \sqrt{\frac{-b_2 + \sqrt{b_2^{\,2} - 4b_1 b_4}}{2b_4}}$$

The complete solution of Eq. (4.31) can be written as

$$\begin{aligned} K(x) &= K_h(x) + K_p(x) \\ &= C_3 e^{k_1 x} + C_4 e^{k_2 x} + C_5 e^{k_3 x} + C_6 e^{k_4 x} + \frac{\bar{p}}{b_1} \end{aligned} \tag{4.36}$$

In the equations (4.28) and (4.36), the six constants $C_1 \sim C_6$ can also be determined by using the boundary conditions as shown in chapter 3. The two functions $K_1(x)$ and $K_2(x)$ can be derived by separating the real part and imaginary part of the complex solution $K(x)$, which is shown in Eq. (4.36). Also, after we get the two functions $K_1(x)$ and $K_2(x)$, we can use the equations (4.9), (4.23), (4.28) and (3.4), (3.9) to get the displacement and resultant force of smart composite laminate beam when there is no external electrical field applied to the present beam model.

In this chapter, we discussed the approximate analytical solution of smart composite laminate beams based on the Reissner-Mindlin plate theory. The numerical results of this approximate analytical solution will be presented in next chapter.

Chapter 5

Results and Discussions

5.1 Introduction

The applications of laminate beams with active and sensory piezoelectric layers (PVDF) are presented in this chapter. The force-vibration of a cantilevered laminated composite beam with surface bonded continuous piezoelectric layers is analyzed. Several examples will be considered in this section. The four-layers and eight-layers laminated beams with different ply orientation of smart composite beams are studied. In all cases, the standard laminate notation is augmented to indicate the lamination and the location of piezoelectric material through the thickness, with the letter *p* indicating the piezoelectric layer. The Software Package MATHEMATICA will be used to calculate the numerical results and graphical representation thereof in this chapter. The next paragraph is the brief introduction of this software package.

- **About Software Package MATHEMATICA**

Mathematica is the world's only fully integrated environment for technical computing. First released in 1988, it has had a profound effect on the way computers are used in many technical and other fields.

It is often said that the release of *Mathematica* marked the beginning of modern technical computing. Ever since the 1960s individual packages had existed for specific numerical, algebraic, graphical and other tasks. But the visionary concept of the package was to create once and for all a single system that could handle all the various aspects of technical computing in a coherent and unified way. The key intellectual advance that made this possible was the invention of a new kind of symbolic computer language that could for the first time manipulate the very wide range of objects involved in technical computing using only a fairly small number of basic primitives.

At first, *Mathematica*'s impact was felt mainly in the physical sciences, engineering and mathematics. But over the years, it has become important in a remarkably wide range of fields. *Mathematica* is used today throughout the sciences—physical, biological, social and other—and counts many of the world's foremost scientists among its enthusiastic supporters. It has played a crucial role in many important discoveries, and has been the basis for thousands of technical papers. In engineering, the software package has become a standard tool for both development and production, and by now many of the world's important new products rely at one stage or another in their design on *Mathematica*. In commerce, *Mathematica* has played a significant role in the growth of sophisticated financial modelling, as well as being widely used in many kinds of general planning and analysis. It has also emerged as an important tool in computer science and software development: its language component is widely used as a research, prototyping and interface environment.

At a technical level, *Mathematica* is widely regarded as a major feat of software engineering. It is one of the largest single application programs ever developed, and it contains a vast array of novel algorithms and important technical innovations. Among these innovations is the concept of platform-independent interactive documents known as notebooks. Notebooks have already become the standard for many kinds of courseware and reports, and with the new capabilities added in *Mathematica* 3.0 they are poised to emerge as a general standard for publishing technical documents on the web and elsewhere.

There are today nearly a hundred specialized commercial packages available for *Mathematica*, as well as several periodicals and more than two hundred books devoted to the system.

5.2 Numerical Results

An intelligent beam structure containing distributed piezoelectric Sensor/Actuator on both the top and bottom surface is shown in Figure 5.1. In this structure, the piezoelectric of the bottom layer is considered as a sensor to sense the strain and generate the electrical potential and the piezoelectric of the top layer as an actuator to control the vibration of the structure. As mentioned before, the model of cantilever beam will be considered in this section. The smart structure can be divided arbitrarily. All material properties used are shown in Table 5.1.

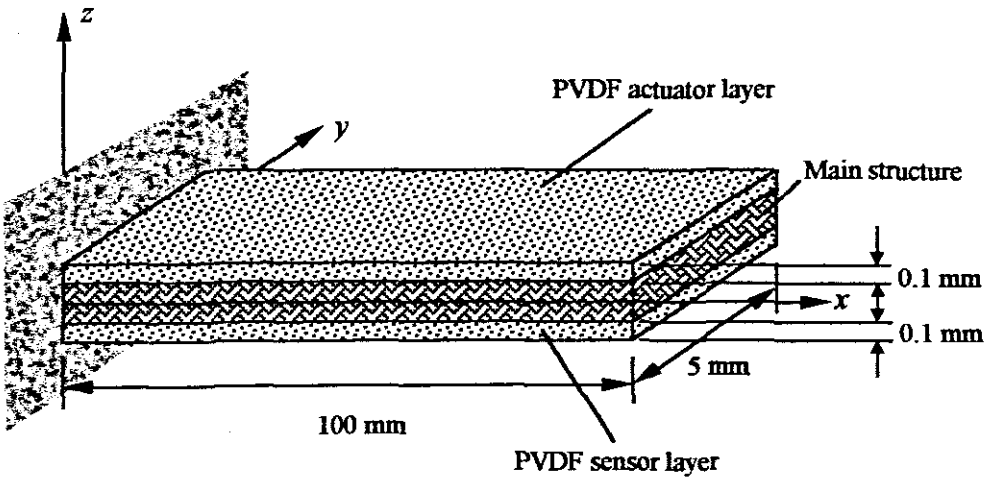

Figure 5.1 A beam with piezoelectric sensor and actuator

In the classical vibration theory, the natural frequency of Bernoulli-Euler cantilever beam can be written as

$$\omega_i = (\beta_i l)^2 \sqrt{\frac{EI}{\rho A l^4}} \qquad i = 1, 2, \cdots$$

For the first natural frequency, the above expression can be rewritten as

$$\omega_1 = 3.515\sqrt{\frac{EI}{\rho A l^4}} \tag{5.1}$$

Table 5.1 The material properties of the main structure and piezoelectric

Property	PVDF	Graphite/Epoxy
E_1	0.2E+10 N/m^2	0.98E+11 N/m^2
E_2	0.2E+10 N/m^2	0.79E+10 N/m^2
G_{12}	0.775E+9 N/m^2	0.56E+10 N/m^2
G_{23}	—	0.385E+10 N/m^2
ν_{12}	0.29	0.28
ρ	1800 kg/m^3	1520 kg/m^3
e_{31}	0.046 C/m^2	—
e_{32}	0.046 C/m^2	—
e_{33}	0.0	—
g_{11}	0.1062E–9 F/m	—
g_{22}	0.1062E–9 F/m	—
g_{33}	0.1062E–9 F/m	—
t	0.1E–3 m	0.125E–3 m

As we know, the Bernoulli-Euler beam does not account for the lateral strain. For thin beams, accurate results can still be obtained. In this project, the present beam model comes from Reissner-Mindlin plate theory. It considers the effect of the transverse strain. Compared to the length of beam, the present beam model is still very thin and we can use Eq. (5.1) to estimate the first natural frequency of different ply orientation of laminated beams. To calculate the equivalent stiffness (EI), we use the stiffness along the length of beam of each layer. That is $\sum_{k=1}^{n} \tilde{Q}_{11k} I_k$, I_k is the moment of inertia to the mid-plane of the laminate beam for k^{th} layer. The first natural frequency of different ply orientation is shown in Table 5.2.

Table 5.2 The first natural frequency of laminated beams

Ply Orientation	Equivalent Stiffness EI (Nm^2)	First Natural Frequency (rad/s)
[0°/0°/0°/0°]	5.30188E–3	342.016
[0°/90°/90°/0°]	4.71529E–3	322.541
[45°/-45°/-45°/45°]	0.87053E–3	138.587
[30°/50°/50°/30°]	1.26172E–3	166.845
[-45°/30°/-30°/45°]	0.927769E–3	143.071
[0°/90°/0°/90°]	2.95553E–3	255.358
[0°/45°/-45°/90°]	2.6949E–3	243.839
[0°/30°/-30°/90°]	2.75214E–3	246.415
[0°/0°/0°/0°/0°/0°/0°/0°]	4.14936E–2	738.502
[0°/0°/90°/90°/90°/90°/0°/0°]	3.68009E–2	695.489
[0°/0°/90°/90°/0°/0°/90°/90°]	2.27228E–2	546.502

A cantilever laminated beam with distributed piezoelectric PVDF layer serving as a distributed actuator on the top surface, and another PVDF on the bottom surface as a distributed sensor, will be used as a case study. The beam dimensions considered are: *length* l = 100 mm and *width* b = 5mm. As we mentioned before, the numerical results of the four layers and eight layers laminated beams will be presented in this chapter. The thickness of the beam can be generally written as $h = n \times 0.125\text{E}{-3}$ m and piezoelectric PVDF layer is taken as 0.1×10^{-3} m (see Table 5.1). The applied transverse load is uniformly distributed and has a magnitude of $p_1(x) = p_2(x) = 2.5\times10^3$ N/m^2.

The transverse displacement for the tip of the laminated cantilever beam with the different ply orientation is obtained using the present method. The transverse displacement of four layers laminated composite beams with actuator and sensor layer on the top and bottom surface respectively, for feedback gains of 0, 40, 100 and 140, are shown in the following figures. Firstly, according to Table 5.2, we take the frequency of the external applied force as 10 Hz.

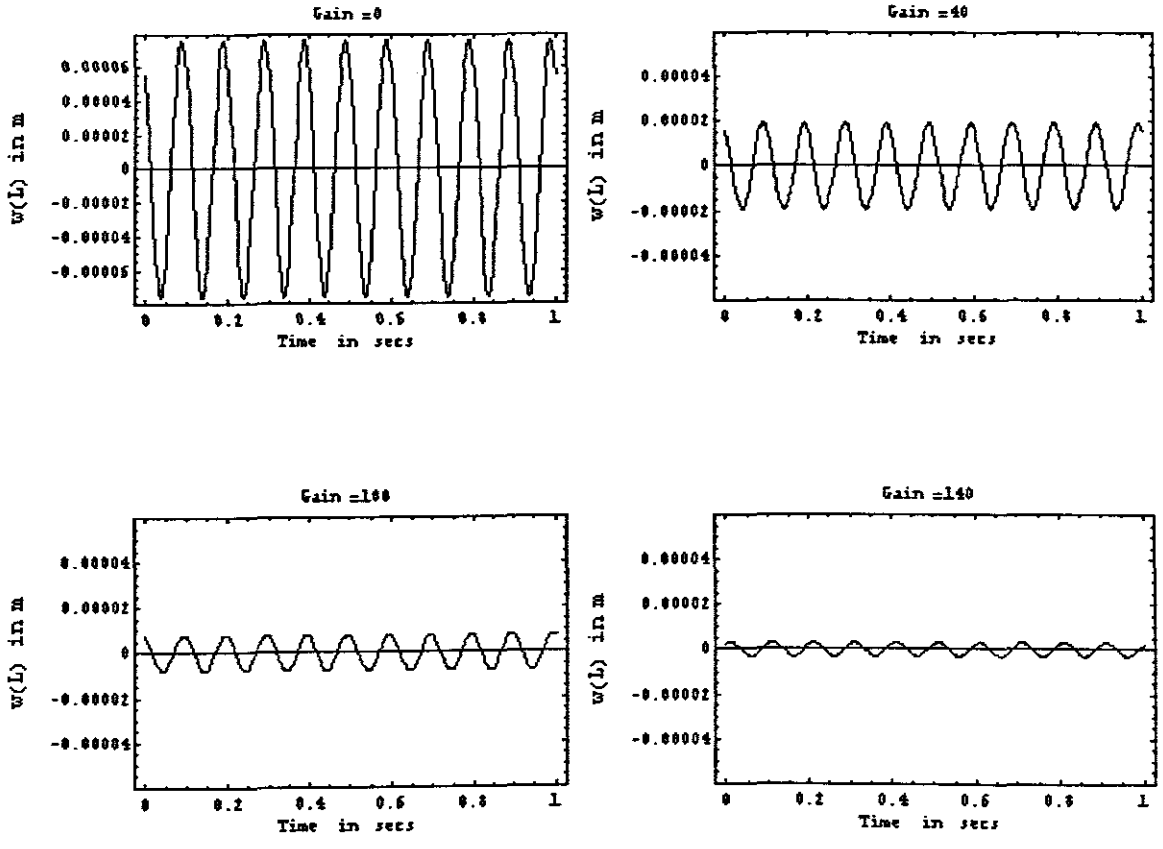

Figure 5.2 Effect of negative velocity feedback gain on the tip transient response [0°/0°/0°/0°]

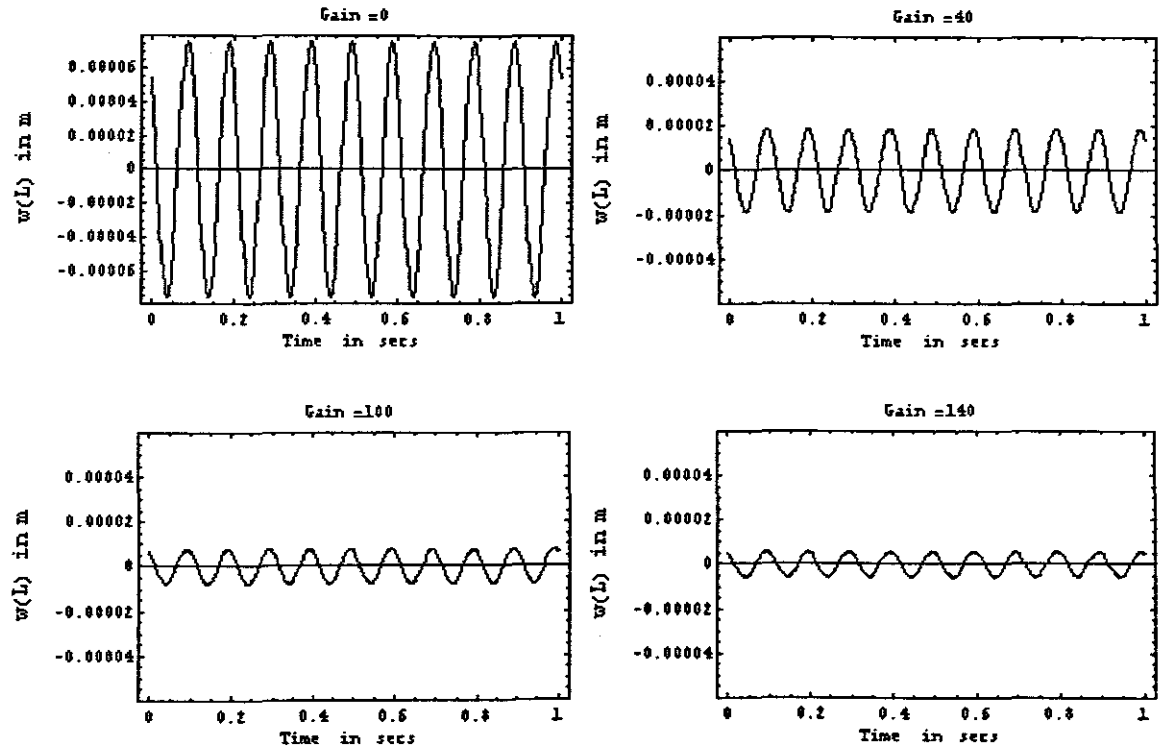

Figure 5.3 Effect of negative velocity feedback gain on the tip transient response [0°/90°/90°/0°]

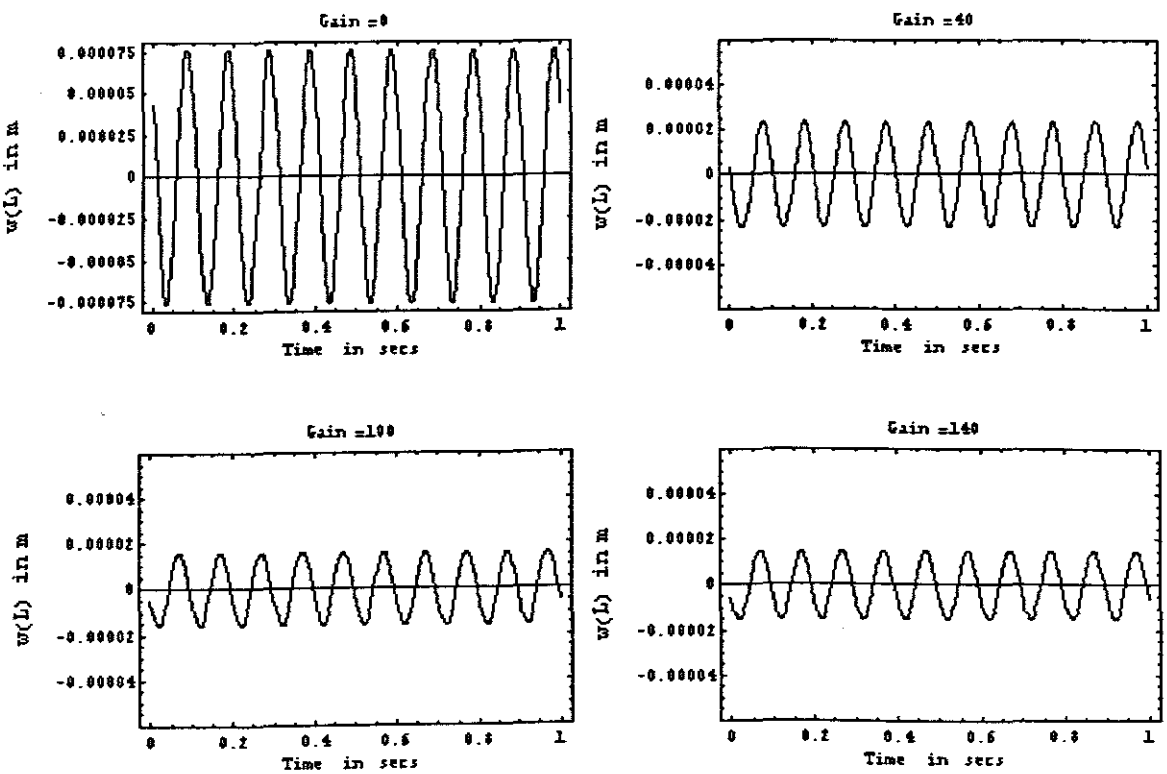

Figure 5.4 Effect of negative velocity feedback gain on the tip transient response [45°/-45°/-45°/45°]

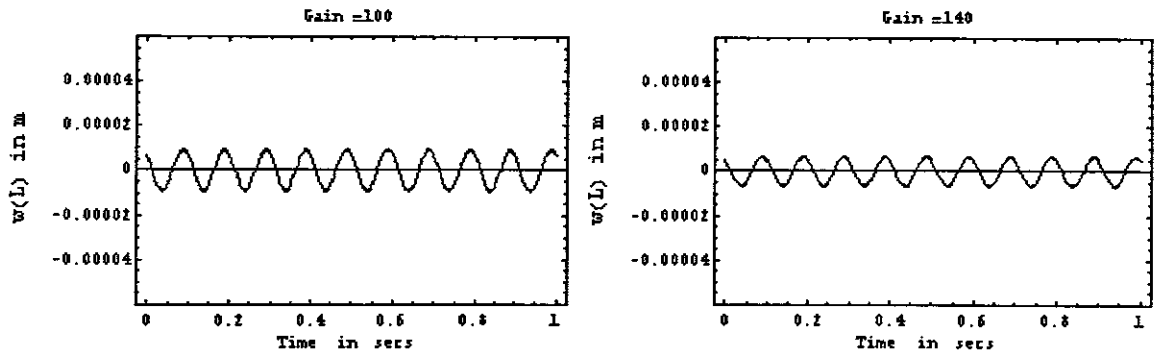

Figure 5.6 Effect of negative velocity feedback gain on the tip transient response [0°/90°/0°/90°]

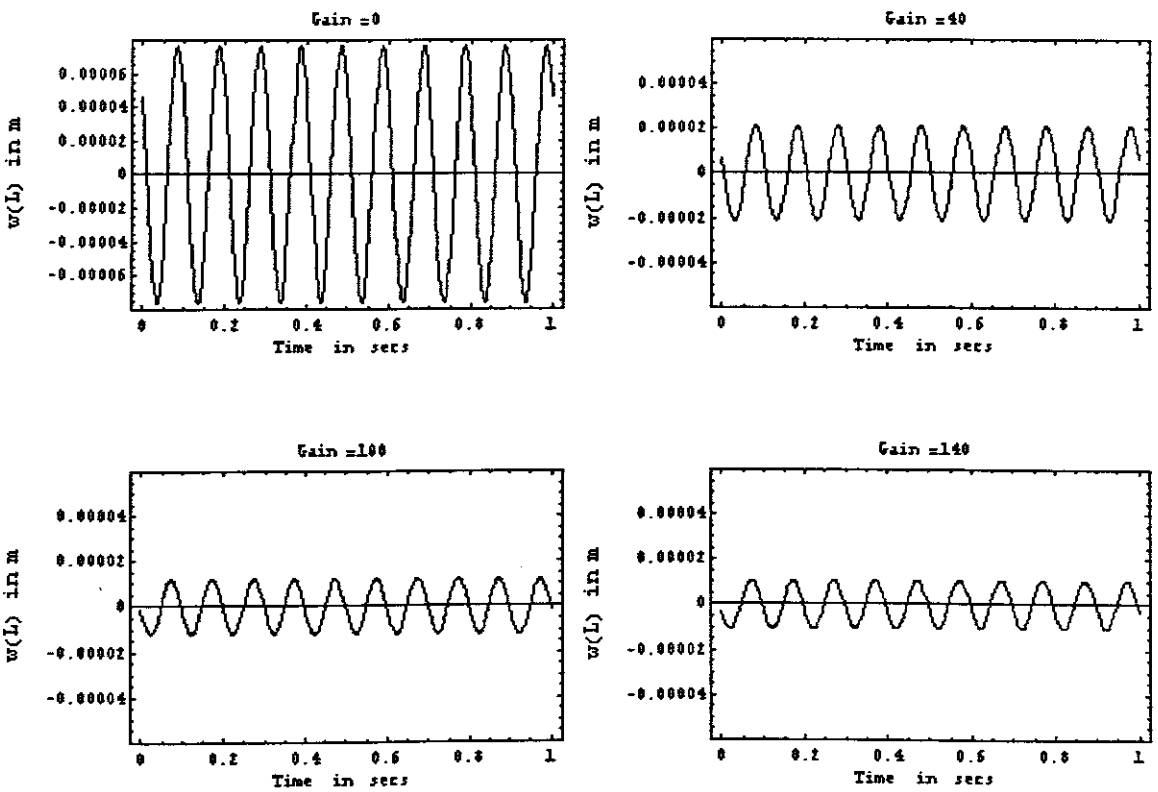

Figure 5.7 Effect of negative velocity feedback gain on the tip transient response [-45°/30°/-30°/45°]

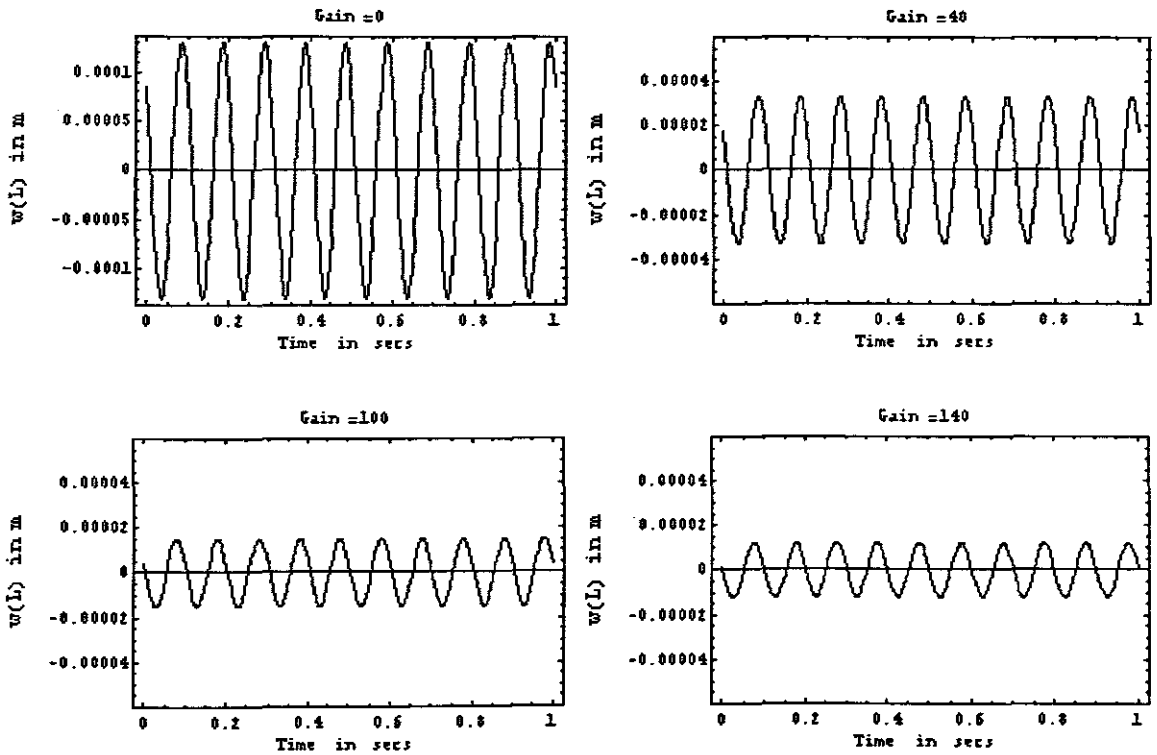

Figure 5.8 Effect of negative velocity feedback gain on the tip transient response [0°/45°/-45/90°]

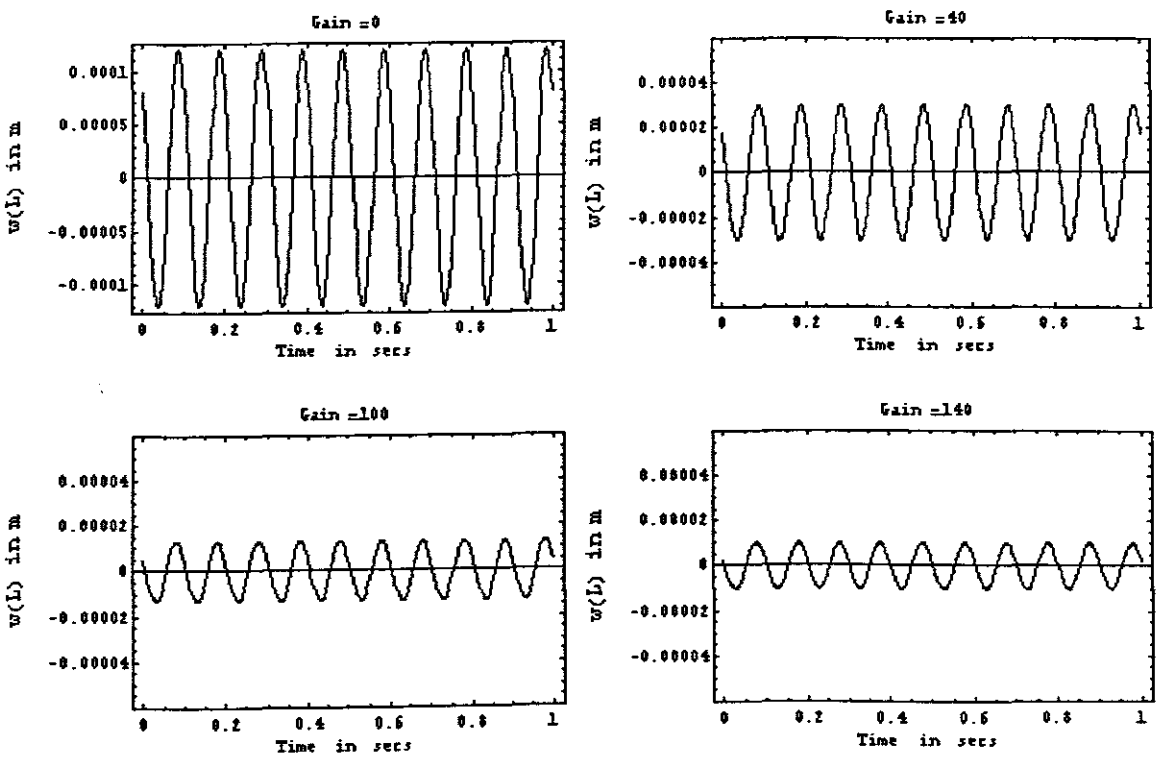

Figure 5.9 Effect of negative velocity feedback gain on the tip transient response [0°/30°/-30°/90°]

From the above figures, it is observed that for orthotropic and cross-ply beams there is hardly a noticeable difference, but there exists a considerable difference in the case of angle-ply beams. Having studied the open loop response, the direct and converse piezoelectric features are coupled with a negative velocity feedback control algorithm in order to analyze the closed loop response. It is evident from all the above graphs that transient tip amplitude of the beam gets damped out quickly when the higher feedback control gains are applied. This also illustrates the applicability of the present approximate solution. From the Figure (5.2) to (5.9), it can be easily observed the significant effect of the lamination scheme or stacking sequences of laminated beams. According to different ply orientation of each layer and lamination scheme, the stiffness of the laminated beam also has significant difference, which is shown in Table 5.2. There is larger amplitude on the tip of the beam if the stiffness of the beam is small. This can be observed from the Figures (5.2) ~ (5.9). This also verified the correctness of the present method. We can also see that the Figures (5.2) and (5.3) show very good control purpose for the general orthotropic and regular symmetric cross-ply laminated beams. From the above results, we can also find that when the feedback control gain $G_i > 100$, the control purpose is not very distinct. In order to analyze the optimal feedback control gain, the following results (The tip deflection of the beam versus feedback control gain for the different ply orientation) will be presented.

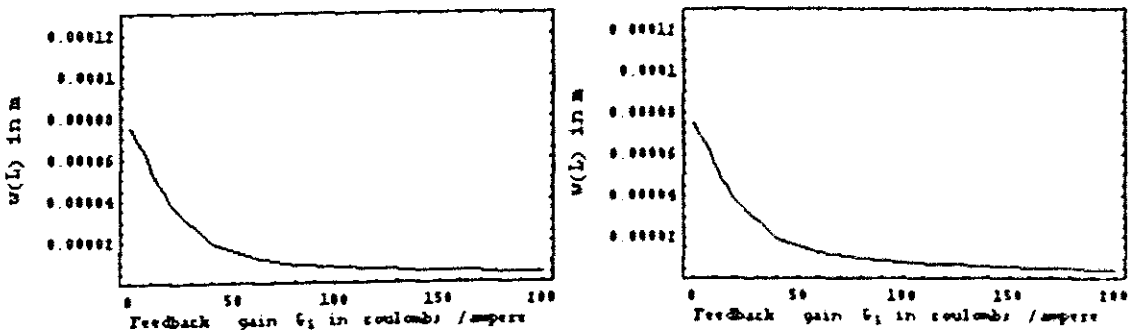

Figure 5.10 *The tip deflection of beam versus feedback control gain*
(a) [0°/0° 0° 0°]; (b) [0° 90° 90° 0°]

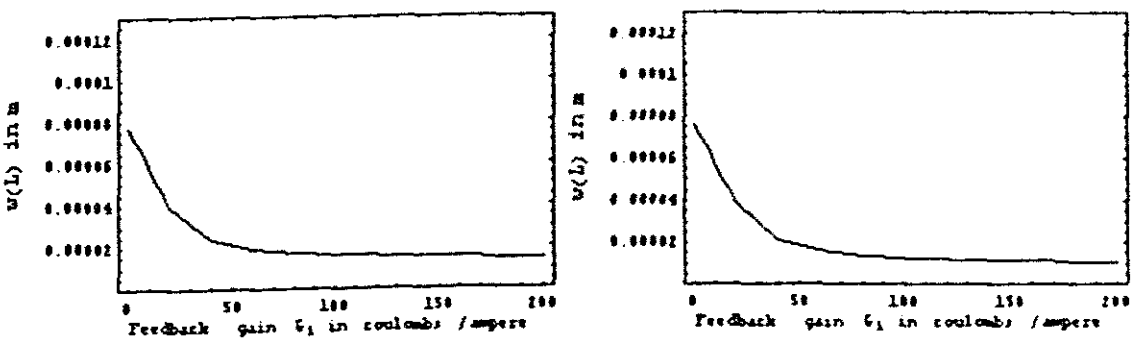

Figure 5.11 The tip deflection of beam versus feedback control gain
(a) [45°/-45°/-45°/45°]; (b) [30°/50°/50°/30°]

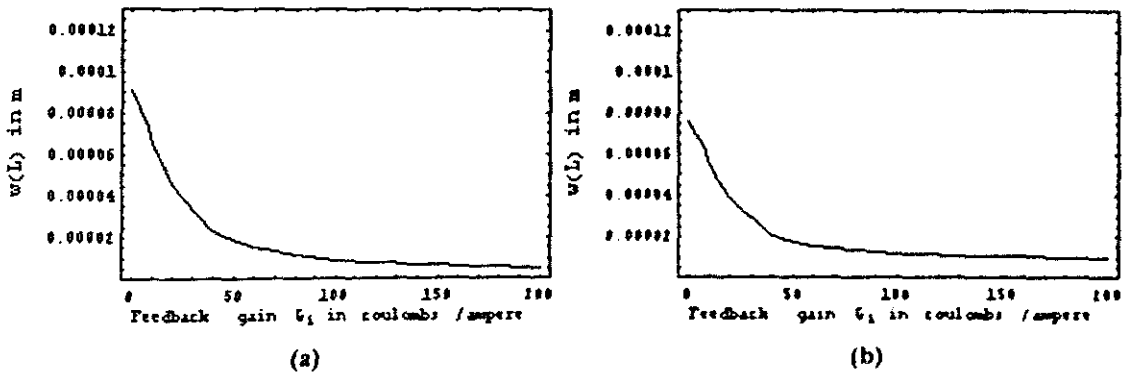

Figure 5.12 The tip deflection of beam versus feedback control gain
(a) [0°/90°/0°/90°]; (b) [-45°/30°/-30°/45°]

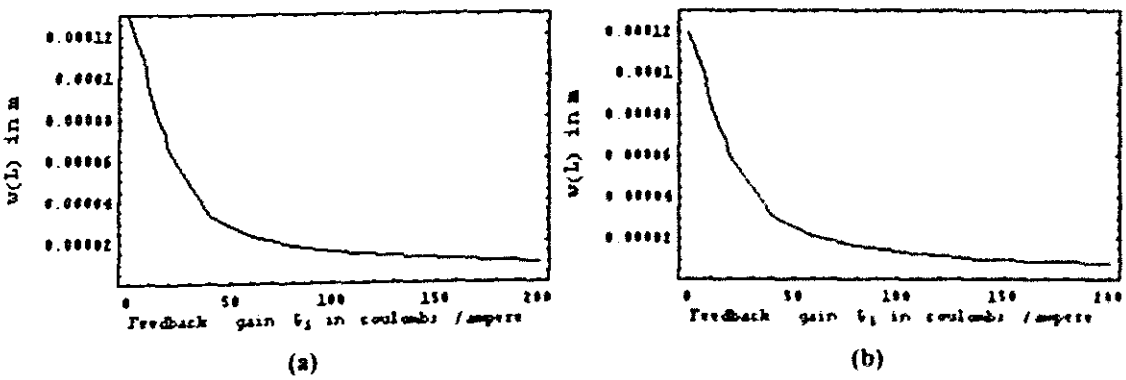

Figure 5.13 The tip deflection of beam versus feedback control gain
(a) [0°/45°/-45°/90°]; (b) [0°/30°/-30°/90°]

The above results show the effect of feedback control gain for the tip deflection of laminated beams. It can be found that the tip deflection (amplitude) of the beam decreases quickly while the feedback control gain increases. When the control gain G_i less than 100 coulombs/ampere, the control purpose is very effective. But when the control gain G_i > 100 coulombs/ampere, the tip deflection decreases very slowly. From all these phenomena, we can say the optimal feedback control gain of present beam model is about 100 coulombs/ampere. From Figure (5.10) to (5.13), we can also see the ply orientation or lamination scheme of the laminated beam really affect the control purpose. The symmetric cross-ply of laminated beams has a good control purpose than symmetric angle-ply, the antisymmetric cross-ply and angle-ply as well.

The output (sensitive) and input (active) voltage is another important feature of smart laminate composite structure. The next results will present the output and input voltage of vibration of smart laminated beams with different ply orientations. The relations

between output voltage and input voltage will also be analyzed. Please note that all of the input and output voltages, which are presented here, is based on the feedback control gain $G_i = 40$ coulombs/ampere.

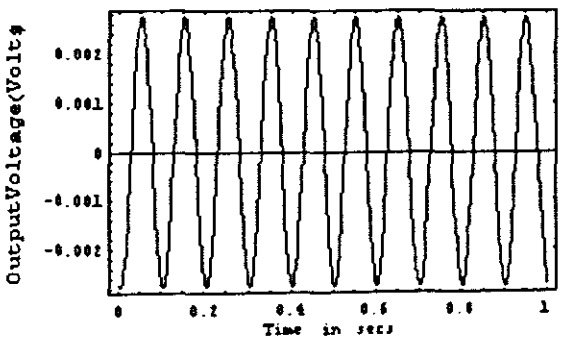

Figure 5.14 The output voltage from sensor layer [0°/90°/90°/0°]

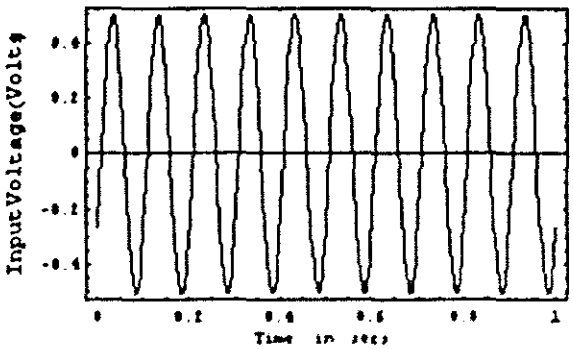

Figure 5.15 The input voltage act on actuator layer [0°/90°/90°/0°]

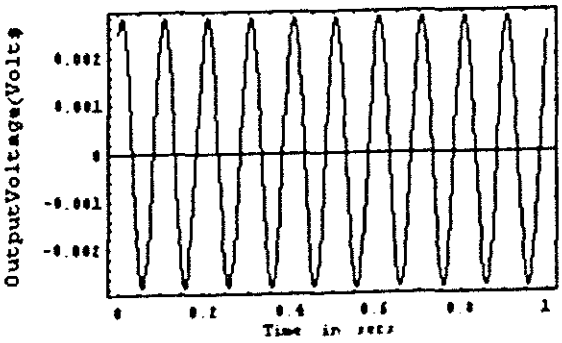

Figure 5.16 The output voltage from sensor layer [45°/-45°/-45°/45°]

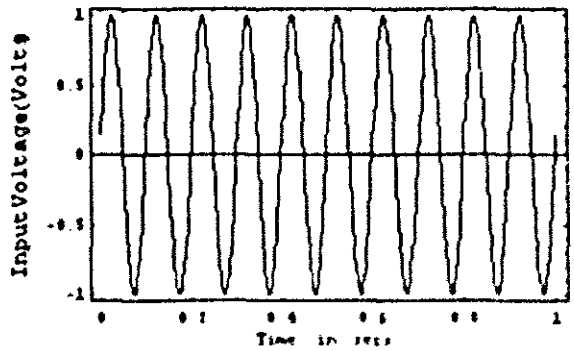

Figure 5.17 The input voltage act on actuator layer [45°/-45°/-45°/45°]

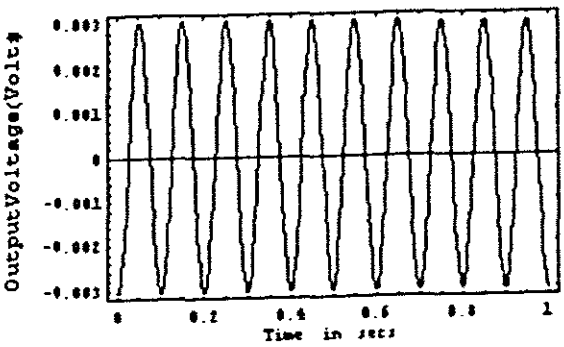

Figure 5.18 The output voltage from sensor layer [0°/90°/0°/90°]

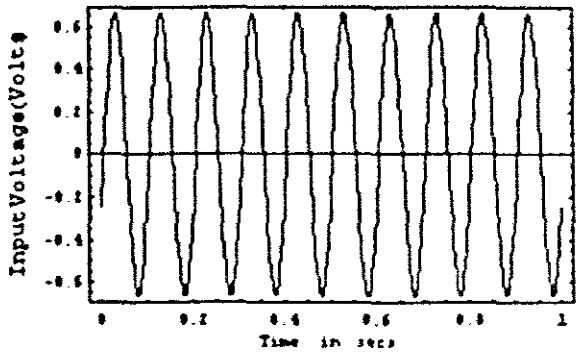

Figure 5.19 The input voltage act on actuator layer [0°/90°/0°/90°]

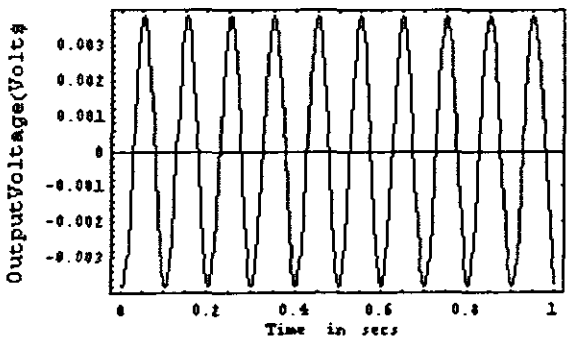

Figure 5.20 The output voltage from sensor layer [0°/45°/-45°/90°]

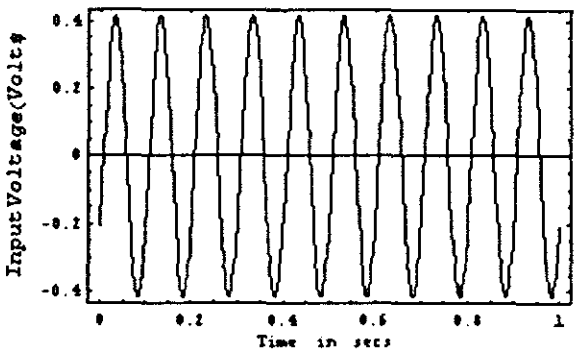

Figure 5.21 The input voltage act on actuator layer [0°/45°/-45°/90°]

The above results showed the output and input voltage from sensor and actuator layers with the different ply orientation, respectively. Firstly, we can observe that the output and input voltage vary as the beam vibrates, and their vibrational period is the same as the period of laminated beam. From the figures, we can also see that there is about a $\pi/2$ phasic difference between input and output voltage. Secondly, from the results, it shows that the different ply orientation causes the different output and input voltage. It is affected by several reasons, such as the stiffness of the beam, the frequency of the external applied force, and so on. In this project, we first assume that the frequency of the external applied force is 10 Hz. For some of the ply orientation laminated beams, this frequency is far from their first natural frequency (such as symmetric cross-ply), but for some of the laminated beams, it is very close to their first natural frequency (such as symmetric angle-ply). Hence, these results show us the very complicated situation of the input and output voltage with the different ply orientation.

In the following section, the vibration control is studied while the higher frequency of external force act on the laminated beam. They included the two cases, the regular symmetric cross-ply ([0°/90°/90°/0°]) laminated beam which applied by the higher frequency (55 Hz) of the external force; the regular symmetric angle-ply ([45°/–45°/–45°/45°]) laminated beam which is subjected to the frequency (25 Hz) of the external applied force. These results serve to illustrate the control effect of the present method if the frequency of external force is more than the first natural frequency of laminated beams.

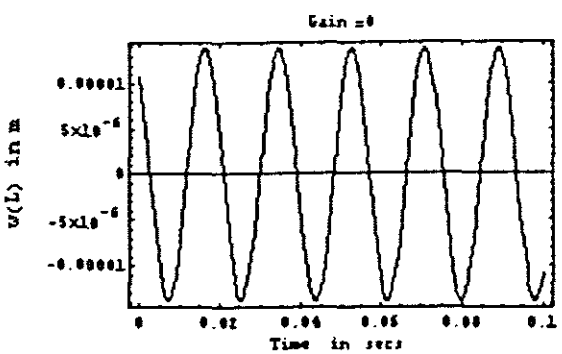

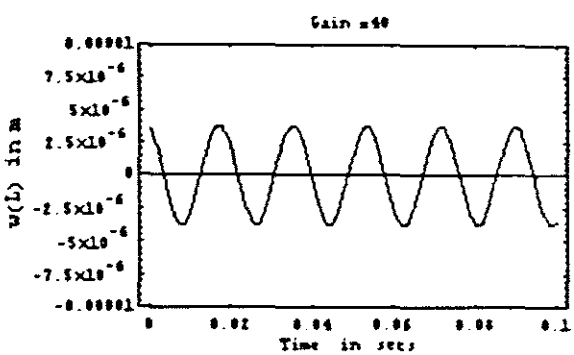

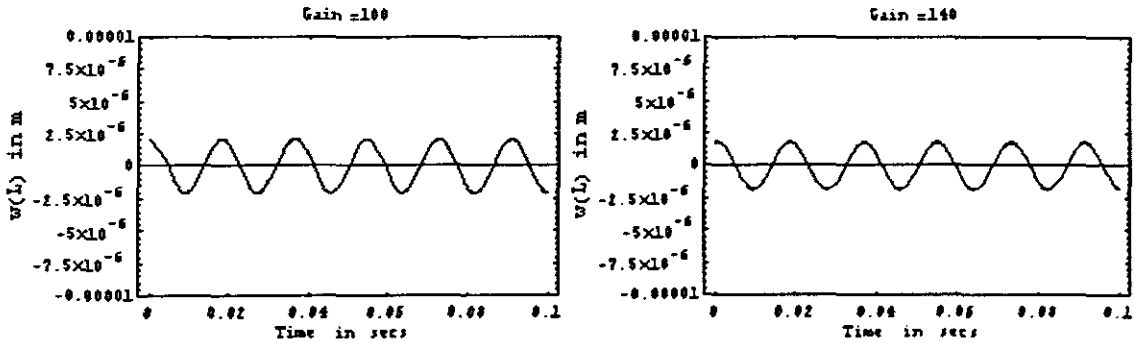

Figure 5.22 Effect of negative velocity feedback gain on the tip transient response [0°/90°/90°/0°]

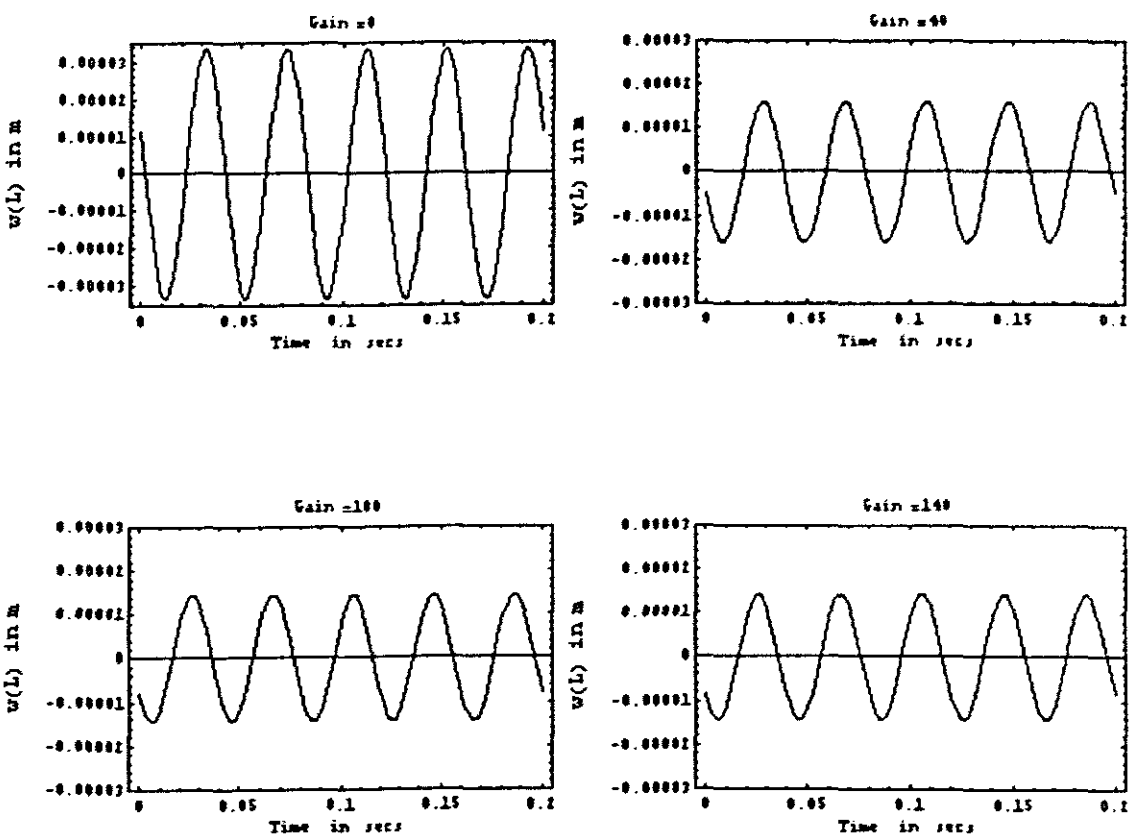

Figure 5.23 Effect of negative velocity feedback gain on the tip transient response [45°/-45°/-45°/45°]

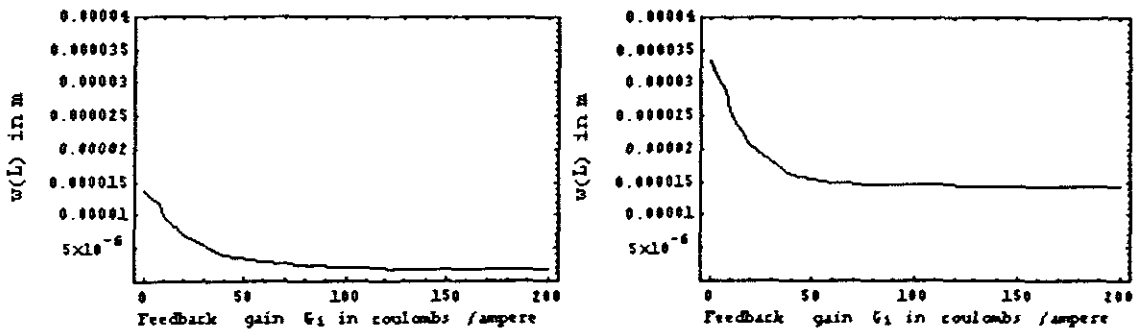

Figure 5.24 The tip deflection of beam versus feedback control gain
(a) [0°/90°/90°/0°]; (b) [45°/-45°/-45°/45°]

The Figures (5.22) and (5.23) contain the amplitude of vibration at the tip of the cantilever beam for two different ply orientations which are subjected to the higher frequency of external force as we mentioned previously. The tip deflection of the beam versus the feedback control gain is shown in Figure (5.24). The Figures (5.22) and (5.23) indicate that control function of the composite beam that is subject to the higher frequency of applied force is very evident. Comparing with the previous results, the results in Figure (5.24) shows that the optimal control gain is about 80 coulombs/ampere, which is subjected to the higher frequency of applied force on the beam. Also, the symmetric cross-ply has the better control purpose than the symmetric angle-ply of the composite beam. The input and output voltage are also shown in the following figures, which indicates that the external force has the high frequency.

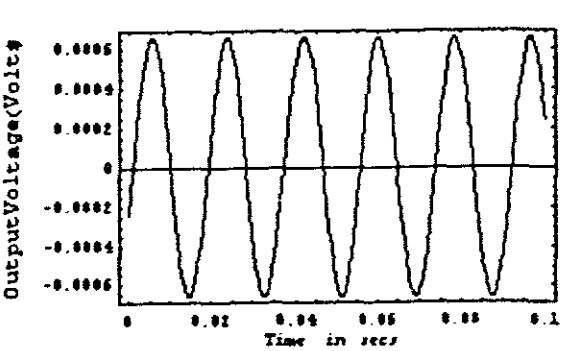

Figure 5.25 The output voltage from sensor layer [0°/90°/90°/0°]

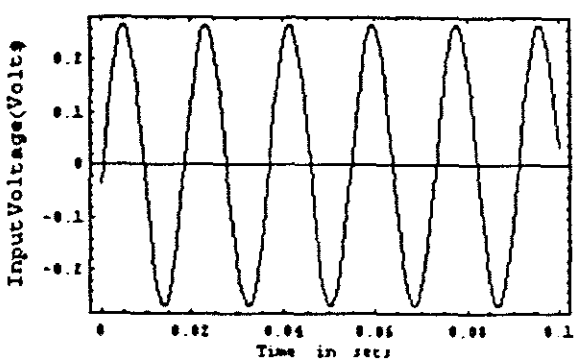

Figure 5.26 The input voltage act on actuator layer [0°/90°/90°/0°]

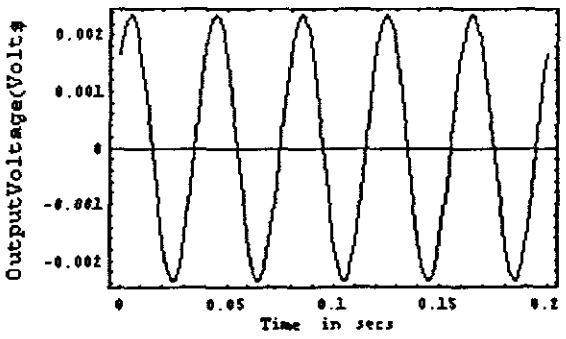

Figure 5.27 The output voltage from sensor layer [45°/-45°/-45°/45°]

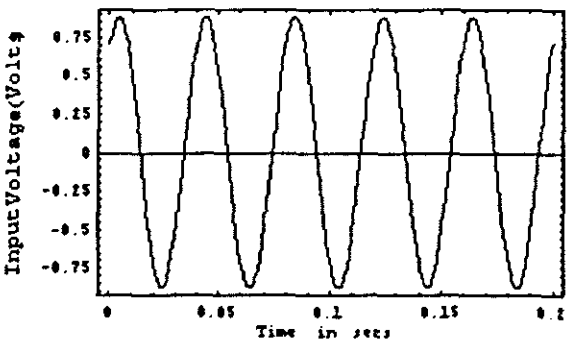

Figure 5.28 The input voltage act on actuator layer [45°/-45°/-45°/45°]

In the previous study, we discussed the behaviour of the four layers smart laminated composite beam with the different lamination schemes or stacking sequences. The results also pointed out predominant effects in the response of composite beams with the lower and higher frequency of external applied force. The next study, we will consider the laminated composite beam with eight different ply orientation layers and discuss the control effects of these cases. According to the Table 5.2, we first take 50 Hz as the frequency of external force.

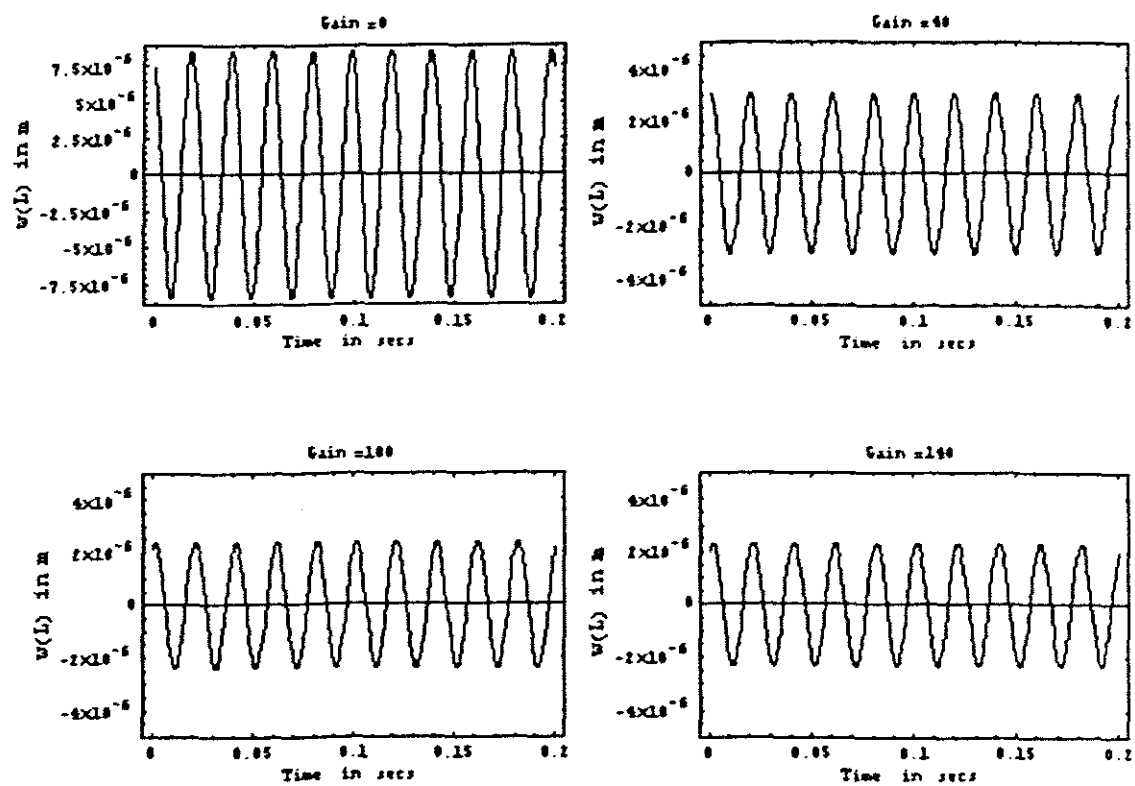

Figure 5.29 Effect of negative velocity feedback gain on the tip transient response [0°/0°/0°/0°/0°/0°/0°/0°]

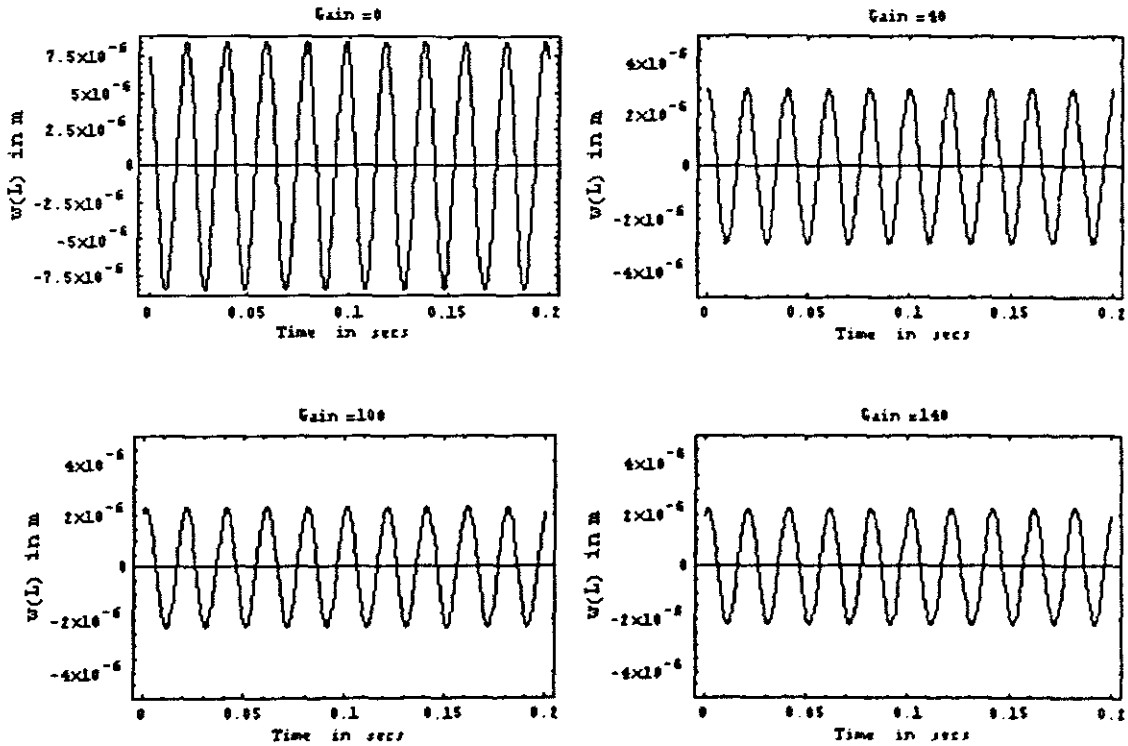

Figure 5.30 Effect of negative velocity feedback gain on the tip transient response
[0°/0°/90°/90°/90°/90°/0°/0°]

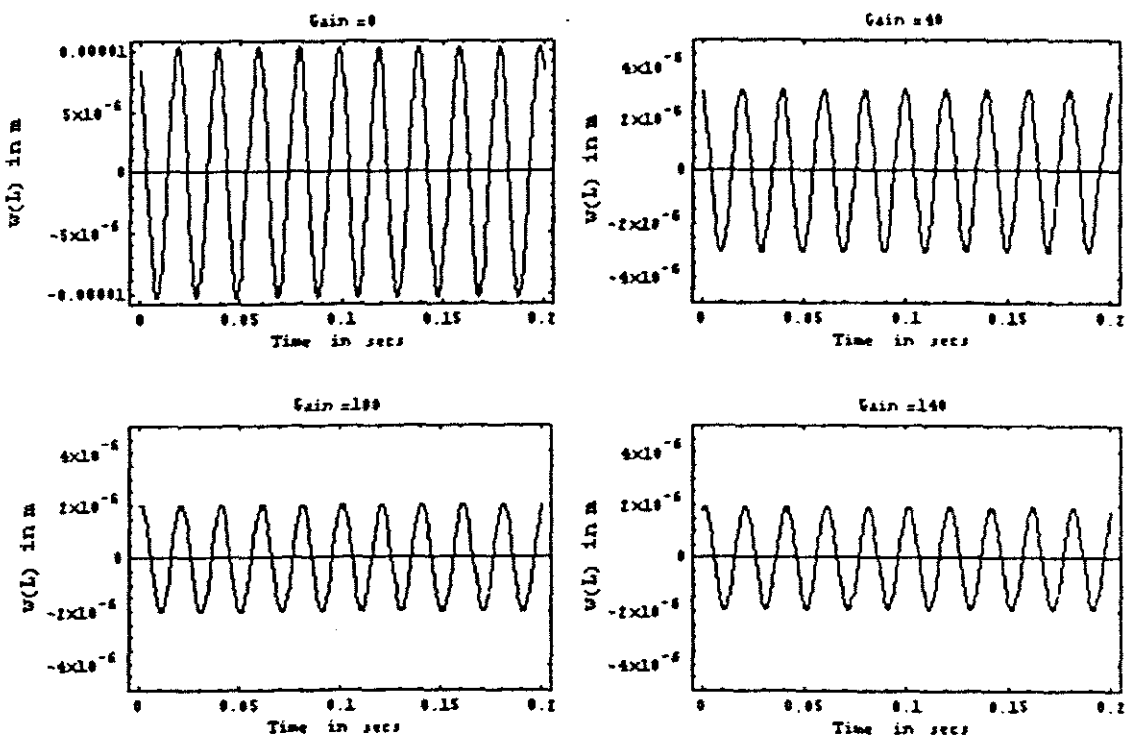

Figure 5.31 Effect of negative velocity feedback gain on the tip transient response
[0°/0°/90°/90°/0°/0°/90°/90°]

The effect of feedback control gain on the tip transverse response of eight-layer laminated beams are shown in Figures (5.29)~(5.31). The amplitude of the beam vibration damped out quickly by increasing the feedback control gain. Comparing with four-layer laminated beams, the eight-layer laminated beam has higher stiffness, which is shown in Table 5.2. The deflection of the eight-layer beam is smaller than four-layer beam when there is no feedback control ($G_i = 0$) and the effect of number of layers with amplitude of vibration of a laminated composite beam can be also noticed. From these figures, the control effect is not very evident between 100 coulombs/ampere and 140 coulombs/ampere of feedback control gain. In order to analyze the optimal feedback gain for the eight-layer laminated beams, the following results have been presented.

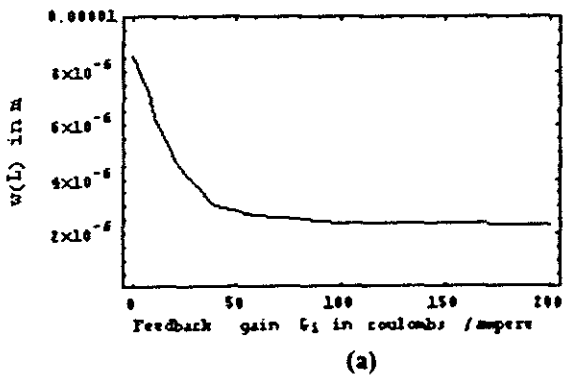

(a)

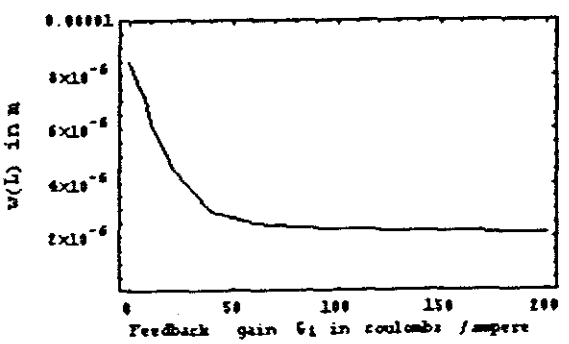

(b)

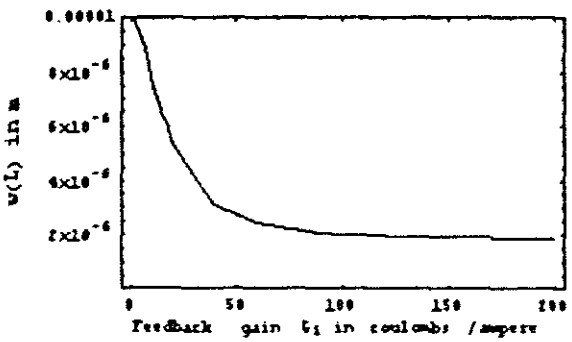

(c)

Figure 5.32 The tip deflection of beam versus feed back control gain
(a) [0°/0°/0°/0°/0°/0°/0°/0°]; (b) [0°/0°/90°/90°/90°/90°/0°/0°]; (c) [0°/0°/90°/90°/0°/0°/90°/90°]

From the Figure (5.32), it is easy to notice the effect of the lamination schemes or stacking sequences, which (b) is called symmetric cross-ply and (c) is called antisymmetric cross-ply. From the above results, we can also observe that the amplitude of vibration damped out very quickly between $G_i = 0$ and $G_i = 50$. After $G_i = 100$ coulombs/ampere, the curve go down smoothly. This shows us that the optimal feedback control gain is also about 100 coulombs/ampere for the eight-layer laminated beam.

Similar to the four-layer laminated beam, in the following results, we will discuss the features of input and output voltage of the eight-layer laminated beam with two different ply orientations.

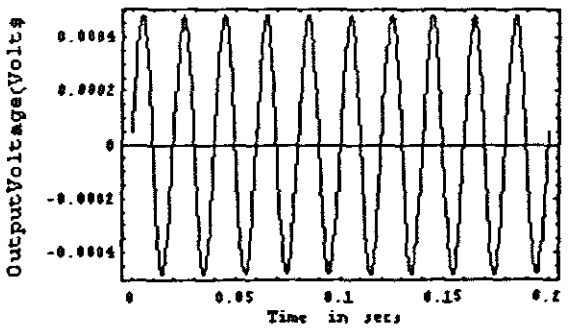

Figure 5.33 The output voltage from sensor layer [0°/0°/90°/90°/90°/90°/0°/0°]

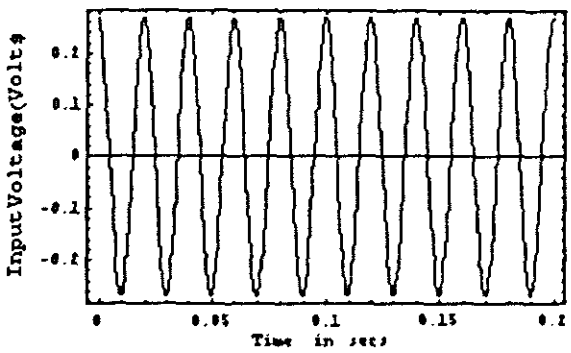

Figure 5.34 The input voltage act on actuator layer [0°/0°/90°/90°/90°/90°/0°/0°]

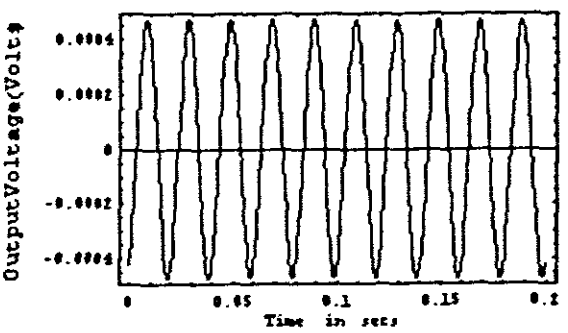

Figure 5.35 The output voltage from sensor layer [0°/0°/90°/90°/0°/0°/90°/90°]

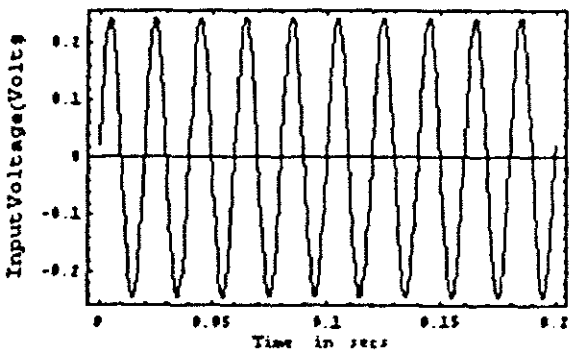

Figure 5.36 The input voltage act on actuator layer [0°/0°/90°/90°/0°/0°/90°/90°]

It should be noted that all the input and output voltage is based on the feedback gain G_f = 40. For the eight-layer smart laminated composite beam, from the above results, we can also observe that input and output voltage vary with the vibration of beam, and they have the same vibrational period with the laminated response. Also, the output voltage has the $\pi/2$ phasic difference with the input voltage of smart beams. In order to illustrate the effects of eight-layer smart laminated beam subjecting to the higher frequency of external force, the following results will be included in this section. For the symmetric cross-ply, the frequency of applied force is 120 Hz (Figure 5.37), and for the antisymmetric cross-ply, it will take 100 Hz (Figure 5.38) as the frequency of external load.

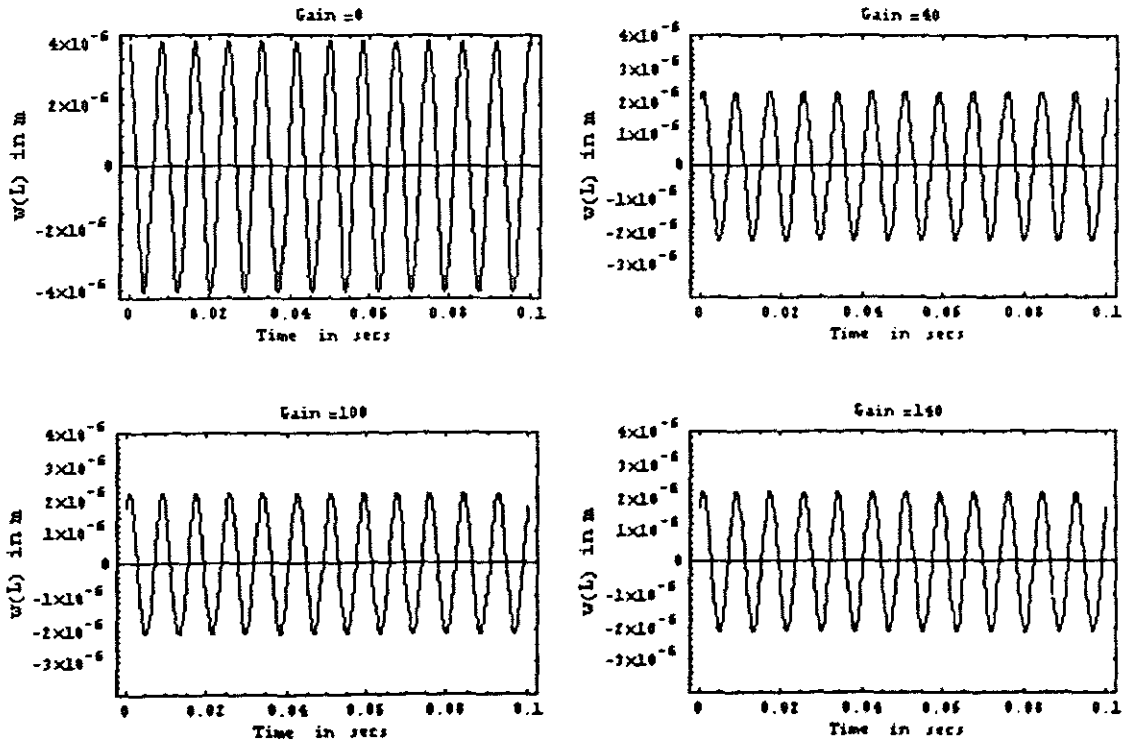

Figure 5.37 Effect of negative velocity feedback gain on the tip transient response
[0°/0°/90°/90°/90°/90°/0°/0°]

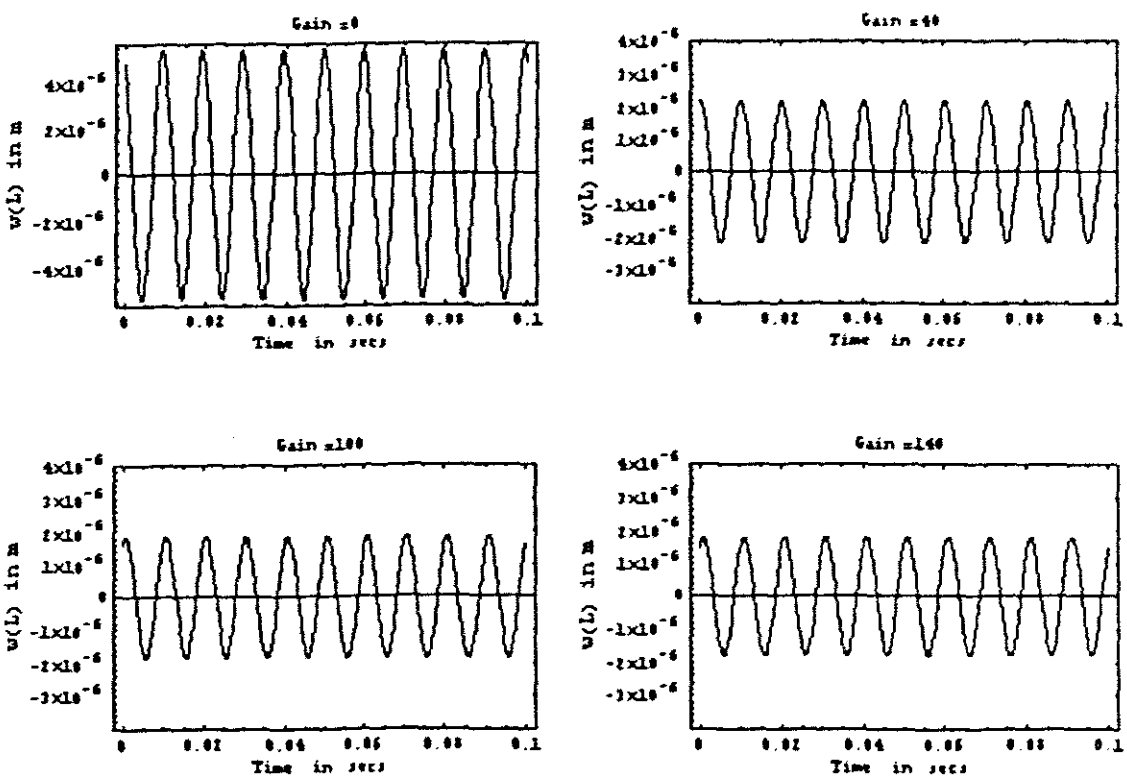

Figure 5.38 Effect of negative velocity feedback gain on the tip transient response
[0°/0°/90°/90°/0°/0°/90°/90°]

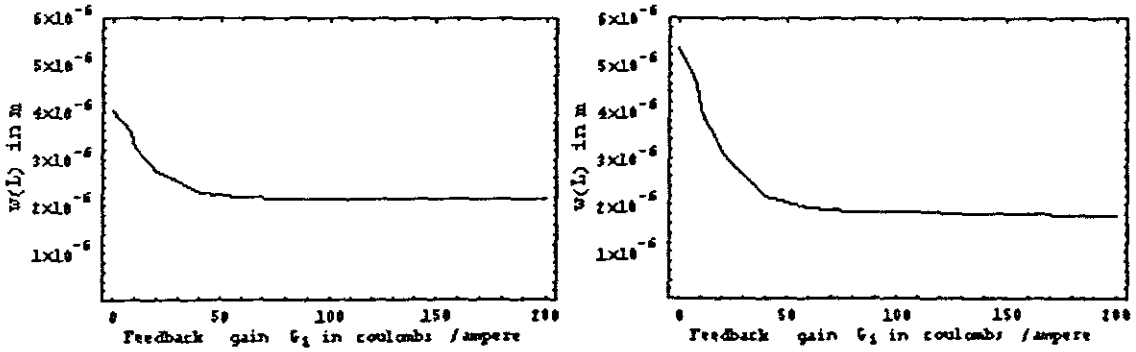

(a) (b)

Figure 5.39 The tip deflection of beam versus feed back control gai
(a) [0°/0°/90°/90°/90°/90°/0°/0°]; (b) [0°/0°/90°/90°/0°/0°/90°/90°]

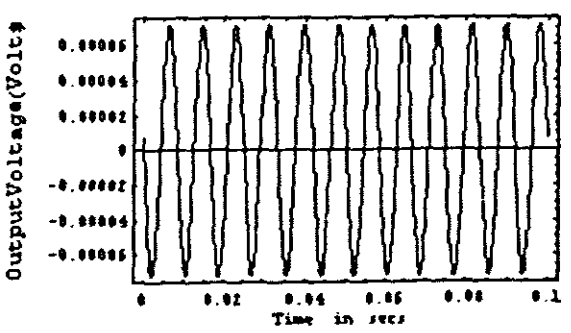

Figure 5.40 The output voltage from sensor layer
[0°/0°/90°/90°/90°/90°/0°/0°]

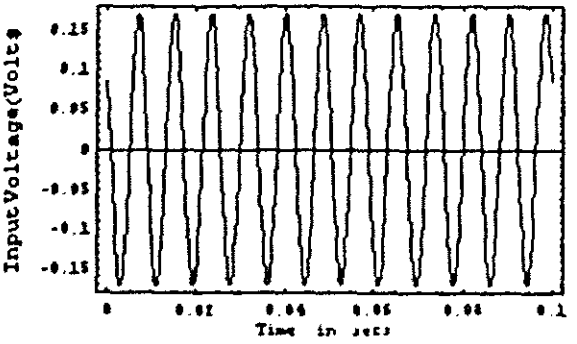

Figure 5.41 The input voltage act on actuator layer
[0°/0°/90°/90°/90°/90°/0°/0°]

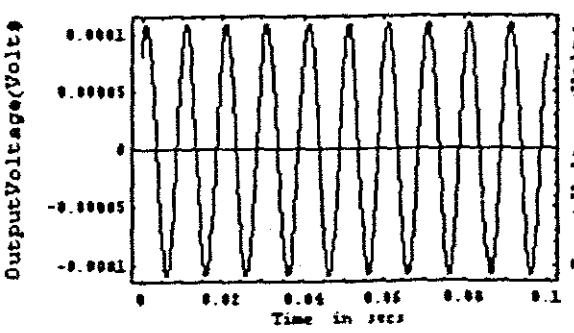

Figure 5.42 The output voltage from sensor layer
[0°/0°/90°/90°/0°/0°/90°/90°]

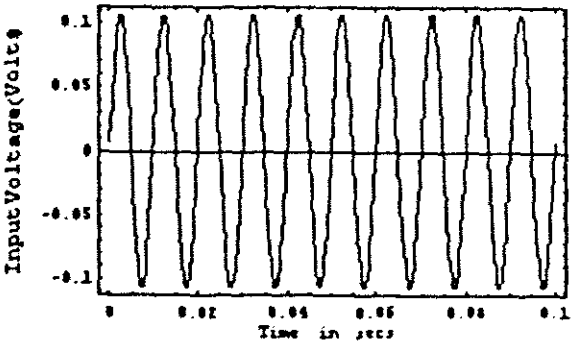

Figure 5.43 The input voltage act on actuator layer
[0°/0°/90°/90°/0°/0°/90°/90°]

The effect of feedback control gain under the higher frequency of external force is shown in Figures (5.37) and (5.38). It can be noticed that the amplitude of vibration reduced quickly. The optimal feedback gain can also be obtained from Figure (5.39), which is about $G_i = 70$ coulombs/ampere. From all these results, we can find that it still has a good control purpose for eight-layer of the present beam model even applied by the higher frequency (120 Hz for the symmetric cross-ply and 100 Hz for the antisymmetric cross-ply) of external force. The input and output voltage of this case are also shown in Figures (5.40)~(5.43).

5.3 Conclusions

Advanced 'intelligent' structures with integrated sensors, actuators and control electronics are becoming increasingly important in high-performance space structures and mechanical systems. In this project, an integrated distributed piezoelectric sensor/actuator for laminated composite beams has been proposed. Laminate and structural mechanics and the corresponding coupled electromechanical model for the dynamic analysis of smart composite beam structures with embedded piezoelectric actuators and sensors were developed and described. The governing equation of smart laminated composite beams and its approximate analytical solutions have also been presented.

Performance of a beam model coupled with the distributed piezoelectric sensor/actuator was studied in a force vibration analysis. Distributed dynamic measurement of the laminated beam was demonstrated and the input and output voltage were studied. It was observed that the input and output voltage vary with the vibration of beam and there is $\pi/2$ phasic difference between input and output voltage. It was also found that the reciprocal relationship between piezoelectric sensors and actuators attest to advantage of control algorithms which combine piezoelectric sensors and actuators. Active distributed vibration suppression and control of the beam was also studied by using negative velocity feedback control law. It can be observed that the amplitude of beam vibration damped out very quickly when the feedback control gain increased. The relation between the amplitude of vibration and feedback control gain was also described and analyzed. From these results, we can approximately estimate the optimal feedback control gain. An approximate analytical solution was developed for analyzing system with complicated stiffness couplings, arbitrary boundary conditions, and external loads. Also, the present beam model is based on the laminated theory. Obviously, different ply orientations would change the frequency predictions and control effect.

In this project, three important issues have been presented. Firstly, at the aspect of mathematical model, the governing equations of the smart laminated composite beam based on the first order shear deformation theory (Reissner-Mindlin plate theory) has been derived by introducing the electric potential function. Comparing with the finite element method which was mentioned in chapter 1, the present governing equation is continuous at both fields of space and time. However for the governing equation of the finite element method, only the field of time is continuous and the field of space is discrete. From this regard, we can easily find that the governing equation of the finite element method is a differential equation and the present governing equation is a partial differential equation. In general, the solution of present governing equation will be more accurate than the finite element method. Secondly, considering the aspect of the

deriving method, the present method creatively introduces a mathematical tool of complex numbers to reduce the two coupled differential equations to one complex differential equation and from twelfth-order differential equation to sixth-order differential equation. This is the first presentation of this method. Finally, from the aspect of solution, the approximate analytical solution of the smart laminated beam under the external harmonic vibration loads has been derived. After reviewing the relative literature, very few papers were found that concentrates on the analytical solution or exact solution of smart laminated composite beam. The present work focuses on this approach and can thus be seen as a foundation for future work.

By observing the Figures (5.10)~(5.13), (5.24), (5.32) and (5.39), the mathematical relation of the amplitude of beam vibration and feedback control gain can be written as

$$f = A(1 - e^{\alpha G_i}) + B \tag{5.2}$$

where f is the amplitude of vibration and G_i is the feedback control gain. The coefficients A, B and α can be determined by choosing three points from the above graphical results.

It should also be noted that the piezoelectric PVDF used in the distributed sensor/actuator of the advanced structure has a 'breakdown' voltage of around 200 volts. When the feedback voltage exceeds this breakdown voltage, the dipolar molecular structure of the PVDF will be destroyed. Additionally, the temperature variation in the piezoelectric crystal could also affect the overall performance, which is not considered in this project. Also, the performance of other piezoelectric materials, such as PZTs, needs to be explored further. The present work is based on the beam model, but it also can be applied to the plate and shell structure. The future work will address this issue.

Bibliography

[1] Bailey, T. and Hubbard, J.E., 1985, Distributed Piezoelectric-Polymer Active Vibration Control of a Cantilever Beam, *Journal of Guidance, Control and Dynamics*, **8**(5), pp.605-611.

[2] Bangera, K.M. and Chandrashekhara, K., 1991, Nonlinear Vibration of Moderately Thick Laminated Beams Using Finite Element Method, *Finite Elements in Analysis and Design*, **9**, pp.321-333.

[3] Barbero, E.J. and Reddy, J.N., 1990, Nonlinear Analysis of Composite Laminates Using A Generalised Laminated Plates Theory, *AIAA Journal*, **28**(11), pp.1987-1994.

[4] Bhimaraddi, A. and Chandrashekhara, K., 1991, Some Observations on the Modeling of Laminated Composite Beams with General Lay-ups, *Composite Structures*, **19**, pp.371-380.

[5] Bhumbla, R., Kosmatka, J.B. and Reddy, J.N., 1990, Free Vibration Behaviour of Spinning Shear-Deformable Plates Composed of Composite Materials, *AIAA Journal*, **28**(11), pp.1962-1970.

[6] Callahan, J. and Baruh, H., 1995, Modal Analysis Using Segmented Piezoelectric Sensors, *AIAA Journal*, **33**(12), pp.2371-2378.

[7] Chandra, R. and Chopra, I., 1993, Structural Modelling of Composite Beams with Induced-Strain Actuators, *AIAA Journal*, **31**(9), pp.1692-1701.

[8] Chandrashekhara, K. and Agarnal, A., 1993, Active Vibration Control of Laminated Composite Plates Using Piezoelectric Device: A Finite element Approach, *Journal of Intelligent Materials Systems & Structures*, **4**, pp.496-508.

[9] Chandrashekhara, K. and Donthireddy, P., 1997, Vibration Suppression of Composite Beams with Piezoelectric Devices Using a Higher Order Theory, *European Journal of Mechanics, A/Solids*, **16**(4), pp.709-721.

[10] Charette, F., Gvigou, C., Berry, A. and Plantier, G., 1994, Asymmetric Actuation and Sensing of a Beam Using Piezoelectric Materials, *Journal of Acoustical Society of America*, **96**(4), pp.2272-2283.

[11] Chen, S.H., Wang, Z.D. and Liu, X.H., 1997, Active Vibration Control and Suppression for Intelligent Structures, *Journal of Sound and vibration*, **200**(2), pp.167-177.

[12] Crawley, E.F. and de Luis, J., 1987, Use of Piezoelectric Actuators as Elements of Intelligent Structures, *AIAA Journal*, (10), pp.1373-1385.

[13] Crawley, E.F. and Lazarus, K.B., 1991, Induced Strain Actuation of Isotropic and Anisotropic Plates, *AIAA Journal*, **29**(6), pp.944-951.

[14] Crawley, E.F., 1994, Intelligent Structures for Aerospace: A Technology Overview and Assessment, *AIAA Journal*, **32**(8), pp.1689-1699.

[15] Culshaw, B., Michie, C., Gardiner, P. and Mcgown, A., 1996, Smart Structures and Applications in Civil Engineering, *Proceeding of The IEEE*, **84**,(1), pp.78-86.

[16] Gerhold, C.H. and Rocha, R., 1989, Active Control of Flexural Vibrations in Beams, *Journal of Aerospace Engineering*, **2**(3), pp.141-154.

[17] Gerhold, C.H. and Rocha, R., 1990, Active Control of Flexural Vibrations in Beams, *Journal of Aerospace Engineering*, **2**, pp.141-154.

[18] Gorman, D.J., 1997, Free Vibration Analysis of MINDLIN Plates with Uniform Elastic Edge Support by the Superposition Method, *Journal of Sound and Vibration*, **207**(3), pp.335-350.

[19] Grandhi, M.V., and Thompson, B.S., Smart Materials and Structures, London: Chapman & Hall.

[20] Ha, S.K., Keilers, C. and Chang, F.K., 1992, Finite Element Analysis of Composite Structures Containing Distributed Piezoceramic Sensors and Actuators, *AIAA Journal*, **30**(3), pp. 772-780.

[21] Hashin, Z., 1983, Analysis of Composite Materials – A Survey, *ASME Journal of Applied Mechanics*, **50**(9), pp.481-505.

[22] Heyliger, P. and Saravanos, D.A., 1995, Exact Free-Vibration Analysis of Laminated Plates with Embedded Piezoelectric Layers, *Journal of Acoustical Society of America*, **98**(3), pp.1547-1557.

[23] Heyliger, P., Exact Solutions for Simply Supported Laminated Piezoelectric Plates, *Journal of Applied Mechanics*, **64**(6), pp.299-306.

[24] Huang, D. and Sun, B.H., 1998, Nonlinear Vibration Analysis of Smart Composite Beams, *Proceedings of the 2nd South Africa Conference on Applied Mechanics, Cape Town*, Vol. 1, pp.481-492.

[25] Huang, D. and Sun, B.H., 1998, Vibration Analysis of Laminated Composite Beams with Piezoelectric Layers Using a Higher Order Theory, *Proceedings of the second International Conference on Composite Science and Technology (ICCST/2), Durban*, pp.395-402.

[26] Huang, Y. and Huang, D., 1998, The Bending and Free Vibrations of Anti-Symmetric Angle-ply Laminated Rectangular Plates, *Proceedings of the 2nd South Africa Conference on Applied Mechanics, Cape Town*, Vol. 1, pp.493-504.

[27] Hwang, W.S. and Park, H.C., 1993, Finite Element Modelling of Piezoelectric Sensors and Actuators, *AIAA Journal*, **31**(5), pp.930-937.

[28] Im, S. and Atluri, S.N., 1989, Effects of a Piezo-Actuator on a Finitely Deformed Beam Subjected to General Lading, *AIAA Journal*, **27**(12), pp.1801-1807.

[29] Jones, R.M., 1975, Mechanics of Composite Materials, Scripta, Washington, DC.

[30] Kapania, R.K. and Raciti, S., 1989, Nonlinear Vibrations of Unsymmetrically Laminated Beams, *AIAA Journal*, **27**(2), pp.201-210.

[31] Lee, C.K. and Moon, F.C., 1990, Modal Sensor/Actuators, *Journal of Applied Mechanics*, **57**(6), pp.434-441.

[32] Lee, C.K., 1990, Theory of Laminated Piezoelectric Plates for the Design of Distributed Sensors/Actuators. Part I: Governing Equations and Reciprocal Relationships, *Journal of Acoustical Society of America*, **87**(3), pp.1144-1158.

[33] Lesieutre, G.A. and Lee, U., 1996, A Finite Element for Beams Having Segmented Active Constrained Layers with Frequency-Dependent Viscoelastics, *Smart Materials and Structures*, **5**, pp.615-627.

[34] Liu, S., 1991, A Vibration Analysis of Composite Laminated Plates, *Finite Element in Analysis and Design*, **9**, pp.295-307.

[35] Lo, K.H., Christensen, R.M. and Wu E.M., 1977, A High-Order Theory of Plate Deformation, Part 2: Laminated Plates, *ASME Journal of Applied Mechanics*, (12), pp.669-676.

[36] Mindlin, R.D., 1965, Influence of Rotatory Inertia and Shear on Flexural Motions of Isotropic, Elastic Plates, *Journal of Applied Mechanics*, **18**, pp.31-38.

[37] Mitchell, J.A. and Reddy, J.N., 1995, A Refined Hybrid Plate Theory for Composite Laminates with Piezoelectric Laminae, *International Journal of Solids Structures*, **32**(16), pp.2345-2367.

[38] Murakami, H., Reissner, E. and Yamakawa, J., 1996, Anisotropic Beam Theories with Shear Deformation, *Journal of Applied Mechanics*, **63**(9), pp.660-668.

[39] Pai, P.F., Nayfeh, A. H., Oh, K. and Mook, D.T., 1993, A Refined Nonlinear Model of Composite Plates With Integrated Piezoelectric Actuators and Sensors, *International Journal of Solids Structures*, **30**(12), pp.1603-1630.

[40] Ramalingeswara, R.S. and Ganesan, N., 1997, Dynamic Response of Non-Uniform Composite Beams, *Journal of Sound and Vibration*, **200**(5), pp.563-577.

[41] Rao, S.S. and Sunar, M., 1994, Piezoelectricity and Its Use in Disturbance Sensing and Control of Flexible Structures: A Survey, *Applied Mechanics Rev.*, **47**(4), pp.113-123.

[42] Reddy, J.N. and Khdeir, A.A., 1989, Buckling and Vibration of Laminated Composite Plates Using Various Plate Theories, *AIAA Journal*, **27**(12), pp.1808-1817.

[43] Reddy, J.N. and Miravete, A., 1995, Practical Analysis of Composite Laminates, CRC Press, Inc.

[44] Reddy, J.N., 1984, A Simple Higher-Order Theory for Laminated Composite Plates, *Journal of Applied Mechanics*, **51**(12), pp.745-752.

[45] Saravanos, D.A., Heyliger, P.R. and Hopkins, D.A., 1997, Layerwise Mechanics and Finite Element for The Dynamic Analysis of Piezoelectric Composite Plates, *International Journal of Solids Structures*, **34**(3), pp.359-378.

[46] Shen, Y. and Yin, L., 1997, Strain Sensor of Composite Plates Subjected to Low Velocity Impact with Distributed Piezoelectric Sensors: A Mixed Finite Element Approach, *Journal of Sound and Vibration*, **199**(1), pp.17-31.

[47] Shieh, R.C., 1994, Governing Equations and Finite Element Models for Multiaxial Piezoelectric Beam Sensors/Actuators, *AIAA Journal*, **32**(6), pp.1250-1258.

[48] Singh, G., Rao, V. and Lyengar, N.G.R., 1991, Analysis of the Nonlinear Vibrations of Unsymmetrically Laminated Composite Beams, *AIAA Journal*, **29**(10), pp.1727-1735.

[49] Sun, B.H. and Huang, D., 1999, On the Feedback Control Gain (G_i) of Smart Laminated Beams, Plates and Shells, 6th *International Conference on Composite Engineering (ICCE/6), Florida, U.S.A*, pp.859-860.

[50] Tzou, H.S. and Gadre, M., 1988, Active Vibration Isolation by Polymeric Piezoelectret with Variable Feedback Gains, *AIAA Journal*, **26**(8), pp.1014-1017.

[51] Tzou, H.S. and Tseng, C.I., 1990, Distributed Piezoelectric Sensor/Actuator Design for Dynamic Measurement/Control of Distributed Parameter Systems: A Piezoelectric Finite Element Approach, *Journal of Sound and Vibration*, **138**(1), pp.17-34.

[52] Wang, B.T., and Rogers, C.A., 1991, Laminated Plate Theory for Spatially Distributed Induced Strain Actuators, *Journal of Composite Materials*, **25**, pp. 433-452.

[53] Wung, P.M. and Reddy, J.N., 1991, A Transverse Deformation Theory of Laminated Composite Plates, *Computers & Structures*, **41**(4), pp.821-833.

[54] Xue, S. and Tobita, J., 1997, Kurita S. and Izumi M., Mechanics and Dynamics of Intelligent Passive Vibration Control System, *Journal of Engineering Mechanics*, 4, pp.322-327.

[55] Yang, S.M. and Lee, G.S., 1997, Vibration Control of Smart Structures by Using Neural Networks, *ASME Journal of Dynamic Systems, Measurement, and Control*, **119**(3), pp.35-39.

[56] Yang, X.X., Shen, S. and Kuang, Z.B., 1997, The Degenerate Solution for Piezothermoelastic Materials, *European Journal of Mechanics, A/Solids*, **16**(5), pp.779-793.

[57] Yellin, J.M. and Shen, I.Y., 1996, A Self-Sensing Active Constrainal Layer Damping Treatment for a Euler-Bernoulli Beam, *Smart Materials and Structures*, **5**, pp.628-637.

Appendix A

Arbitrary Transformation of Constitutive Equations

1. Constitutive equations for piezoelectric composite structures

For an orthotropic laminate, the constitutive equations in the principal material axes including the piezoelectric effect are given as (Eq. 2.11):

$$\begin{Bmatrix}\sigma_1\\ \sigma_2\\ \tau_{23}\\ \tau_{13}\\ \tau_{12}\end{Bmatrix}_k = \begin{bmatrix}\hat{Q}_{11} & \hat{Q}_{12} & 0 & 0 & 0\\ \hat{Q}_{12} & \hat{Q}_{22} & 0 & 0 & 0\\ 0 & 0 & \hat{Q}_{44} & 0 & 0\\ 0 & 0 & 0 & \hat{Q}_{55} & 0\\ 0 & 0 & 0 & 0 & \hat{Q}_{66}\end{bmatrix}_k \begin{Bmatrix}\varepsilon_1\\ \varepsilon_2\\ \gamma_{23}\\ \gamma_{13}\\ \gamma_{12}\end{Bmatrix}_k - \begin{bmatrix}0 & 0 & e_{31}\\ 0 & 0 & e_{32}\\ 0 & e_{24} & 0\\ e_{15} & 0 & 0\\ 0 & 0 & 0\end{bmatrix}_k \begin{Bmatrix}E_1\\ E_2\\ E_3\end{Bmatrix}_k \tag{A.1}$$

$$\begin{Bmatrix}D_1\\ D_2\\ D_3\end{Bmatrix}_k = \begin{bmatrix}0 & 0 & 0 & e_{15} & 0\\ 0 & 0 & e_{24} & 0 & 0\\ e_{31} & e_{32} & 0 & 0 & 0\end{bmatrix}_k \begin{Bmatrix}\varepsilon_1\\ \varepsilon_2\\ \gamma_{23}\\ \gamma_{13}\\ \gamma_{12}\end{Bmatrix}_k + \begin{bmatrix}g_{11} & 0 & 0\\ 0 & g_{22} & 0\\ 0 & 0 & g_{33}\end{bmatrix}_k \begin{Bmatrix}E_1\\ E_2\\ E_3\end{Bmatrix}_k \tag{A.2}$$

However, laminates are constructed in such a manner that the principal material co-ordinate system do not coincide with the natural co-ordinate system of the reference body. Given the constitutive model, we use the transformation $\hat{Q}_{ij} = e_{im}e_{jn}\overline{Q}_{mn}$ to obtain the constitutive model in an arbitrary co-ordinate system. We now represent $T_1 = e_{ij}$ and $T_2 = e_{im}e_{jn}$ as first and second order transformation matrices, respectively.

First, we introduce the transformation matrix $[T_0]$, $[T]$ and Reuter's matrix $[R]$, such that

$$[T] = \begin{bmatrix}\cos^2\theta & \sin^2\theta & 0 & 0 & 2\cos\theta\sin\theta\\ \sin^2\theta & \cos^2\theta & 0 & 0 & -2\cos\theta\sin\theta\\ 0 & 0 & \cos\theta & -\sin\theta & 0\\ 0 & 0 & \sin\theta & \cos\theta & 0\\ -\cos\theta\sin\theta & \cos\theta\sin\theta & 0 & 0 & \cos^2\theta-\sin^2\theta\end{bmatrix}, \quad [T]^{-1} = [T(-\theta)]$$

$$[T_0] = \begin{bmatrix}\cos\theta & -\sin\theta & 0\\ \sin\theta & \cos\theta & 0\\ 0 & 0 & 1\end{bmatrix}, \quad [T_0]^{-1} = [T_0(-\theta)]$$

$$[R]=\begin{bmatrix}1&0&0&0&0\\0&1&0&0&0\\0&0&2&0&0\\0&0&0&2&0\\0&0&0&0&2\end{bmatrix},\quad [R]^{-1}=\begin{bmatrix}1&0&0&0&0\\0&1&0&0&0\\0&0&\frac{1}{2}&0&0\\0&0&0&\frac{1}{2}&0\\0&0&0&0&\frac{1}{2}\end{bmatrix}$$

Our aim is to determine material properties in the arbitrary direction when those in the principal material co-ordinate are known. Here, some important relationships have been considered. These transform as follows:

$$\begin{Bmatrix}\sigma_1\\\sigma_2\\\tau_{23}\\\tau_{31}\\\tau_{12}\end{Bmatrix}=[T]\begin{Bmatrix}\sigma_x\\\sigma_y\\\tau_{yz}\\\tau_{xz}\\\tau_{xy}\end{Bmatrix},\quad \begin{Bmatrix}\varepsilon_1\\\varepsilon_2\\\frac{1}{2}\gamma_{23}\\\frac{1}{2}\gamma_{31}\\\frac{1}{2}\gamma_{12}\end{Bmatrix}=[T]\begin{Bmatrix}\varepsilon_x\\\varepsilon_y\\\frac{1}{2}\gamma_{yz}\\\frac{1}{2}\gamma_{xz}\\\frac{1}{2}\gamma_{xy}\end{Bmatrix} \qquad \text{(A.3a~b)}$$

$$\begin{Bmatrix}E_1\\E_2\\E_3\end{Bmatrix}=[T_0]\begin{Bmatrix}E_x\\E_y\\E_z\end{Bmatrix},\quad \begin{Bmatrix}D_1\\D_2\\D_3\end{Bmatrix}=[T_0]\begin{Bmatrix}D_x\\D_y\\D_z\end{Bmatrix} \qquad \text{(A.3c~d)}$$

Using the Reuter's matrix [R], we can define the following relationships:

$$\begin{Bmatrix}\varepsilon_1\\\varepsilon_2\\\gamma_{23}\\\gamma_{31}\\\gamma_{12}\end{Bmatrix}=[R]\begin{Bmatrix}\varepsilon_1\\\varepsilon_2\\\frac{1}{2}\gamma_{23}\\\frac{1}{2}\gamma_{31}\\\frac{1}{2}\gamma_{12}\end{Bmatrix},\quad \begin{Bmatrix}\varepsilon_x\\\varepsilon_y\\\gamma_{yz}\\\gamma_{xz}\\\gamma_{xy}\end{Bmatrix}=[R]\begin{Bmatrix}\varepsilon_x\\\varepsilon_y\\\frac{1}{2}\gamma_{yz}\\\frac{1}{2}\gamma_{xz}\\\frac{1}{2}\gamma_{xy}\end{Bmatrix} \qquad \text{(A.4a~b)}$$

Substituting the expressions (A.3a~d), (A.4a~b) and matrices [T], [T_0], [R] in Eqs. (A.1) and (A.2), we can have

$$\begin{Bmatrix}\sigma_x\\\sigma_y\\\tau_{yz}\\\tau_{xz}\\\tau_{xy}\end{Bmatrix}=[T]^{-1}[\hat{Q}][R][T][R]^{-1}\begin{Bmatrix}\varepsilon_x\\\varepsilon_y\\\gamma_{yz}\\\gamma_{xz}\\\gamma_{xy}\end{Bmatrix}-[T]^{-1}[e]^T[T_0]\begin{Bmatrix}E_x\\E_y\\E_z\end{Bmatrix}$$

$$=[T^{-1}][\hat{Q}][T]^{-T}\begin{Bmatrix}\varepsilon_x\\\varepsilon_y\\\gamma_{yz}\\\gamma_{xz}\\\gamma_{xy}\end{Bmatrix}-[T]^{-1}[e]^T[T_0]\begin{Bmatrix}E_x\\E_y\\E_z\end{Bmatrix}$$

$$\begin{Bmatrix} D_x \\ D_y \\ D_z \end{Bmatrix} = [T_0]^{-1}[e][R][T][R]^{-1}\begin{Bmatrix} \varepsilon_x \\ \varepsilon_y \\ \gamma_{yz} \\ \gamma_{xz} \\ \gamma_{xy} \end{Bmatrix} + [T_0]^{-1}[g][T_0]\begin{Bmatrix} E_x \\ E_y \\ E_z \end{Bmatrix}$$

$$= [T_0]^{-1}[e][T]^{-T}\begin{Bmatrix} \varepsilon_x \\ \varepsilon_y \\ \gamma_{yz} \\ \gamma_{xz} \\ \gamma_{xy} \end{Bmatrix} + [T_0]^{-1}[g][T_0]\begin{Bmatrix} E_x \\ E_y \\ E_z \end{Bmatrix}$$

where $[T]^{-T} = [R][T][R]^{-1}$

Expanding the above equations, we can obtain the following constitutive equations as:

$$\begin{Bmatrix} \sigma_x \\ \sigma_y \\ \tau_{yz} \\ \tau_{xz} \\ \tau_{xy} \end{Bmatrix} = \begin{bmatrix} \bar{Q}_{11} & \bar{Q}_{12} & 0 & 0 & \bar{Q}_{16} \\ \bar{Q}_{12} & \bar{Q}_{22} & 0 & 0 & \bar{Q}_{26} \\ 0 & 0 & \bar{Q}_{44} & \bar{Q}_{45} & 0 \\ 0 & 0 & \bar{Q}_{45} & \bar{Q}_{55} & 0 \\ \bar{Q}_{16} & \bar{Q}_{26} & 0 & 0 & \bar{Q}_{66} \end{bmatrix}\begin{Bmatrix} \varepsilon_x \\ \varepsilon_y \\ \gamma_{yz} \\ \gamma_{xz} \\ \gamma_{xy} \end{Bmatrix} - \begin{bmatrix} 0 & 0 & \bar{e}_{31} \\ 0 & 0 & \bar{e}_{32} \\ \bar{e}_{14} & \bar{e}_{24} & 0 \\ \bar{e}_{15} & \bar{e}_{25} & 0 \\ 0 & 0 & \bar{e}_{36} \end{bmatrix}\begin{Bmatrix} E_x \\ E_y \\ E_z \end{Bmatrix} \tag{A.5}$$

$$\begin{Bmatrix} D_x \\ D_y \\ D_z \end{Bmatrix} = \begin{bmatrix} 0 & 0 & \bar{e}_{14} & \bar{e}_{15} & 0 \\ 0 & 0 & \bar{e}_{24} & \bar{e}_{25} & 0 \\ \bar{e}_{31} & \bar{e}_{32} & 0 & 0 & \bar{e}_{36} \end{bmatrix}\begin{Bmatrix} \varepsilon_x \\ \varepsilon_y \\ \gamma_{yz} \\ \gamma_{xz} \\ \gamma_{xy} \end{Bmatrix} + \begin{bmatrix} \bar{g}_{11} & \bar{g}_{12} & 0 \\ \bar{g}_{12} & \bar{g}_{22} & 0 \\ 0 & 0 & \bar{g}_{33} \end{bmatrix}\begin{Bmatrix} E_x \\ E_y \\ E_z \end{Bmatrix} \tag{A.6}$$

where

$$\bar{Q}_{11} = \hat{Q}_{11}\cos^4\theta + 2(\hat{Q}_{12} + 2\hat{Q}_{66})\sin^2\theta\cos^2\theta + \hat{Q}_{22}\sin^4\theta$$
$$\bar{Q}_{12} = (\hat{Q}_{11} + \hat{Q}_{22} - 4\hat{Q}_{66})\sin^2\theta\cos^2\theta + \hat{Q}_{12}(\sin^4\theta + \cos^4\theta)$$
$$\bar{Q}_{22} = \hat{Q}_{11}\sin^4\theta + 2(\hat{Q}_{12} + 2\hat{Q}_{66})\sin^2\theta\cos^2\theta + \hat{Q}_{22}\cos^4\theta$$
$$\bar{Q}_{16} = (\hat{Q}_{11} - \hat{Q}_{12} - 2\hat{Q}_{66})\sin\theta\cos^3\theta + (\hat{Q}_{12} - \hat{Q}_{22} + 2\hat{Q}_{66})\sin^3\theta\cos\theta$$
$$\bar{Q}_{26} = (\hat{Q}_{11} - \hat{Q}_{12} - 2\hat{Q}_{66})\sin^3\theta\cos\theta + (\hat{Q}_{12} - \hat{Q}_{22} + 2\hat{Q}_{66})\sin\theta\cos^3\theta$$
$$\bar{Q}_{66} = (\hat{Q}_{11} + \hat{Q}_{22} - 2\hat{Q}_{12} - 2\hat{Q}_{66})\sin^2\theta\cos^2\theta + \hat{Q}_{66}(\sin^4\theta + \cos^4\theta)$$
$$\bar{Q}_{44} = \hat{Q}_{44}\cos^2\theta + \hat{Q}_{55}\sin^2\theta$$
$$\bar{Q}_{45} = (\hat{Q}_{55} - \hat{Q}_{44})\sin\theta\cos\theta$$
$$\bar{Q}_{55} = \hat{Q}_{44}\sin^2\theta + \hat{Q}_{55}\cos^2\theta$$

and

$$\bar{e}_{14} = (e_{15} + e_{24})\sin\theta\cos\theta$$
$$\bar{e}_{24} = e_{24}\cos^2\theta - e_{15}\sin^2\theta$$
$$\bar{e}_{15} = e_{15}\cos^2\theta - e_{24}\sin^2\theta$$
$$\bar{e}_{25} = -(e_{15} + e_{24})\sin\theta\cos\theta$$
$$\bar{e}_{31} = e_{31}\cos^2\theta + e_{32}\sin^2\theta$$
$$\bar{e}_{32} = e_{31}\sin^2\theta + e_{32}\cos^2\theta$$
$$\bar{e}_{36} = (e_{31} - e_{32})\sin\theta\cos\theta$$

$$\bar{g}_{11} = g_{11}\cos^2\theta + g_{22}\sin^2\theta$$
$$\bar{g}_{12} = (g_{22} - g_{11})\sin\theta\cos\theta$$
$$\bar{g}_{22} = g_{11}\sin^2\theta + g_{22}\cos^2\theta$$
$$\bar{g}_{33} = g_{33}$$

2. The relations between the coefficients $\tilde{Q}_{ij}$ and $\bar{Q}_{ij}$

In Chapter 2, we have the constitutive equation for smart composite structure in the arbitrary direction, such as:

$$\sigma_x = \bar{Q}_{11}\varepsilon_x + \bar{Q}_{12}\varepsilon_y + \bar{Q}_{16}\gamma_{xy} - \bar{e}_{31}E_z^k$$
$$\sigma_y = \bar{Q}_{12}\varepsilon_x + \bar{Q}_{22}\varepsilon_y + \bar{Q}_{26}\gamma_{xy} - \bar{e}_{31}E_z^k$$
$$\tau_{yz} = \bar{Q}_{44}\gamma_{yz} + \bar{Q}_{45}\gamma_{xz}$$
$$\tau_{xz} = \bar{Q}_{45}\gamma_{yz} + \bar{Q}_{55}\gamma_{xz}$$
$$\tau_{xy} = \bar{Q}_{16}\varepsilon_x + \bar{Q}_{26}\varepsilon_y + \bar{Q}_{66}\gamma_{xy}$$

For the beam problem, we set $\sigma_y = \tau_{yz} = \tau_{xy} = 0$, such that

$$\begin{cases} \bar{Q}_{12}\varepsilon_x + \bar{Q}_{22}\varepsilon_y + \bar{Q}_{16}\gamma_{xy} - \bar{e}_{31}E_z^k = 0 \\ \bar{Q}_{44}\gamma_{yz} + \bar{Q}_{45}\gamma_{xz} = 0 \\ \bar{Q}_{16}\varepsilon_x + \bar{Q}_{26}\varepsilon_y + \bar{Q}_{66}\gamma_{xy} = 0 \end{cases} \quad \text{(A.7a~c)}$$

From expressions (A.7), we can get

$$\gamma_{yz} = -\frac{\bar{Q}_{45}}{\bar{Q}_{44}}\gamma_{xz} \quad \text{(A.8a)}$$

$$\gamma_{xy} = \frac{\bar{Q}_{26}\bar{e}_{31}E_z^k - (\bar{Q}_{12}\bar{Q}_{26} - \bar{Q}_{16}\bar{Q}_{22})\varepsilon_x}{\bar{Q}_{26}^2 - \bar{Q}_{22}\bar{Q}_{66}} \quad \text{(A.8b)}$$

$$\varepsilon_y = \frac{\bar{Q}_{66}\bar{e}_{31}E_z^k - (\bar{Q}_{12}\bar{Q}_{66} - \bar{Q}_{16}\bar{Q}_{26})\varepsilon_x}{\bar{Q}_{22}\bar{Q}_{66} - \bar{Q}_{26}^2} \quad \text{(A.8c)}$$

Substitution of (A.8b), (A.8c) and (A.8a) in the expression σ_x and γ_{xz}, respectively, we can get the following expressions as:

$$\sigma_x = \left[\bar{Q}_{11} + \frac{\bar{Q}_{16}\bar{Q}_{26} - \bar{Q}_{12}\bar{Q}_{66}}{\bar{Q}_{22}\bar{Q}_{66} - \bar{Q}_{26}^2}\bar{Q}_{12} + \frac{\bar{Q}_{12}\bar{Q}_{26} - \bar{Q}_{16}\bar{Q}_{22}}{\bar{Q}_{22}\bar{Q}_{66} - \bar{Q}_{26}^2}\bar{Q}_{16}\right]\varepsilon_x - \left[1 - \frac{\bar{Q}_{12}\bar{Q}_{66} - \bar{Q}_{16}\bar{Q}_{26}}{\bar{Q}_{22}\bar{Q}_{66} - \bar{Q}_{26}^2}\right]\bar{e}_{31}E_z^k$$

$$\tau_{xz} = \left(\bar{Q}_{55} - \frac{\bar{Q}_{45}^2}{\bar{Q}_{44}}\right)\gamma_{xz}$$

By setting

$$\begin{cases} \tilde{Q}_{11} = \bar{Q}_{11} + \dfrac{\bar{Q}_{16}\bar{Q}_{26} - \bar{Q}_{12}\bar{Q}_{66}}{\bar{Q}_{22}\bar{Q}_{66} - \bar{Q}_{26}^2}\bar{Q}_{12} + \dfrac{\bar{Q}_{12}\bar{Q}_{26} - \bar{Q}_{16}\bar{Q}_{22}}{\bar{Q}_{22}\bar{Q}_{66} - \bar{Q}_{26}^2}\bar{Q}_{16} \\ \tilde{Q}_{55} = \bar{Q}_{55} - \dfrac{\bar{Q}_{45}^2}{\bar{Q}_{44}} \\ \tilde{e}_{31} = (1 - \dfrac{\bar{Q}_{12}\bar{Q}_{66} - \bar{Q}_{16}\bar{Q}_{26}}{\bar{Q}_{22}\bar{Q}_{66} - \bar{Q}_{26}^2})\bar{e}_{31} \end{cases}$$

then, we can obtain the constitutive equations of smart composite beams as:

$$\begin{Bmatrix} \sigma_x \\ \tau_{xz} \end{Bmatrix}_k = \begin{bmatrix} \tilde{Q}_{11} & 0 \\ 0 & \tilde{Q}_{55} \end{bmatrix}_k \begin{Bmatrix} \varepsilon_x \\ \gamma_{xz} \end{Bmatrix}_k - \begin{Bmatrix} \tilde{e}_{31} \\ 0 \end{Bmatrix}_k E_z^k \qquad \text{(A.9)}$$

Appendix B

Calculation of Derivative Operators

From chapter 3, we have the derivative operators as

$$L_{11} = -a\frac{\partial^2}{\partial x^2} + I_1\frac{\partial^2}{\partial t^2} + G_i\alpha_1\frac{\partial^3}{\partial x^2\partial t}, \quad L_{12} = L_{21} = 0$$

$$L_{13} = -b\frac{\partial^2}{\partial x^2} + I_2\frac{\partial^2}{\partial t^2} + G_i\alpha_2\frac{\partial^3}{\partial x^2\partial t}$$

$$L_{22} = I_1\frac{\partial^2}{\partial t^2} - \bar{A}_{55}\frac{\partial^2}{\partial x^2}, \quad L_{23} = -\bar{A}_{55}\frac{\partial}{\partial x}$$

$$L_{31} = -b\frac{\partial^2}{\partial x^2} + I_2\frac{\partial^2}{\partial t^2} + G_i\alpha_1\frac{\partial^3}{\partial x^2\partial t}, \quad L_{32} = \bar{A}_{55}\frac{\partial}{\partial x}$$

$$L_{33} = -d\frac{\partial^2}{\partial x^2} + I_3\frac{\partial^2}{\partial t^2} + G_i\alpha_2\frac{\partial^3}{\partial x^2\partial t} + \bar{A}_{55}$$

then the following derivative operators will be calculated.

$$L_1 = -L_{13}L_{32} = \bar{A}_{55}b\frac{\partial^3}{\partial x^3} - \bar{A}_{55}I_2\frac{\partial^3}{\partial x\partial t^2} - \bar{A}_{55}G_i\alpha_2\frac{\partial^4}{\partial x^3\partial t}$$

$$-L_{11}L_{33} = -ad\frac{\partial^4}{\partial x^4} + (I_3a + I_1d)\frac{\partial^4}{\partial x^2\partial t^2} + G_i(a\alpha_2 + d\alpha_1)\frac{\partial^5}{\partial x^4\partial t} - G_i(I_1\alpha_2 + I_3\alpha_1)\frac{\partial^5}{\partial x^2\partial t^3} -$$
$$- G_i^2\alpha_1\alpha_2\frac{\partial^6}{\partial x^4\partial t^2} + \bar{A}_{55}a\frac{\partial^2}{\partial x^2} - I_1I_3\frac{\partial^4}{\partial t^4} - \bar{A}_{55}I_1\frac{\partial^2}{\partial t^2} - \bar{A}_{55}G_i\alpha_1\frac{\partial^3}{\partial x^2\partial t}$$

$$L_{13}L_{31} = b^2\frac{\partial^4}{\partial x^4} - 2I_2b\frac{\partial^4}{\partial x^2\partial t^2} - G_i(b\alpha_1 + b\alpha_2)\frac{\partial^5}{\partial x^4\partial t} + G_i(I_2\alpha_1 + I_2\alpha_2)\frac{\partial^5}{\partial x^2\partial t^3} +$$
$$+ I_2^2\frac{\partial^4}{\partial t^4} + G_i\alpha_1\alpha_2\frac{\partial^6}{\partial x^4\partial t^2}$$

$$L_2 = -L_{11}L_{33} + L_{13}L_{31}$$
$$= (b^2 - ad)\frac{\partial^4}{\partial x^4} + (I_3a + I_1d - 2I_2b)\frac{\partial^4}{\partial x^2\partial t^2} + G_i(a\alpha_2 + d\alpha_1 - b\alpha_1 - b\alpha_2)\frac{\partial^5}{\partial x^4\partial t} +$$
$$+ G_i(I_2\alpha_1 + I_2\alpha_2 - I_1\alpha_2 - I_3\alpha_1)\frac{\partial^5}{\partial x^2\partial t^3} + (I_2^2 - I_1I_3)\frac{\partial^4}{\partial t^4} + \bar{A}_{55}a\frac{\partial^2}{\partial x^2}$$
$$- \bar{A}_{55}I_1\frac{\partial^2}{\partial t^2} - \bar{A}_{55}G_i\alpha_1\frac{\partial^3}{\partial x^2\partial t}$$

$$L_3 = L_{11}L_{32} = -\bar{A}_{55}a\frac{\partial^3}{\partial x^3} + \bar{A}_{55}I_1\frac{\partial^3}{\partial x\partial t^2} + \bar{A}_{55}G_i\alpha_1\frac{\partial^4}{\partial x^3\partial t}$$

$$\begin{aligned}
L_{22}L_2 = {} & (-\bar{A}_{55}b^2 + \bar{A}_{55}ad)\frac{\partial^6}{\partial x^6} + [-\bar{A}_{55}(I_3a + I_1d - 2I_2b) + I_1(b^2 - ad)]\frac{\partial^6}{\partial x^4\partial t^2} + \\
& + [-\bar{A}_{55}G_i(a\alpha_2 + d\alpha_1 - b\alpha_1 - b\alpha_2)]\frac{\partial^7}{\partial x^6\partial t} + (-\bar{A}_{55}{}^2a)\frac{\partial^4}{\partial x^4} + \\
& + [-\bar{A}_{55}G_i(I_2\alpha_1 + I_2\alpha_2 - I_1\alpha_2 - I_3\alpha_1) + I_1G_i(a\alpha_2 + d\alpha_1 - b\alpha_1 - b\alpha_2)]\frac{\partial^7}{\partial x^4\partial t^3} + \\
& + [-\bar{A}_{55}(I_2{}^2 - I_1I_3) + I_1(I_3a + I_1d - 2I_2b)]\frac{\partial^6}{\partial x^2\partial t^4} + (\bar{A}_{55}{}^2I_1 + \bar{A}_{55}I_1a)\frac{\partial^4}{\partial x^2\partial t^2} + \\
& + I_1G_i(I_2\alpha_1 + I_2\alpha_2 - I_1\alpha_2 - I_3\alpha_1)\frac{\partial^7}{\partial x^2\partial t^5} + \bar{A}_{55}{}^2G_i\alpha_1\frac{\partial^5}{\partial x^4\partial t} - \bar{A}_{55}I_1G_i\alpha_1\frac{\partial^5}{\partial x^2\partial t^3} \\
& + I_1(I_2{}^2 - I_1I_3)\frac{\partial^6}{\partial t^6} - \bar{A}_{55}I_1{}^2\frac{\partial^4}{\partial t^4}
\end{aligned}$$

$$L_{23}L_3 = \bar{A}_{55}a\frac{\partial^4}{\partial x^4} - \bar{A}_{55}{}^2I_1\frac{\partial^4}{\partial x^2\partial t^2} - \bar{A}_{55}{}^2G_i\alpha_1\frac{\partial^5}{\partial x^4\partial t}$$

Appendix C

Input and Output Files of MATLAB

Input file

```
K0=dsolve('A6*D6K+A4*D4K+A2*D2K+A0*K=0','x')
```

Output file

```
K0 =

C1*exp(1/6/A6/(36*A2*A4*A6-108*A0*A6^2-8*A4^3+12*3^(1/2)*(4*A2^3*A6-
A2^2*A4^2-
18*A2*A4*A6*A0+27*A0^2*A6^2+4*A0*A4^3)^(1/2)*A6)^(1/3)*3^(1/2)*2^(1/2)*(
-A6*(36*A2*A4*A6-108*A0*A6^2-8*A4^3+12*3^(1/2)*(4*A2^3*A6-A2^2*A4^2-
18*A2*A4*A6*A0+27*A0^2*A6^2+4*A0*A4^3)^(1/2)*A6)^(1/3)*(2*A4*(36*A2*A
4*A6-108*A0*A6^2-8*A4^3+12*3^(1/2)*(4*A2^3*A6-A2^2*A4^2-
18*A2*A4*A6*A0+27*A0^2*A6^2+4*A0*A4^3)^(1/2)*A6)^(1/3)-(36*A2*A4*A6-
108*A0*A6^2-8*A4^3+12*3^(1/2)*(4*A2^3*A6-A2^2*A4^2-
18*A2*A4*A6*A0+27*A0^2*A6^2+4*A0*A4^3)^(1/2)*A6)^(2/3)+12*A2*A6-
4*A4^2))^(1/2)*x)+C2*exp(-1/6/A6/(36*A2*A4*A6-108*A0*A6^2-
8*A4^3+12*3^(1/2)*(4*A2^3*A6-A2^2*A4^2-
18*A2*A4*A6*A0+27*A0^2*A6^2+4*A0*A4^3)^(1/2)*A6)^(1/3)*3^(1/2)*2^(1/2)*(
-A6*(36*A2*A4*A6-108*A0*A6^2-8*A4^3+12*3^(1/2)*(4*A2^3*A6-A2^2*A4^2-
18*A2*A4*A6*A0+27*A0^2*A6^2+4*A0*A4^3)^(1/2)*A6)^(1/3)*(2*A4*(36*A2*A
4*A6-108*A0*A6^2-8*A4^3+12*3^(1/2)*(4*A2^3*A6-A2^2*A4^2-
18*A2*A4*A6*A0+27*A0^2*A6^2+4*A0*A4^3)^(1/2)*A6)^(1/3)-(36*A2*A4*A6-
108*A0*A6^2-8*A4^3+12*3^(1/2)*(4*A2^3*A6-A2^2*A4^2-
18*A2*A4*A6*A0+27*A0^2*A6^2+4*A0*A4^3)^(1/2)*A6)^(2/3)+12*A2*A6-
4*A4^2))^(1/2)*x)+C3*exp(-1/3/A6/(36*A2*A4*A6-108*A0*A6^2-
8*A4^3+12*3^(1/2)*(4*A2^3*A6-A2^2*A4^2-
18*A2*A4*A6*A0+27*A0^2*A6^2+4*A0*A4^3)^(1/2)*A6)^(1/3)*3^(1/2)*(-
9*A2*A4*A6^2+27*A0*A6^3+2*A4^3*A6-3*3^(1/2)*(4*A2^3*A6-A2^2*A4^2-
18*A2*A4*A6*A0+27*A0^2*A6^2+4*A0*A4^3)^(1/2)*A6^2+3*A6^2*(36*A2*A4*
A6-108*A0*A6^2-8*A4^3+12*3^(1/2)*(4*A2^3*A6-A2^2*A4^2-
18*A2*A4*A6*A0+27*A0^2*A6^2+4*A0*A4^3)^(1/2)*A6)^(1/3)*A2-
A6*(36*A2*A4*A6-108*A0*A6^2-8*A4^3+12*3^(1/2)*(4*A2^3*A6-A2^2*A4^2-
18*A2*A4*A6*A0+27*A0^2*A6^2+4*A0*A4^3)^(1/2)*A6)^(1/3)*A4^2-
A6*(36*A2*A4*A6-108*A0*A6^2-8*A4^3+12*3^(1/2)*(4*A2^3*A6-A2^2*A4^2-
18*A2*A4*A6*A0+27*A0^2*A6^2+4*A0*A4^3)^(1/2)*A6)^(2/3)*A4-
9*i*A6^2*3^(1/2)*A2*A4+27*i*A6^3*3^(1/2)*A0+2*i*A6*3^(1/2)*A4^3-
9*i*A6^2*(4*A2^3*A6-A2^2*A4^2-
18*A2*A4*A6*A0+27*A0^2*A6^2+4*A0*A4^3)^(1/2)-3*i*A6^2*(36*A2*A4*A6-
108*A0*A6^2-8*A4^3+12*3^(1/2)*(4*A2^3*A6-A2^2*A4^2-
18*A2*A4*A6*A0+27*A0^2*A6^2+4*A0*A4^3)^(1/2)*A6)^(1/3)*3^(1/2)*A2+i*A6
```

*(36*A2*A4*A6-108*A0*A6^2-8*A4^3+12*3^(1/2)*(4*A2^3*A6-A2^2*A4^2-
18*A2*A4*A6*A0+27*A0^2*A6^2+4*A0*A4^3)^(1/2)*A6)^(1/3)*3^(1/2)*A4^2)^(1
/2)*x)+**C4***exp(1/3/A6/(36*A2*A4*A6-108*A0*A6^2-
8*A4^3+12*3^(1/2)*(4*A2^3*A6-A2^2*A4^2-
18*A2*A4*A6*A0+27*A0^2*A6^2+4*A0*A4^3)^(1/2)*A6)^(1/3)*3^(1/2)*(-
9*A2*A4*A6^2+27*A0*A6^3+2*A4^3*A6-3*3^(1/2)*(4*A2^3*A6-A2^2*A4^2-
18*A2*A4*A6*A0+27*A0^2*A6^2+4*A0*A4^3)^(1/2)*A6^2+3*A6^2*(36*A2*A4*
A6-108*A0*A6^2-8*A4^3+12*3^(1/2)*(4*A2^3*A6-A2^2*A4^2-
18*A2*A4*A6*A0+27*A0^2*A6^2+4*A0*A4^3)^(1/2)*A6)^(1/3)*A2-
A6*(36*A2*A4*A6-108*A0*A6^2-8*A4^3+12*3^(1/2)*(4*A2^3*A6-A2^2*A4^2-
18*A2*A4*A6*A0+27*A0^2*A6^2+4*A0*A4^3)^(1/2)*A6)^(1/3)*A4^2-
A6*(36*A2*A4*A6-108*A0*A6^2-8*A4^3+12*3^(1/2)*(4*A2^3*A6-A2^2*A4^2-
18*A2*A4*A6*A0+27*A0^2*A6^2+4*A0*A4^3)^(1/2)*A6)^(2/3)*A4-
9*i*A6^2*3^(1/2)*A2*A4+27*i*A6^3*3^(1/2)*A0+2*i*A6*3^(1/2)*A4^3-
9*i*A6^2*(4*A2^3*A6-A2^2*A4^2-
18*A2*A4*A6*A0+27*A0^2*A6^2+4*A0*A4^3)^(1/2)-3*i*A6^2*(36*A2*A4*A6-
108*A0*A6^2-8*A4^3+12*3^(1/2)*(4*A2^3*A6-A2^2*A4^2-
18*A2*A4*A6*A0+27*A0^2*A6^2+4*A0*A4^3)^(1/2)*A6)^(1/3)*3^(1/2)*A2+i*A6
*(36*A2*A4*A6-108*A0*A6^2-8*A4^3+12*3^(1/2)*(4*A2^3*A6-A2^2*A4^2-
18*A2*A4*A6*A0+27*A0^2*A6^2+4*A0*A4^3)^(1/2)*A6)^(1/3)*3^(1/2)*A4^2)^(1
/2)*x)+**C5***exp(1/3/A6/(36*A2*A4*A6-108*A0*A6^2-
8*A4^3+12*3^(1/2)*(4*A2^3*A6-A2^2*A4^2-
18*A2*A4*A6*A0+27*A0^2*A6^2+4*A0*A4^3)^(1/2)*A6)^(1/3)*3^(1/2)*(-
9*A2*A4*A6^2+27*A0*A6^3+2*A4^3*A6-3*3^(1/2)*(4*A2^3*A6-A2^2*A4^2-
18*A2*A4*A6*A0+27*A0^2*A6^2+4*A0*A4^3)^(1/2)*A6^2+3*A6^2*(36*A2*A4*
A6-108*A0*A6^2-8*A4^3+12*3^(1/2)*(4*A2^3*A6-A2^2*A4^2-
18*A2*A4*A6*A0+27*A0^2*A6^2+4*A0*A4^3)^(1/2)*A6)^(1/3)*A2-
A6*(36*A2*A4*A6-108*A0*A6^2-8*A4^3+12*3^(1/2)*(4*A2^3*A6-A2^2*A4^2-
18*A2*A4*A6*A0+27*A0^2*A6^2+4*A0*A4^3)^(1/2)*A6)^(1/3)*A4^2-
A6*(36*A2*A4*A6-108*A0*A6^2-8*A4^3+12*3^(1/2)*(4*A2^3*A6-A2^2*A4^2-
18*A2*A4*A6*A0+27*A0^2*A6^2+4*A0*A4^3)^(1/2)*A6)^(2/3)*A4+9*i*A6^2*3^
(1/2)*A2*A4-27*i*A6^3*3^(1/2)*A0-2*i*A6*3^(1/2)*A4^3+9*i*A6^2*(4*A2^3*A6-
A2^2*A4^2-
18*A2*A4*A6*A0+27*A0^2*A6^2+4*A0*A4^3)^(1/2)+3*i*A6^2*(36*A2*A4*A6-
108*A0*A6^2-8*A4^3+12*3^(1/2)*(4*A2^3*A6-A2^2*A4^2-
18*A2*A4*A6*A0+27*A0^2*A6^2+4*A0*A4^3)^(1/2)*A6)^(1/3)*3^(1/2)*A2-
i*A6*(36*A2*A4*A6-108*A0*A6^2-8*A4^3+12*3^(1/2)*(4*A2^3*A6-A2^2*A4^2-
18*A2*A4*A6*A0+27*A0^2*A6^2+4*A0*A4^3)^(1/2)*A6)^(1/3)*3^(1/2)*A4^2)^(1
/2)*x)+**C6***exp(-1/3/A6/(36*A2*A4*A6-108*A0*A6^2-
8*A4^3+12*3^(1/2)*(4*A2^3*A6-A2^2*A4^2-
18*A2*A4*A6*A0+27*A0^2*A6^2+4*A0*A4^3)^(1/2)*A6)^(1/3)*3^(1/2)*(-
9*A2*A4*A6^2+27*A0*A6^3+2*A4^3*A6-3*3^(1/2)*(4*A2^3*A6-A2^2*A4^2-
18*A2*A4*A6*A0+27*A0^2*A6^2+4*A0*A4^3)^(1/2)*A6^2+3*A6^2*(36*A2*A4*
A6-108*A0*A6^2-8*A4^3+12*3^(1/2)*(4*A2^3*A6-A2^2*A4^2-
18*A2*A4*A6*A0+27*A0^2*A6^2+4*A0*A4^3)^(1/2)*A6)^(1/3)*A2-
A6*(36*A2*A4*A6-108*A0*A6^2-8*A4^3+12*3^(1/2)*(4*A2^3*A6-A2^2*A4^2-
18*A2*A4*A6*A0+27*A0^2*A6^2+4*A0*A4^3)^(1/2)*A6)^(1/3)*A4^2-
A6*(36*A2*A4*A6-108*A0*A6^2-8*A4^3+12*3^(1/2)*(4*A2^3*A6-A2^2*A4^2-
18*A2*A4*A6*A0+27*A0^2*A6^2+4*A0*A4^3)^(1/2)*A6)^(2/3)*A4+9*i*A6^2*3^

```
(1/2)*A2*A4-27*i*A6^3*3^(1/2)*A0-2*i*A6*3^(1/2)*A4^3+9*i*A6^2*(4*A2^3*A6-
A2^2*A4^2-
18*A2*A4*A6*A0+27*A0^2*A6^2+4*A0*A4^3)^(1/2)+3*i*A6^2*(36*A2*A4*A6-
108*A0*A6^2-8*A4^3+12*3^(1/2)*(4*A2^3*A6-A2^2*A4^2-
18*A2*A4*A6*A0+27*A0^2*A6^2+4*A0*A4^3)^(1/2)*A6)^(1/3)*3^(1/2)*A2-
i*A6*(36*A2*A4*A6-108*A0*A6^2-8*A4^3+12*3^(1/2)*(4*A2^3*A6-A2^2*A4^2-
18*A2*A4*A6*A0+27*A0^2*A6^2+4*A0*A4^3)^(1/2)*A6)^(1/3)*3^(1/2)*A4^2)^(1
/2)*x)
```